Reconstructing the erosional history of the Upper Mississippi River from magnetic, isotopic, and geomorphic evidence

A DISSERTATION
SUBMITTED TO THE FACULTY OF THE GRADUATE SCHOOL
OF THE UNIVERSITY OF MINNESOTA
BY

Dylan John Blumentritt

IN PARTIAL FULFILLMENT OF THE REQUIREMENTS
FOR THE DEGREE OF
DOCTOR OF PHILOSOPHY

Daniel R. Engstrom and Herbert E. Wright, Jr., advisers

August 2013

Acknowledgements

I have had the good fortune of interacting with many kind and talented people while working on my PhD at the University of Minnesota, and I could not have completed this work without their help and support. I give my sincerest gratitude to all those who have helped me along my way. My co-adviser, Herb Wright, Jr., has been an inspiration and a guide. It was Herb who, after much persistence, convinced me to pursue my PhD. Periodically, he would come into my office in the basement of Pillsbury Hall to talk about Lake Pepin, and our conversations usually ended with him convincing me that what we talked about would make a good PhD project. He was right. I thank Herb for our wonderful conversations and for being a supportive adviser as well as a good friend. Dan Engstrom, my other co-adviser and Director of the St. Croix Watershed Research Station (SCWRS), deserves much credit for my development as a scientist. He is patient, supportive, and offers gentle criticism when deserved, all qualities that make him an excellent teacher. I had many productive conversations and brainstorming sessions with Shawn Schottler, a senior scientist at the SCWRS, who also provided entertainment while in the field. Carrie Jennings of the Minnesota Geological Survey has been a valuable mentor since I came to the University of Minnesota. David Fox, Karen Gran, and Bruce Moskowitz served on my examining committee and helped to direct my projects from the early stages. I would also like to thank all those at the SCWRS for allowing me to infiltrate their tight-knit community. In particular, Erin Mortenson and Jill Coleman Wasik were a tremendous help in the lab, and Sharon Mallman for general

guidance. Amy Myrbo, Kristina Brady, Anders Noren, and Ryan O'Grady of the Limnological Research Center improved this project with their expertise and made for a fun working environment. Ioan Lascu along with Mike Jackson, and Peter Solheid of the Institute for Rock Magnetism helped me to discover the finer points of magnetism. Staff at the Metropolitan Council Environmental Services was kind enough to provide support, Scott Schellhaass and Scott Haire collected many large water samples and Karen Jensen provided data and modeling guidance. Additionally, I would like to thank the staff in the Earth Science Department, Sharon Kressler, Kathy Ohler, Mark Griffith, Doug Johnson, and Greg Gambeski, for helping me find my way through University mazes.

I have made many friends while working in the Department of Earth Sciences and SCWRS, many of which were graduate students who provided the kind of support and friendship that only fellow graduate students could. I'd like to thank Ioan Lascu, Robert Dietz, Laura Triplett, Avery Cook-Shinneman, Marylee Murphy, Annia Fayon, Rory McFadden, Eric Goergen, Seth Kruckenberg, Nick Pester, Anna Henderson, Sam Matson, Andrew Haveles, Laura Vietti, Peter Rose, Andrew Luhmann, Ted Fuller, and Stephanie Day for enhancing my experience at Minnesota. My family has been supportive in all that I do, but I now know that this support knows no limitations. Debra Cadwell, my mother, taught me the intrinsic value of nature and the joys of being outdoors, all of which drove me towards geology. Tony Blumentritt, my father, instilled the values of hard work and integrity, which have helped me achieve my goals. My sisters, Keely and Leah, always inspire me to be a better person. Finally, I'd like to thank my wife Erin. Her kindness, support, and truly endless patience make anything possible.

Abstract

Excess sediment affects many streams and rivers throughout the world and has a negative impact on the ecological health of surface waters. The unifying objective of this dissertation is to better understand sediment dynamics and how sediment is measured in large river systems, particularly where excess sediment is related to anthropogenic landscape modifications. Lake Pepin, the principal focus of this study, is a natural riverine impoundment that traps sediment eroding from three major sub-watersheds of the upper Mississippi River (UMR), the St. Croix, headwater Mississippi, and Minnesota rivers. Sediment accumulation in Lake Pepin has increased nearly 10-fold since the onset of Euro-American settlement c. 1830. This dissertation explores: (1) the geological evolution of the UMR and Lake Pepin, (2) the most recent sediment-accumulation trends in Lake Pepin, (3) the deconstruction of magnetic susceptibility profiles in a Lake Pepin core, and (4) an evaluation of direct atmospheric deposition of ^{210}Pb to the river surface and its consequences for geochemical fingerprinting. The four study elements are summarized as follows:

(Chapter 1) Lake Pepin currently occupies 34 km of the Mississippi River valley, but it extended nearly 81 km further up-river at its inception approximately 10,000 years ago. Sediment fans deposited by several tributaries (the Chippewa, Cannon, and Vermillion rivers) entering the valley segmented this early Lake Pepin into several smaller lake sections. Later, accretion of the Chippewa fan surpassed that of the tributary fans to create a single large lake. Since that time, the length of Lake Pepin has decreased progressively as its delta prograded downstream from present-day St. Paul. Based on geomorphic evidence, the delta is estimated to have migrated past Hastings c. 6.0 ka and Red Wing c. 1.4 ka.

(Chapter 2) A new method was developed to measure recent sediment accumulation rates in Lake Pepin by aligning new cores to a previous set of cores with an established chronology. This method relies on prominent magnetic susceptibility peaks ubiquitous throughout the lake to align the new cores with the older core set. The amount

of recent (1996–2008) bulk sediment, total phosphorus, and mercury at each core site was extrapolated to the depositional area of the lake to estimate whole-basin loads. These core-based estimates of recent sediment loads compared well (<3%) with load estimates from monitored inflow data, validating the alignment procedure and multiple-core approach. Recent (1996–2008) bulk sediment accumulation remains high (772,000 t/yr), and almost an order of magnitude greater than pre-settlement accumulation rates. Total phosphorus deposition remains constant and mercury continues to decline following peaks in the 1960s.

(Chapter 3) Three techniques for measuring magnetic susceptibility were compared using a single sediment core from Lake Pepin: (1) loop-sensor logging on wet sediment of the intact core; (2) point-sensor logging on wet sediment of a split (lengthwise) core; and (3) discrete measurements of dried subsamples (2-cm intervals) using a susceptibility bridge. Overall trends agree reasonably well among the three techniques. Profiles from the loop-sensor and susceptibility bridge were most similar, while the point sensor profile provided higher down-core temporal resolution. All three techniques captured two distinct magnetic susceptibility excursions c. 1900 and 1940. Concentrations of ferrimagnetic components were modeled to further explore the magnetic sources of these susceptibility peaks. Model results indicate that the two prominent excursions were a result of higher superparamagnetic particle concentrations (<30 nm). A later peak (1980) was present in the point-sensor and susceptibility bridge logs, but was not obvious in the loop-sensor log. This 1980 peak corresponded to higher concentrations of interacting single domain (<0.1 μm) and multi-domain (>1–10 μm) ferrimagnetic particles, but not superparamagnetic particles, as did the two earlier excursions. These results highlight the likely causes for discrepancies among magnetic susceptibility techniques on sediment cores.

(Chapter 4) Geochemical fingerprinting using atmospheric radioisotopes (ARI) such as ^{210}Pb is an important tool for quantifying riverine sediment sources. Although sediment fingerprinting methods are well established, they rely on the assumption that direct deposition of ARI to the river surface is negligible relative to that derived indirectly from watershed erosion. In this study a strategy was developed for quantifying

the amount of ^{210}Pb deposited directly to the river surface (i.e., ^{210}Pb not entering on eroded particles) by exploiting the initial disequilibrium between newly deposited ^{210}Pb and its granddaughter ^{210}Po. Direct ^{210}Pb deposition (Pb_w) was estimated by modeling ^{210}Po ingrowth based on repeated measurements of the same sample over the course of a year. A significant amount of Pb_w was detected at each site, ranging from 20–90% of the total unsupported annual ^{210}Pb load, and generally increasing with watershed size. This method provides an important correction to atmospheric radioisotope fingerprinting, particularly in larger watersheds.

This dissertation offers several key findings that help to better understand sediment movement in the upper Mississippi River system and provide innovative and novel approaches to more accurately measure sediment dynamics in general. There is now a new understanding of the early history of Lake Pepin and the Mississippi River valley it occupies. There is also a new method for determining recent trends in sediment and contaminant accumulation by building on previously analyzed cores, and results show that despite efforts to remediate high sediment loads in the UMR, Lake Pepin is still filling in at an alarming rate. There is now a better understanding of the ubiquitous magnetic susceptibility peaks in Lake Pepin cores that have been important stratigraphic markers in prior studies. It is now understood the two most prominent peaks (1900 and 1940) are associated with a greater influx of superparamagnetic particles, and the most recent (1980) peak is heavily influenced by greater concentrations of interacting single domain and multi-domain ferrimagnetic particles. Finally, efforts to determine sediment sources with atmospheric radioisotopes have neglected the influence of isotopes deposited directly to the river surface, largely because there was not a viable method to estimate this component. There is now a new method to measure atmospherically deposited ^{210}Pb, which provides an important correction for these types of studies.

Table of Contents

List of Tables

List of Figures

Introduction

The motivation for the work presented in this dissertation centers around understanding how human influences on our landscape affect sediment erosion in our waterways. Sediment is the central theme, and Lake Pepin is the main character. Lake Pepin, a natural riverine lake on the Mississippi River in southeastern Minnesota, is a fortunate natural occurrence because its watershed drains almost the entire southern half of Minnesota and it has been in existence for almost 10,000 years; thus, the sediment in Lake Pepin records the erosional history of southern Minnesota.

A suite of 25 sediment cores was collected in 1996 from throughout Lake Pepin in earlier work by Engstrom et al. (2009). In their study they determined that the sediment accumulation rate in Lake Pepin had increased almost ten-fold in the past two centuries. Further work by Kelley and Nater (2000) concluded that an overwhelming majority of sediment entering Lake Pepin (80–90%) comes from the Minnesota River basin. Combined, these two studies have formed the scientific basis for many other studies focused on excess sediment in southern Minnesota (Belmont, 2011; Belmont et al., 2011; Blumentritt et al., 2013; Blumentritt et al., 2009; Gran et al., 2009; Kelley et al., 2006; Knox, 2001; Schottler et al., 2010; Schottler et al., 2013). There has been much interest in addressing the issue of excess sediment in southern Minnesota in recent years by the State of Minnesota and various other stakeholders; Lake Pepin and the Minnesota River are currently the subjects of larger-scale total maximum daily load (TMDL) reduction efforts for excess sediment.

The goal of the work presented in this dissertation is a clearer understanding of sediment dynamics in the large rivers of southern Minnesota, particularly the Minnesota River and the Mississippi River between St. Paul and Lake Pepin. A significant portion of this work focuses on improving the methods used to measure sediment in large rivers and lakes. The subsequent four chapters are inter-related papers prepared for publication in scientific journals. Each chapter benefitted tremendously from co-authors who improved both the ideas and the writing.

Chapter 1, "Formation and early history of Lakes Pepin and St. Croix of the upper Mississippi River," examines the Mississippi River valley over the past 10,000 years and builds on earlier work by Zumberge (1952), who first recognized that Lake Pepin extended from its current location to St. Paul. We examined recent borings from several bridge and dam sites between St. Paul and Lake Pepin and discovered that many had two lake layers. This study furthers our understanding of Lake Pepin, which was previously thought to extend as a single lake from St. Paul to the Chippewa River fan. From this work, we know early Lake Pepin was segmented by the Cannon River and Vermillion River fans; later, the Chippewa River fan growth surpassed the growth of the Cannon and Vermillion fans to create a longer, less-segmented Lake Pepin. This paper was co-authored by Herb E. Wright, Jr. and Vania Stefanova. Wright provided much guidance for interpreting the bore records and was ultimately responsible for organizing the complete manuscript. Although Wright's contribution to this paper could have earned him lead author, he insisted that it be I because, as he put it, 'I provided the new information.' Chapter 1 of this dissertation is not the entire paper, but the portion of the

original paper that I consider myself the primary contributor. Stefanova provided pollen analysis and composed several of the figures in the original paper. This paper, in its entirety, was published in the Journal of Paleolimnology (2009, DOI 10.1007/s10933-008-9291-6) as the first paper in the special issue "Recent environmental history of the Upper Mississippi River" edited by Daniel R. Engstrom.

Chapter 2, "A novel repeat-coring approach to reconstruct recent sediment, phosphorus, and mercury loading from the upper Mississippi River to Lake Pepin, USA," develops a simple method to date the most recent portion of repeat-cores where an initial paleo-study had been performed and more recent information is desired. We re-cored the exact location of ten primary cores used in the initial study that looked at whole-basin accumulation rates in Lake Pepin (Engstrom et al., 2009) to obtain more recent sediment, phosphorus, and mercury accumulation rates. Our re-core method relies on an immobile stratigraphic marker; here we used prominent magnetic susceptibility peaks. The amount of new sediment is the difference in dry mass above the tie points between the original core and the most recent core. We extrapolated this new accumulation rate of each of the ten cores to a representative portion of the basin to estimate whole-basin accumulation rates. Estimates from our re-core method compared well (within 3%) with estimates from monitored suspended sediment loads near the inflow to Lake Pepin. Both sediment and phosphorus accumulation rates remain high, while mercury accumulation is declining. The original paper was published in the Journal of Paleolimnology (2013, DOI 10.1007/s10933-013-9724-8), co-authored by Daniel R. Engstrom and Steven J. Balogh. Engstrom provided guidance throughout this study, from developing the re-core

methodology to preparing the manuscript for publication. Balogh performed the mercury analysis and provided insightful discussion.

Chapter 3 "A comparison of magnetic susceptibility measurement techniques and ferrimagnetic component analysis from recent sediments in Lake Pepin (USA)" explores the advantages and difficulties of measuring magnetic susceptibility using three different techniques: (1) whole-core scanning with a loop sensor susceptibility meter, (2) split-core scanning with a point sensor susceptibility meter, and (3) single-sample measurements on discrete intervals using a susceptibility bridge. We compared magnetic susceptibility profiles for these three acquisition techniques on a single core from Lake Pepin, which displays several prominent magnetic susceptibility peaks. Further motivation for this study was to explore the causes of these magnetic susceptibility peaks, which are found throughout Lake Pepin. We applied the recently developed model of Lascu et al. (2010) that successfully untangles the ferrimagnetic components using standard bulk magnetic measurements. Results indicate that small increases in the superparamagnetic ferrimagnetic fraction (<30 nm) can have dramatic effects on magnetic susceptibility. However, magnetic susceptibility peaks were also tied to increases in multi-domain (>1–10 μm) and interacting single domain (<0.1 μm) components, but these required larger concentrations than the SP component. This chapter is co-authored by Ioan Lascu, who provided very useful discussion, the ferrimagnetic component analysis, and much laboratory guidance at the Institute for Rock Magnetism (University of Minnesota).

In **Chapter 4,** "Investigation of direct deposition of atmospheric ^{210}Pb to river

surfaces: Implications for sediment fingerprinting," we develop a new approach for estimating the amount of ^{210}Pb deposited directly from the atmosphere to the surface of rivers. Sediment fingerprinting using atmospheric radioisotopes (ARI) has been an important tool for measuring the provenance of sediment in rivers. A central assumption of the ARI fingerprinting method is that the source of ARI is sorbed onto eroded sediment particles and did not enter the river directly from the atmosphere. As a result, most successful ARI sediment fingerprinting work has been performed on smaller watersheds. Our goal was to assess the contribution of atmospheric ARI on large river systems and provide a correction for sediment fingerprinting. Our method relies on disequilibrium between freshly deposited ^{210}Pb and its granddaughter ^{210}Po. If there is a significant amount of ^{210}Pb deposited directly to the water (Pb_w), we can measure the appearance of ^{210}Po after sample collection. If ^{210}Pb[^{210}Po] are in equilibrium, there will be no appearance of additional ^{210}Po. Using this disequilibrium technique, we measured Pb_w at four different locations with a range of watershed sizes. Our sample sites included the Minnesota River at Jordan (42,000 km^2) and Fort Snelling (44,000 km^2) and the Mississippi River at St. Paul (95,000 km^2) and Lock and Dam 3 (123,000 km^2), which is just upstream of Lake Pepin. A significant portion of the total ^{210}Pb was attributed to Pb_w at each of our sample sites. Pb_w was present, but less significant (20–50%) at Jordan and Ft. Snelling, providing an important correction to sediment fingerprinting. At St. Paul and Lock and Dam 3, however, Pb_w was much more significant (60–90%), calling into question the feasibility of ARI fingerprinting on watersheds as large as these. This chapter is co-authored by Shawn Schottler and Daniel R. Engstrom, as both provided

strong guidance in developing this new method.

Chapter 1: Formation and early history of Lakes Pepin and St. Croix of the Mississippi River

Dylan Blumentritt, Herbert E. Wright, Jr., Vania Stefanova

Department of Earth Sciences, University of Minnesota, Minneapolis, MN, USA

Reprinted from the Journal of Paleolimnology, Vol. 41 (4), DOI 10.1007/s10933-008-9291-6,

Study of Lake Pepin and Lake St. Croix began more than a century ago, but new information has permitted a closer look at the geologic history of these two riverine lakes located on the upper Mississippi River system. Drainages from large proglacial lakes Agassiz and Duluth at the end of the last glaciation helped shape the current valleys. As high-discharge outlet waters receded, tributary streams deposited fans of sediment in the incised river valleys. These tributary fans dammed the main river, forming riverine lakes. Lake Pepin was previously thought to be a single long continuous lake, extending for 80 km from its dam at the Chippewa River fan all the way up to St. Paul, with an arm extending up the St. Croix valley. Recent borings taken at bridge and dam locations show more than a single section of lake sediments, indicating a more complex history.

A sediment core taken in Lake Pepin near Lake City had a piece of wood in gravels just below lake sediments that dated to 10.3 ka cal. BP, indicating that the lake formed as the Chippewa River fan grew shortly after the floodwaters of Lakes Agassiz and Duluth receded. Data from new borings indicate small lakes were dammed behind several tributary fans in the Mississippi River valley between the modern Lake Pepin and St. Paul. One tributary lake, here called Early Lake Vermillion, may have hydraulically dammed the St. Croix River, creating an incipient Lake St. Croix. The tributary fans from the Vermillion River, the Cannon River, and the Chippewa River all served to segment the main river valley into a series of riverine lakes. Later the growth of the Chippewa fan surpassed that of the Vermillion and Cannon fans to create a single large lake, here called late Lake Pepin, which extended upstream to St. Paul.

Sediment cores taken from Lake Pepin did not have significant organic matter to develop a chronology from radiocarbon dating. Rather, magnetic features were matched with those from a Lake St. Croix core, which did have a known radiocarbon chronology. The Pepin delta migration rate was then estimated by projecting the elevations of the top of the buried lake sediments to the dated Lake Pepin core, using an estimated slope of 10 cm/km, the current slope of Lake Pepin sediment surface. By these approximations, the Lake Pepin delta prograded past Hastings 6.0 ka cal BP and Red Wing 1.4 ka cal BP.

Keywords: Mississippi River • Holocene • sediments • Minnesota • Wisconsin

1.1 Introduction

Lake Pepin is a riverine lake that lies on the upper Mississippi River, forming a natural boundary between Minnesota and Wisconsin in the United States. Lake St. Croix occupies the St. Croix River valley, a major tributary to the Mississippi (Fig. 1.1A and B). The origin of Lakes Pepin and St. Croix was broadly understood already more than a century ago as a result of the pioneering work of Winchell and Upham (1884) on the glacial history of Minnesota, but recent studies of the sediment-stratigraphies of the Mississippi and St. Croix river valley and the application of radiocarbon dating now permit a more detailed reconstruction of the related histories of the two lakes. Of especial aid in reconstructing the geologic history have been the availability of new topographic maps and aerial photographs, the detailed geologic maps of the Minnesota Geological Survey, and new borings through the floodplain that help to unravel the complicated history of sedimentation. For the development of the lakes themselves after their geologic establishment, sediment cores were taken from the middle of Lake Pepin off Lake City and from Lake St. Croix in mid-lake near Bayport, south of Stillwater (Fig. 1.1B).

1.2 Ice Lobes, Proglacial Lakes, and Catastrophic Floods

The early work recognized that most of the landscape of southern Minnesota was fashioned by two major ice lobes of the Laurentide ice sheet, one on the east extending southward beyond the Lake Superior lowland, and the other on the west advancing from

the Red River Valley across southern Minnesota (Fig. 1.2). The Superior lobe deposited the prominent St. Croix moraine across the St. Croix River valley and covered most of eastern Minnesota with reddish glacial deposits. Later the Des Moines lobe from the west covered most of western and southern Minnesota with grey drift (light brown where oxidized). An eastward protrusion of this lobe (Grantsburg sublobe) even crossed the state and covered the lower part of the St. Croix Valley. The Des Moines lobe proper reached to the edge of St. Paul and extended southward into Iowa. Outwash from these ice lobes provided extensive gravel deposits in the Mississippi and St. Croix River valleys.

The early work also demonstrated that, with the retreat of these two ice lobes across the continental drainage divide in the north, huge proglacial lakes filled the lowlands previously occupied by ice. Glacial Lake Duluth filled the Lake Superior basin, and Glacial Lake Agassiz submerged the Red River lowland (Fig. 1.1A). Outlets of these huge lakes brought great floods down the St. Croix and Minnesota River valleys, dissecting the earlier outwash deposits. When the ice lobes retreated enough to uncover lower outlets to the east and northwest, the southward floods ceased, and the subsequent river discharges were insufficient to remove sediment from tributaries. In the case of the Mississippi River, Lake Pepin was thereby created by a fan of the tributary Chippewa River (Fig. 1.1B). Later work by Zumberge (1952) showed that Lake Pepin once reached up-river to St. Paul (Fig. 1.3). A long arm extending up the St. Croix River valley was cut off by the advancing Mississippi River delta during its southward advance.

The occasion to elaborate the history of Lake Pepin and Lake St. Croix comes with the re-examination of the borings on the Mississippi floodplain used by Zumberge, along with additional borings at bridge sites. The finding that most borings had two sections of lake sediments rather than just one implied that a single upstream growth of Lake Pepin, followed by the reduction by delta advance, was too simple a reconstruction. Sediment cores from both lakes provided another approach to the history. The new geological maps of southeastern Minnesota allowed the reconstruction of the history to be set in a larger context, with a focus on the drainage history of the major rivers in southeastern Minnesota.

1.3 Tributary Fans

When the high flows from Lake Agassiz and Lake Duluth ceased, the tributary streams to the Mississippi River deposited alluvial fans across the valley, because the residual flow of the Mississippi was insufficient to transport these contributions. One such fan was that of the Chippewa River on the eastern (Wisconsin) side, and it served to dam up the main river, forming Lake Pepin (Fig. 1.1B). Similar tributary fans from both sides of the valley downstream to Iowa and beyond have segmented the river into a series of riverine lakes, of which Lake Pepin is the northernmost and most distinctive. Upstream from Lake Pepin the smaller fans of the Cannon and Vermillion rivers also dammed the Mississippi to make small lakes, as described below.

Core P89 in Lake Pepin off Lake City yielded a piece of wood in the gravel just beneath the lake sediment. The ^{14}C date, 9180 yr BP (10.3 ka cal BP), which serves to

record the inception of Lake Pepin, is slightly younger than the 10.6 ka cal BP date at the Lake Agassiz outlet for the last episode of River Warren (Fisher, 2003a). The difference may represent the time for Lake Pepin to expand headward the 12 km from the Chippewa fan to the coring site off Lake City.

1.4 Borings

For the history of Lake Pepin after its initial formation Zumberge (1952) compiled data from floodplain borings at Red Wing, Hastings, and St. Paul, which showed that the basal gravels were overlain by silty lake sediments and these by sandy delta alluvium. He determined that the Mississippi delta has prograded almost 80 km into Lake Pepin, and that it is still advancing past the mouth of the Cannon River at Red Wing (Fig. 1.3). No estimates of the radiocarbon chronology of these events were possible at the time of his analysis.

Zumberge's interpretations can now be supplemented as a result of re-examination of the core logs as well as by data from additional borings at bridge sites. Boring logs with sediment information were obtained from the United States Army Corps of Engineers (USACE) for Lock and Dam 2 (LD2) near Hastings and for Lock and Dam 3 (LD3) near Red Wing, and logs of bridge borings for St. Paul and West St. Paul (Wakota) were obtained from the Minnesota Department of Transportation. It is apparent that two sections of buried lake sediments, rather than just one, are present at all boring sites except St. Paul. In addition, archeological projects yielded radiocarbon dates from sediments in the fan of the Cannon River near Red Wing (Dobbs and Mooers, 1990;

Mrachek et al., 1994). Boring logs for Lake St. Croix are available in Eyster-Smith (1977).

Elevations of the stratigraphic units were determined from cross-sections drawn from multiple-core transects. The available data are shown graphically, with all figures converted to metric. The several stratigraphic columns plotted to scale show the lake-sediment segments, which are designated according to different lake units, controlled by elevation, on each column (Fig. 1.4). This figure forms the basis for a continuous longitudinal profile of these sediments in the Mississippi River valley from Lake Pepin to St. Paul, showing the lakes formed behind tributary fans as well as the extension of Lake Pepin (Fig. 1.5).

The high elevation of the basal gravel from Prescott south to Lake City records a drowned glacial outwash terrace. It had been dissected by the combined flows of the Glacial River Warren from Lake Agassiz and the Glacial St. Croix River from Glacial Lake Duluth, producing the deep trough that extends from LD2 Hastings up the Mississippi to Wakota.

Once the strong discharges of the River Warren and the St. Croix River ceased, the Mississippi channel was locally dammed by tributary fans, not only by that of the Chippewa River but also by those of the Cannon and Vermillion Rivers. The Vermillion River, which enters the Mississippi from the west at Hastings, is smaller than the Cannon, but today the deposition of its sediment is enough to force the Mississippi River to the far side of the valley floor from Hastings downstream for 20 km, despite the additional input of flow from the St. Croix River on that side.

For the time in question the sediment of the Vermillion fan may have dammed the Mississippi River enough to create what is here called early Lake Vermillion (Fig. 1.4 unit V_E at LD2 Hastings), which was much longer than the modern Spring Lake behind LD2, for it extended 25 km upstream to the Wakota Bridge, where the unit V_E, 4 m thick, has about the same elevation as unit V_E at LD2 (7.5 m thick).

Early Lake Vermillion may have reduced the flow of the incoming St. Croix River enough to create by hydraulic damming an incipient Lake St. Croix, which must have extended all the way to Bayport, where the basal sediment of the Lake St. Croix core has a date of 10.8 ka cal BP, corrected by 980 yr for the near-surface date for the rise in ragweed pollen (see below). This date is not much different from that of the cessation of flow from Glacial Lake Duluth (10.6 ka cal BP) according to the finding at Upper Lake St. Croix.

Early Lake Vermillion became filled with sediment from the Mississippi and Vermillion rivers. Meanwhile early Lake Pepin had extended from the Chippewa fan past the Lake City site and reached upstream beyond the mouth of the Cannon River, whose fan was not broad and high enough at the time to block the growth of early Lake Pepin (Fig. 1.5). This early Lake Pepin is represented by unit P_E beneath the Cannon fan and at LD3 Red Wing (Fig. 1.4). It was subsequently filled with alluvium of the Mississippi and Cannon Rivers.

During this time the build-up of the Vermillion fan was enough to produce a late Lake Vermillion, represented by the lower portion of the 19 m of lake sediment (V_L) at LD2 Hastings (Fig. 1.4). By this time the Cannon fan, supplemented by the fan of the

Trembelle River from the opposite side of the valley, was high enough to form Lake Cannon (Fig. 1.5). Continued build-up of the Chippewa fan caused late Lake Pepin to deepen and advance upstream over the Cannon fan (P_L on Fig. 1.4) and LD3 Red Wing, topping Lake Cannon and extending up to Prescott and then to LD2 Hastings, where it deposited the very upper portion of the 19 m of lake sediment. It reached upstream all the way to St. Paul. This late Lake Pepin would have also extended up the St. Croix arm, deepening the lake that was already there.

The subsequent progradation of the Mississippi delta into late Lake Pepin is described by Zumberge in his original reconstruction, and as the delta passed the mouth of the St. Croix the influx of the latter became restricted at the toe of the Vermillion fan by the formation of the sand bar of Douglas Point.

Figure 1.6 consists of block diagrams reconstructing the history of the Mississippi River Valley from St. Paul to Lake City during successive phases of lake formation and delta growth.

1.5 Magnetic Chronology of Lake Pepin Sediments

No datable organic macro-remains were found in the Lake Pepin core, except for the wood in the gravels beneath, so the core was dated by a series of steps based on the magnetic properties of the sediment and their correlation with the sediment record of Lake St. Croix, which does have a chronology. The Lake Pepin chronology is potentially useful in dating indirectly the progression of the Mississippi River delta from St. Paul into Lake Pepin, as indicated by Zumberge.

The correlation of Lake Pepin with the Lake St. Croix chronology was worked out largely by Brachfeld (Brachfeld and Banerjee, 2000; Kelley et al., 2006) on the basis of earlier work by Lund on the magnetic properties of the Lake St. Croix core (Lund and Banerjee, 1985).

With the chronology of the Lake Pepin core determined by the correlation of the magnetic stratigraphy with that of the dated St. Croix core, the opportunity came to calculate the rate of advance of the delta of the Mississippi River into the head of the main branch of Lake Pepin (Fig. 1.1B), and also to date the cut-off of Lake St. Croix, as postulated by Zumberge (1952).

Dates for the delta advance were estimated by assuming that the present slope of the sediment surface of Lake Pepin (southward 0.0001 or 10 cm per km), as estimated from bathymetric maps, had the same slope as the sediment surface in the past, so that this slope could be projected from the top of the upper section of lake sediments at the different borings southward to the dated Lake Pepin P89 core near Lake City. The intersections would yield the estimated dates for the progression of the delta at the boring locations. Thus for Lock and Dam 3 (Red Wing) the top of the 4.5 m section of lake sediments dates to 1500 ^{14}C yr BP (1.4 ka cal BP), and the delta passed Lock and Dam 2 (Hastings) about ^{14}C 5200 yr BP (6.0 ka cal BP), giving migration rates for the delta of 12.8 and 7.7 m/yr, respectively. This method assumes Lake Pepin was continuous and not affected by the Cannon fan. A check on the method is provided by the date of 620 ^{14}C yr BP (580 cal BP) (average of 560 ± 70 and 690 ± 90 ^{14}C yr BP) at the top of lake sediments at a depth of 280 cm at a floodplain site at 204 m elevation at a place where the

Mississippi delta is joined by the fan of the Cannon River (Dobbs and Mooers, 1990), approximately 3.5 km downstream from Lock and Dam 3 near Red Wing. The 580 cal BP date on the Lake City core is at a depth of 300 cm according to the chronology of Kelley et al. (2006), so the slope of this horizon is thus 9.2 m over the distance of 33.5 km (0.0003), rather than the postulated 0.0001 (10 cm per km). The discrepancy may be a result of the fact that the date of Dobbs and Mooers came from the bulge on the Mississippi floodplain produced by the Cannon River fan. Specifically, the top of these upper lake-sediments at this site has an elevation of approximately 204 m, more than 9 m higher than the top of the lake sediments at LD3 just upstream.

1.6 Conclusions

The sections of buried lake sediments in the borings may not record simply the extension of Lake Pepin to St. Paul and up the St. Croix valley as the result of the gradual rise of the Lake Pepin level, responding to continued build-up of the Chippewa fan, as Zumberge indicated. Rather the sequence of events postulated here takes into account the fact that the borings show two lacustrine phases rather than one, and that these can be traced by elevation control from St. Paul downstream all the way past Hastings to Red Wing. They may record instead separate lakes and different phases of lake-development. In the Hastings area the fan of the Vermillion River added to the height of the outwash terrace left by the dissection of outwash gravels, thereby deepening the adjacent low area and forming early Lake Vermillion, which extended up the Mississippi River to the Wakota Bridge in West St. Paul, as well as an arm extending up the St. Croix Valley to

Stillwater as incipient Lake St. Croix. The Wakota arm of Lake Vermillion became filled with delta sediment generated by post-glacial erosion of River Warren terrace sediments in the Minnesota River Valley. When this delta reached the Hastings area it may have partially cut off the St. Croix arm, which was not being filled because the St. Croix River carries relatively little sediment. In the main valley a fan of the tributary Cannon River produced a dam that formed a small early Lake Cannon, and subsequently it was filled with delta sediments of the Mississippi River.

All this time the Chippewa fan was growing, causing Lake Pepin to deepen and extend northward, submerging early Lake Cannon and early Lake Vermillion and reaching to St. Paul and up the St. Croix Valley to Stillwater, as Zumberge originally proposed. This maximum Lake Pepin extent in the main valley then became progressively shortened by the growth of the Mississippi River delta, as previously described, with strengthening of the barrier to Lake St. Croix near Hastings. This barrier did not function as a dam, however, for the surface elevation of Lake St. Croix is no higher than that of the Mississippi at the junction, so it was more a hydraulic dam than a dam of sediment.

Figures

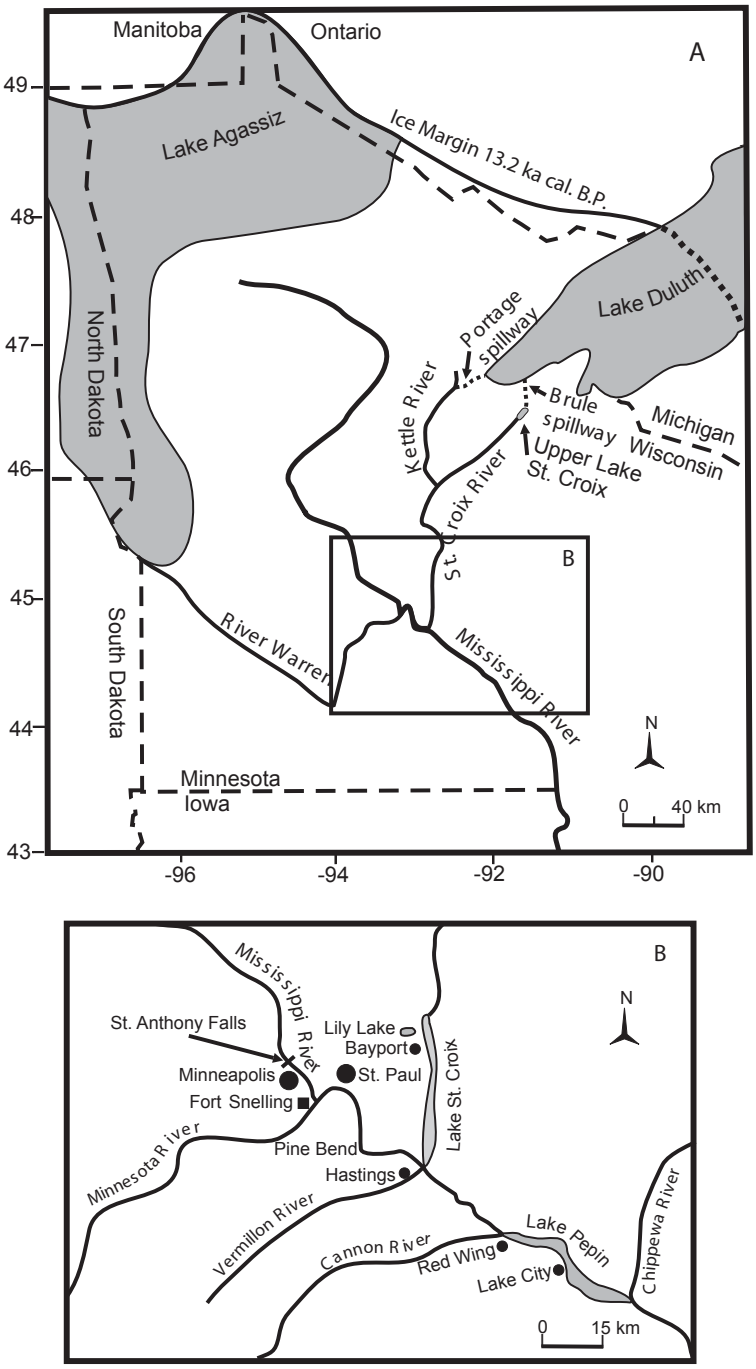

Fig. 1.1 (A) Map showing extent of Lake Agassiz and Lake Duluth at about 13.2 ka cal BP (11.3 14C ka BP) (Teller, 1987), as well as other features mentioned in the text. (B) Map of the Lake Pepin/Lake St. Croix area showing location of features mentioned in the text.

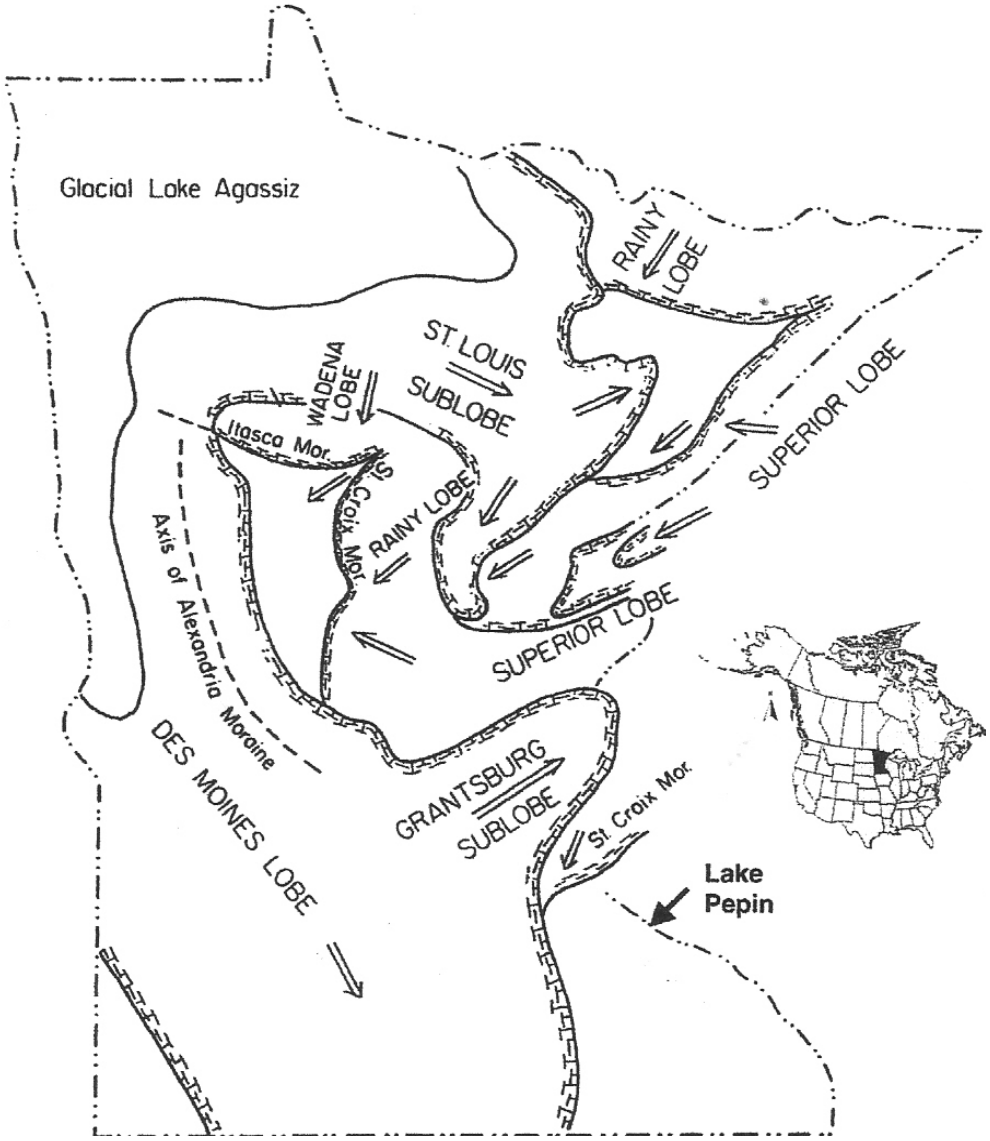

Fig. 1.2 Map showing the extent of ice lobes of the Laurentide ice sheet in Minnesota during the last glaciation, as well as the Minnesota portion of Glacial Lake Agassiz (Wright, 1993).

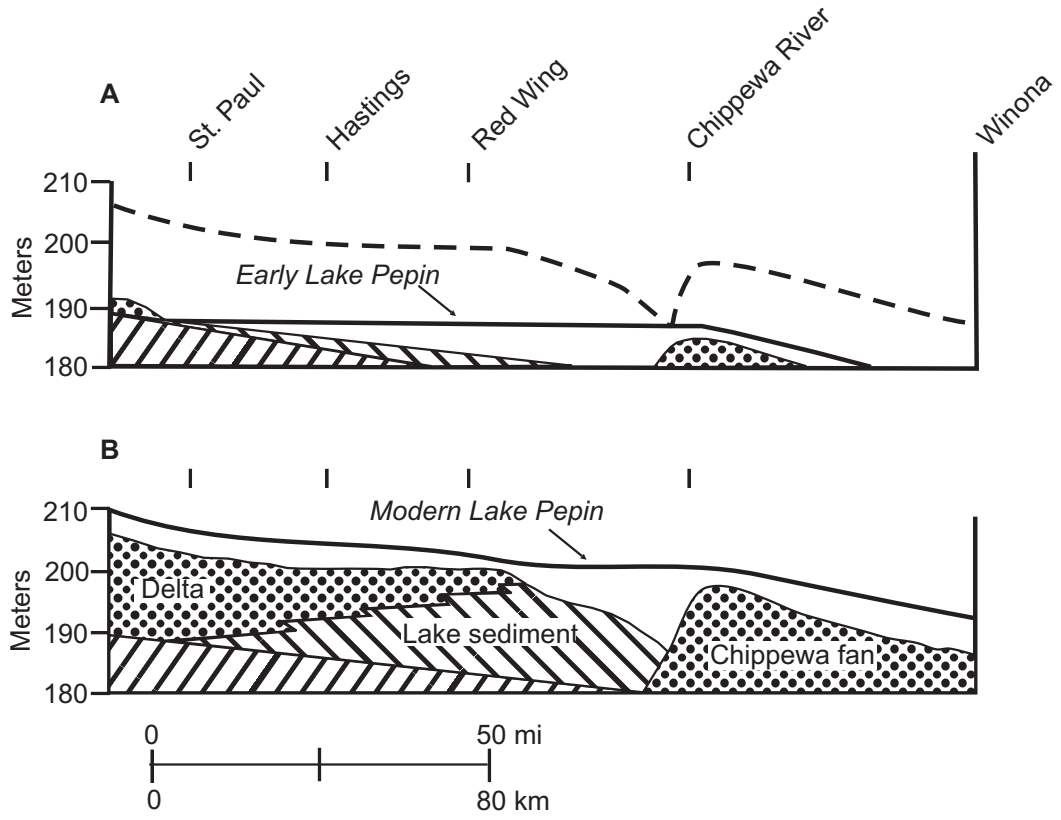

Fig. 1.3 Progression of the Mississippi River delta into Lake Pepin. From Zumberge, 1952.

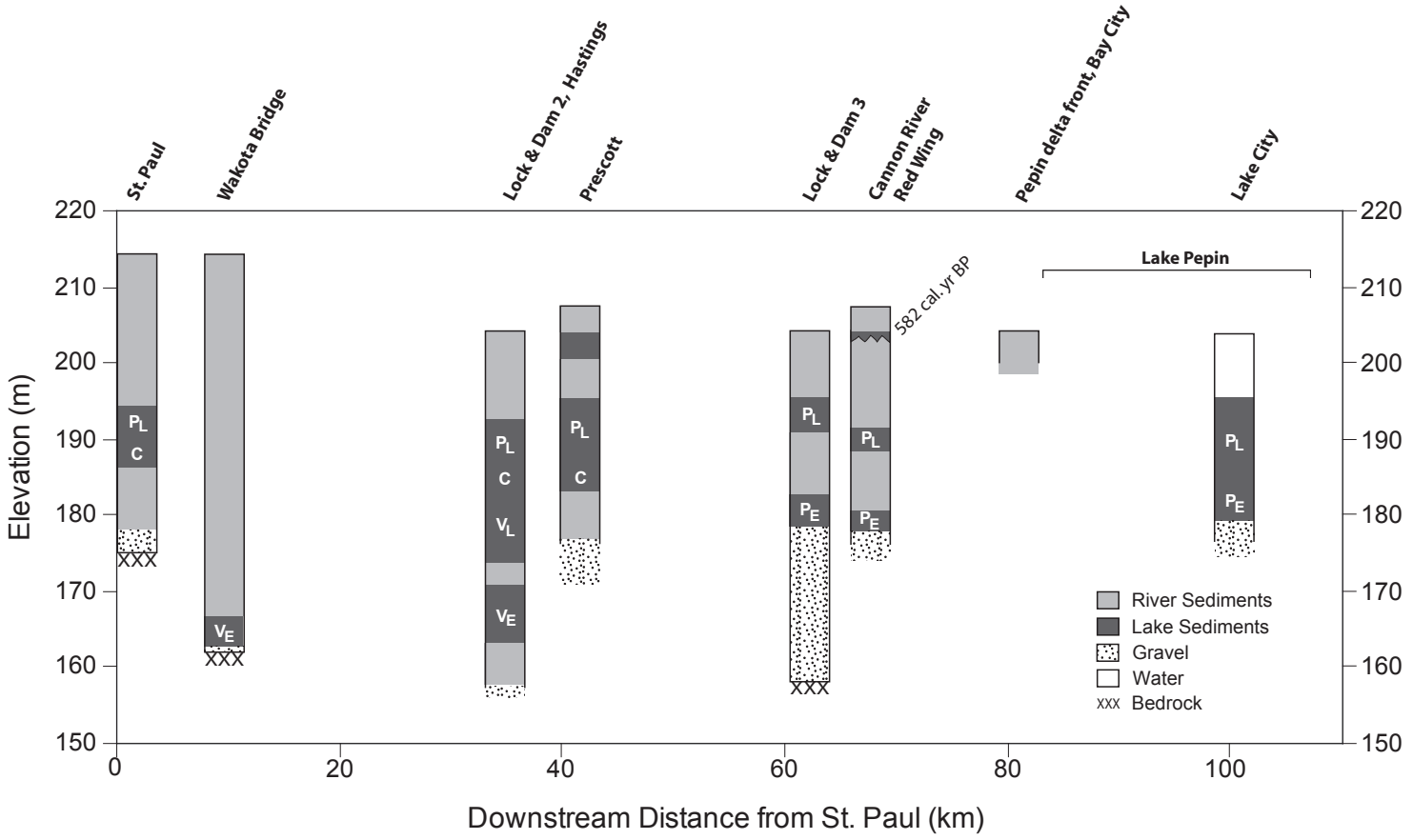

Fig. 1.4 Sediment stratigraphy in borings from the surface of the Mississippi River floodplain. The lake phases in each boring are as follows: V_E is Early Lake Vermillion, V_L is Late Lake Vermillion, C is Lake Cannon, P_E is Early Lake Pepin, and P_L is Late Lake Pepin. Lake layers not labeled are from a single bore at that location and may be a floodplain deposit.

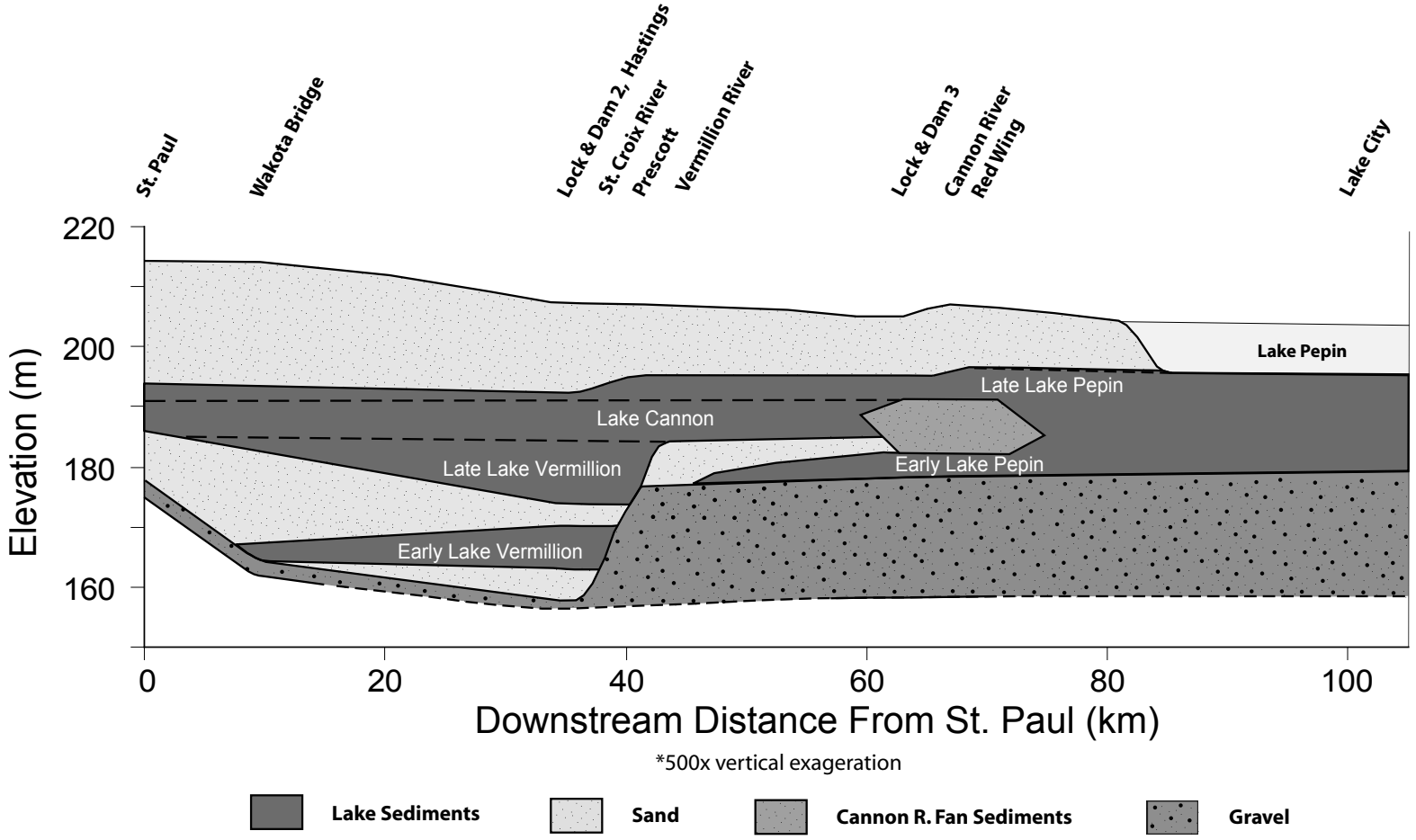

Fig. 1.5 Longitudinal profile of Mississippi River floodplain sediments from St. Paul to Lake City showing various stages of lake development.

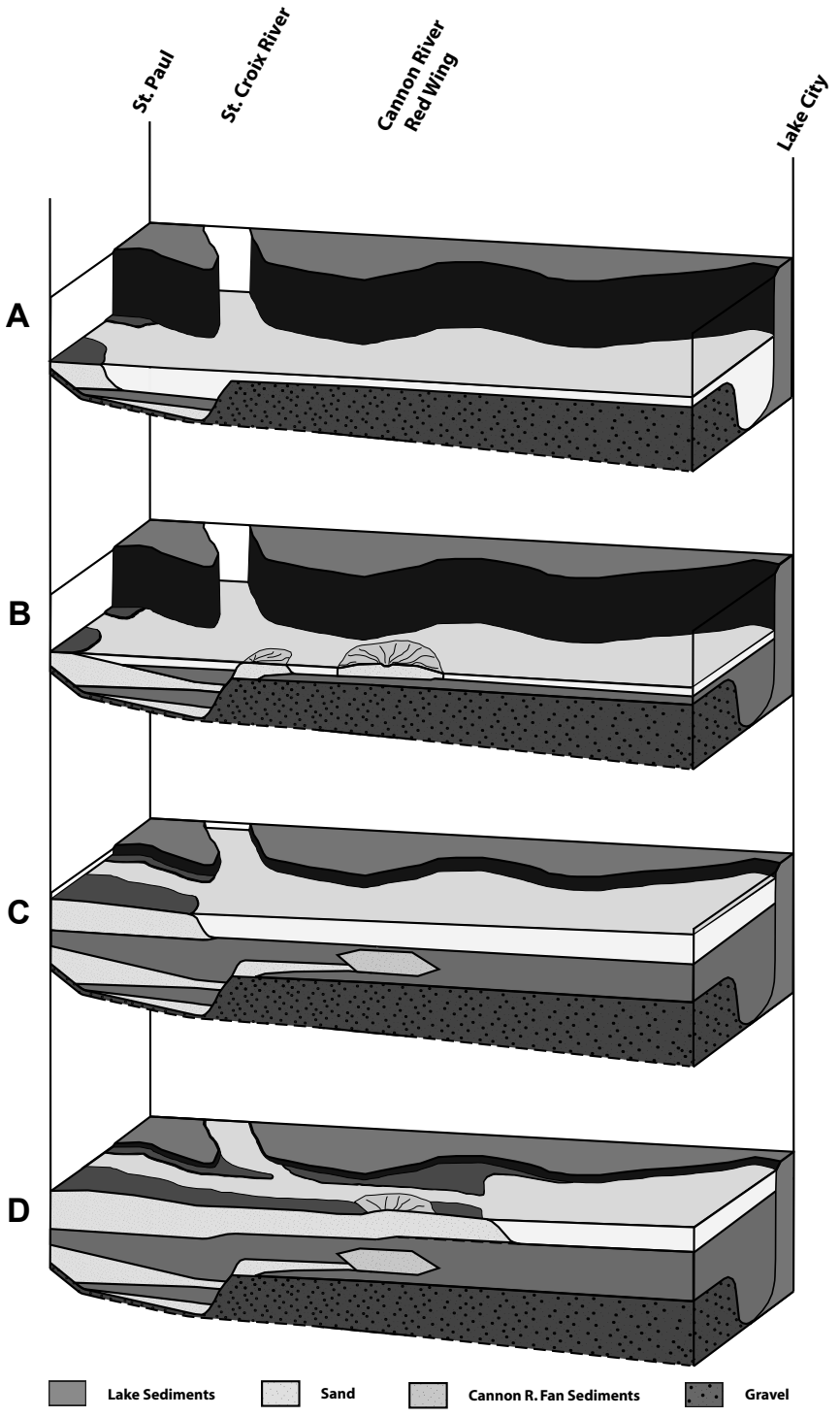

Fig. 1.6 Block diagrams showing relations during the existence of (A) early Lake Vermillion with incipient Lake St. Croix, (B) later Lake Vermillion, Lake Cannon, and early Lake Pepin, (C) later Lake Pepin and later Lake St. Croix, and (D) modern Lake Pepin/Lake St.Croix with Douglas Point at the mouth of Lake St. Croix.

Chapter 2: A novel repeat-coring approach to reconstruct recent sediment, phosphorus, and mercury loading from the upper Mississippi River to Lake Pepin, USA

Dylan J. Blumentritt[1], Daniel R. Engstrom[2], Steven J. Balogh[3]

[1]*Department of Earth Sciences, University of Minnesota, Minneapolis, MN, USA*

[2]*St. Croix Watershed Research Station, Science Museum of Minnesota, St. Paul, MN, USA*

[3]*Metropolitan Council Environmental Services, St. Paul, MN, USA*

Reprinted from the Journal of Paleolimnology, DOI 10.1007/s10933-013-9724-8,

It can be advantageous to revisit coring locations in lakes years after an initial paleolimnological study is completed, to assess environmental changes in the intervening time interval. We revisited sediment core sites in Lake Pepin (Minnesota, Wisconsin) more than a decade after an original set of 10 cores was collected, dated radiometrically, and studied in 1996. Prominent magnetic susceptibility features were used to align the new core set with the older set, such that traditional radiometric dating was not necessary to obtain a chronology for the new cores. The procedure used to align the two core sets accounted for compaction of former surface sediments by burial with new sediment. The amount of new sediment, mercury, and phosphorus accumulated at each core site was determined and extrapolated to the depositional area of the lake to estimate recent (1996-2008) whole-basin loads. Recent sediment accumulation in Lake Pepin compared well (within 3%) with monitored inflow data from a gauging station on the upper Mississippi River just before it enters the lake. Bulk sediment accumulation rate remained very high (772,000 t/yr) for the recent period (1996–2008), down slightly from the peak in 1990–1996 (876,000 t/yr), and almost an order of magnitude above pre-settlement rates. Total phosphorus deposition remained constant since a peak in the 1960s, but was also well above pre-settlement rates. Mercury continued its precipitous decline since peaking in the 1960s.

Keywords: Lake Pepin • Mississippi River • Dating • Repeat-core • Sediment accumulation

2.1 Introduction

Sediment cores have been used extensively to study environmental changes in lakes and their watersheds. In many cases it may be desirable to revisit a previously studied lake system to build on prior work. Conditions may then be determined to have improved or deteriorated as a result of land use change, in-lake manipulations, climate, or other natural forces. Bennion and Battarbee (2007) recommend re-coring as a cost-effective way to measure the effectiveness of management efforts in a lake watershed. Other studies have re-cored varved lakes to assess carbon and nitrogen (C and N) loss over time (Gälman et al., 2008), as well as mercury stability (Rydberg et al., 2008) and ^{137}Cs diffusion (Klaminder et al., 2012) in the sediment record. Re-core efforts have been used in non-varved lake systems to assess post-burial C diagenesis (Hodell and Schelske, 1998) and the impacts of hurricanes on lake sediment profiles (James et al., 2008; Liu and Fearn, 1993).

Significant challenges arise when attempting a re-core study. Sediment re-coring hinges on the ability to accurately and precisely match the new cores to the old cores stratigraphically, so a reliable marker is imperative for this method in non-varved systems. Various approaches have been used for cross-correlation among cores, including non-destructive, whole-core scans of magnetic susceptibility (Birks and Birks, 2006; Thompson et al., 1975; Thompson et al., 2012), diatom biostratigraphy (Battarbee, 1978), pollutant markers (e.g. spheroidal carbonaceous particles (SCPs); (Rose and Yang, 2007), and lithostratigraphy (Rippey et al., 2008). As with all sediment-core studies, accurate dating is a concern. If, however, the original cores were well-dated and the re-

core study is done shortly after the original study, which is the case here (12 years), dates can be assigned to the re-core profiles with sufficient chronological resolution and without the need for further radiometric dating. It is also important to be able to relocate the original sediment core positions with a high degree of certainty. GPS technology enables identifying previous core locations to within several meters. Finally, it is necessary to account for compaction and dewatering of older sediment as it is buried by newer sediment over time.

The aim of this study was to demonstrate the utility of the re-core approach in a multiple-core analysis of whole-lake sedimentation in a large riverine lake. We: (1) developed a novel method for cross-correlating and dating repeat core records in non-varved lake sediments so that re-core efforts can build upon the existing chronology of previous studies with minimal effort; (2) measured the mass accumulation of sediment, phosphorus (P), and mercury (Hg) over a recent 12-year period (1996-2008) in Lake Pepin, a natural impoundment of the upper Mississippi River, and determined if there had been reductions in river loads as a consequence of changing agricultural practices, wastewater treatment, precipitation, or river flows; and (3) estimated recent whole-lake sediment accumulation rates, based on multiple cores, and compared those rates with monitoring data to assess the accuracy of the multi-core approach.

2.1.1 Study area

The Lake Pepin watershed comprises three large river systems, the St. Croix, Minnesota, and headwater Mississippi rivers (Fig. 2.1). Combined, they drain 122,000

km^2, including the southern half of Minnesota and parts of Wisconsin and the Dakotas. The Minnesota River joins the Mississippi in St. Paul, and the confluence with the St. Croix River is 40 km downstream from there. These three major rivers converge and flow through Lake Pepin, which occupies a wide, slow portion of the Mississippi River along a reach that borders southeastern Minnesota and western Wisconsin. Lake Pepin has a surface area of 103 km^2, an average width of 3 km, a mean depth of 5.4 m, a maximum depth of 18 meters near the outlet (transect V), and stretches 34 km from northwest to southeast, with two sweeping bends (Fig. 2.1). Water residence time varies from around 6 days during high flow to 47 days during low flow (Heiskary and Vavricka, 1993). About 80–90% of the sediment deposited in Lake Pepin comes from the Minnesota River basin (Kelley et al., 2006; Kelley and Nater, 2000). An analysis of sediment cores taken from Lake Pepin in 1996 indicated that sediment accumulation rates had increased by almost an order of magnitude since Euro-American settlement in the region (*ca.* 1830) (Engstrom et al., 2009). During that time, most of the Minnesota River basin was converted from native prairies and wetlands to agricultural land use, which now comprises 78% of the basin (Musser et al., 2009).

The Lake Pepin watershed has also undergone a large population increase, especially in the Twin Cities metropolitan area (seven counties surrounding Minneapolis and St. Paul), which today has 2.9 million people, compared to 1.0 million people in 1940 (Gumus-Dawes, 2012). Effluent from the Metropolitan Wastewater Treatment Plant (Metro Plant), which serves 63% of residents in the Twin Cities area, is released into the Mississippi River above Lake Pepin. In 1974, 40% of the phosphorus entering Lake

Pepin was from wastewater treatment plants in the Minneapolis/St. Paul metropolitan area (Mulla and Sekely 2009). By the mid-1990s this waste load was reduced to 30%, with much of the decrease attributed to the ban on phosphate detergents in 1976 and the implementation of advanced secondary treatment at the Metro Plant in 1984 (Johnson and Aasen, 1989). Further improvements were made to the Metro Plant in 2005, integrating biological P-removal into the secondary treatment process, further reducing the effluent P load to approximately 140 t yr^{-1} (10% of the total phosphorus load to Lake Pepin).

2.1.2 Geologic history

Lake Pepin is a unique natural impoundment in that its sediments record the environmental history of more than half the state of Minnesota over the past 11,000 years (Blumentritt et al., 2009; Engstrom et al., 2009; Wright et al., 1998). This depositional basin provides the opportunity to estimate natural "background" rates of sediment accumulation and to track erosion and nutrient loading brought about by land-use changes that began with Euro-American settlement in the region more than 150 years ago.

The geomorphic history of the upper Mississippi River and Lake Pepin is described in detail by Blumentritt et al. (2009); briefly, the Des Moines Lobe of the Laurentide ice sheet retreated into Canada following its maximum, and a large pro-glacial water body, Lake Agassiz, formed in western Minnesota. The southern outlet of Lake Agassiz drained through what is now the Minnesota River valley and eventually the Mississippi River valley below its confluence in St. Paul, and ultimately into the Gulf of Mexico. That high-discharge river, Glacial River Warren, flowed intermittently from the

inception of Lake Agassiz 11,800 ^{14}C yr B.P. (13,700 cal yr) (Lepper et al., 2007; Shay, 1967) until the southern outlet was abandoned 9,400 ^{14}C yr B.P. (10,600 cal yr) (Fisher, 2003b). Subsequently, the Chippewa River began depositing its sediment load in the Mississippi River valley and created a natural riverine impoundment, Lake Pepin.

2.2 Materials and methods

2.2.1 Sediment coring

Sediment cores were collected from ten widely spaced locations along the flow-path of Lake Pepin (Fig. 2.1). These sites, among a total of 25 locations, had been cored in 1996 to reconstruct whole-lake accumulation rates for sediments, phosphorus, and metal contaminants (Balogh et al., 2009; Balogh et al., 1999; Engstrom et al., 2009). The sites selected for re-coring were those from which the most intensively analyzed cores, i.e. "primary" cores, were taken in previous studies. The original cores were dated using radiometric ^{210}Pb, ^{137}Cs, and ^{14}C techniques, along with pollen. Dating uncertainty, spatial variability, and the calculation of whole-lake accumulation rates were described in detail in Engstrom et al. (2009). We revisited three of the coring locations (II.3, IV.2, and V.1) in July 2006 and the remaining seven (I.2, I.3, II.1, III.2, III.4, IV.2, and V.4) in June 2008 (Fig. 2.1). Coordinates for the 1996 cores were determined precisely by differential GPS, so each new core location was located to within several meters of the original site using an on-board GPS unit.

Sediments were collected using a piston corer fitted with a 2-m-long, 7-cm-diameter polycarbonate tube. The top 14–20 cm of each core was sectioned in the field at

2-cm intervals and the remaining length was transported to the laboratory and scanned for magnetic susceptibility using a Geotek Multi-Sensor Core Logger. Cores were then split lengthwise into two halves; one half was stored at the National Lacustrine Core Facility (LacCore) at the University of Minnesota, and the other half was taken to the St. Croix Watershed Research Station where it was sectioned at 2-cm intervals. An aliquot of wet sediment was weighed, dried and re-weighed to estimate percent dry mass and water content. Next, organic matter content in dry sediment was estimated by weight loss on ignition (LOI) (Dean, 1974; Heiri et al., 2001). Remaining portions of each interval were placed in polypropylene jars and freeze-dried.

2.2.2 Core stratigraphic correlation and accumulation rates

Varves and other laminations have been used successfully to cross-correlate repeat cores from the same location by aligning distinctive sequences (Gälman et al., 2006; Rydberg et al., 2008). Because Lake Pepin sediments are visually homogenous, new cores were stratigraphically matched to their older counterparts using prominent excursions in magnetic susceptibility. These susceptibility features are typical in lakes where land use disturbances have increased erosion of surface soils (Eriksson and Sandgren, 1999; Thompson et al., 1975; Triplett et al., 2009). Six of these features are traceable across the entire Lake Pepin basin. Four date from *ca.* 1830 to 1964, whereas two others predate Euro-American settlement (Engstrom et al., 2009). Although we chose to use magnetic susceptibility for core correlation, our approach is equally

applicable using other immobile stratigraphic markers, provided sufficient resolution is achieved.

A major obstacle in determining the amount of new sediment at any core location is accounting for compaction and dewatering of sediment that was once at the sediment surface, but has been subsequently buried by more recent deposition. Because each core has a different amount of new sediment, there are varying degrees of compaction. To account for variable compaction, cores were aligned using the most recent and prominent magnetic features to determine the linear depth offset (Fig. 2.2). These features ranged in depth from 80 cm in the lower accumulation zones at the downstream end of Lake Pepin to 160 cm in the higher accumulation zones of the upstream end of the lake. All were well below the effects of compaction resulting from new sediment overburden. The inventory of inorganic dry mass, established from LOI measurement, was determined above the tie point in both the original core and the new core at each location. The amount of new sediment is simply the difference between masses (Fig. 2.3). The average accumulation rate for the period between coring expeditions (1996–2008) was calculated by dividing the dry mass of newly deposited sediment by the time elapsed. The accumulation rate of each core was extrapolated to an assigned area of the accumulation zone for that particular core, roughly one tenth of the Lake Pepin depositional area, using the same delineation employed by Engstrom et al. (2009). Mass accumulation rates for each core area were summed to estimate the whole-basin sediment accumulation rate. These recent (1996-2008) accumulation rates were compared to previous rates estimated by Engstrom et al. (2009) for the time periods 1980-1990 and 1990-1996.

2.2.3 Phosphorus and mercury analysis

For each of the ten "primary" cores, seven of the previously sectioned discrete intervals were selected at evenly spaced intervals for total phosphorus (TP) and mercury (Hg) determination; five were from post-1996 sediment, whereas two deeper intervals overlapped with the older core set. These overlapping samples were intended to approximate TP and Hg values between the two core sets, as sampling intervals did not match precisely. All intervals were 2 cm except the three cores with the highest accumulation rates (I.2, I.3, and III.2); those samples were composed of two amalgamated intervals to create a 4-cm sample interval. The mean TP and Hg concentration in each core was calculated as the arithmetic mean of the amalgamated samples from 1996 to 2008. Recent (1996–2008) accumulation rates were calculated by multiplying the mean TP and Hg concentration in each core by the recent sediment accumulation rate.

Phosphorus extractions followed procedures adapted from Engstrom and Wright (1984). Freeze-dried samples were reacted sequentially with 30% H_2O_2 and 0.5M HCl to convert all P to phosphate, and extracts were measured using the ascorbic-acid method on a Lachat Quikchem 8000 flow-injection autoanalyzer. Extraction temperatures were maintained in a hot-water bath, and extracts were separated from sediment residue by centrifugation. All dilutions were done according to weight on an electronic balance. TP check standards were within 5% of expected concentrations, and the mean relative percent difference between method duplicate (n = 6) and instrument duplicate (n = 7)

analyses was < 2%. Matrix spike recoveries averaged 94% (n = 3), and blank (n = 3) concentrations were below detection limits.

Mercury concentrations were determined by cold vapor atomic fluorescence spectrometry with single gold trap amalgamation according to methods outlined in Balogh et al. (1999). Two certified reference materials (BCR-320 River Sediment and MESS-3 Marine Sediment) were analyzed along with the Pepin samples. Mean concentrations of total Hg were 1,025 ng g^{-1} in BCR-320 (n=9; relative standard deviation (RSD) = 6%; certified value = 1,030 ng g^{-1}) and 89 ng g^{-1} in MESS-3 (n = 5; RSD = 2%; certified value = 91 ng g^{-1}). Matrix spike recoveries averaged 103% (n = 5), and the mean RSD of five separate triplicate analyses was 3%. Blank concentrations were below our method detection limit of 2 ng g^{-1}.

2.2.4 River monitoring

Total suspended solids (TSS), volatile suspended solids (VSS), and TP have been continuously measured on a weekly basis since 1980 by Metropolitan Council Environmental Services (MCES) at Lock and Dam 3, approximately 15 km upstream of Lake Pepin. Data were compiled and annual loads calculated by MCES staff using Flux32 software (Walker, 1999). In this study, we compared Lake Pepin sediment records (composed of fine-grained silts and clays) to suspended loads (TSS), because it is that fraction of the total sediment load in the river that is delivered to the depositional area of the lake. The bedload fraction of the river sediment (sand and coarser particles) is

preferentially deposited in the delta of the Mississippi River at the head of Lake Pepin and is therefore not considered here.

2.3 Results

Magnetic susceptibility profiles from recent cores (2006, 2008) matched well with earlier (1996) cores at almost all core sites. Transects II through V have good alignment on the basis of prominent magnetic features, ranging in depth from approximately 160 cm in transect II to 80 cm in transect V (Fig. 2.2). Recent cores from transect I did not reach the depth of these prominent magnetic susceptibility excursions. Visual alignment was instead applied to the smaller features throughout the overlapping portion of the cores. Overall, this method provides an excellent way to align overlapping sediment cores taken at different times, especially where there are prominent features in the magnetic susceptibility profile.

Based on core-matching from magnetic susceptibility profiles, the two core sites in the upstream end of Lake Pepin had the most new sediment from 1996 to 2008; site I.2 had 40 cm of new sediment and site I.3 had 41 cm (Fig. 2.2). The two cores from transect II were quite consistent in the amount of new sediment; site II.1 had 22 cm and II.3 had 24 cm. Site III.4 had the least amount of new sediment (8 cm), but that was balanced within the transect by core III.2, which had 32 cm. Core sites IV.2 and IV.4 had 20 cm and 17 cm of new sediment, respectively. And in the lowermost accumulation zone, site V.1 had 18 cm and site V.4 had 13 cm of new sediment.

Sediment dry-mass accumulation (DMA) rates decline progressively from the upstream end of Lake Pepin to the downstream end. Present-day DMA ranges from 21 kg m^{-2} yr^{-1} in the upper lake transect (average of cores I.2 and I.3) to 4.5 kg m^{-2} yr^{-1} in the lower lake transect (average of cores V.1 and V.4) (Fig. 2.4A). DMA decreased between the 1990–1996 and 1996–2008 time intervals in all but two cores, with the greatest decreases occurring in the upper portion of the lake at core sites I.2 and II.1. DMA decreased from 32 to 21 kg m^{-2} yr^{-1} at I.2 and from 15 to 9.4 kg m^{-2} yr^{-1} at II.1. Proportionally, the greatest decreases occurred at mid-lake site III.4 (from 6.9 to 2.6 kg m^{-2} yr^{-1}; a 62% decline) and site V.4 (from 5.1 to 2.6 kg m^{-2} yr^{-1}; a 49% decline). Cores II.3 and V.1 are the two sites where DMA increased between 1990–1996 and 1996–2008. DMA rates rose from 9.6 to 12 kg m^{-2} yr^{-1} in core II.3 and from 5.0 to 6.3 kg m^{-2} yr^{-1} in core V.1. Extending these core-specific accumulation rates to the entire depositional area of the lake, Lake Pepin accumulated sediment at an estimated rate of 772,000 metric tons per year (t yr^{-1}) in the interval 1996–2008, which represents a 12% decrease from 876,000 t yr^{-1} in the period 1990–1996 (Fig. 2.5A). The corresponding mean areal rates estimated for the depositional zone are 10.4 kg m^{-2} yr^{-1} in 1996–2008 vs. 11.7 kg m^{-2} yr^{-1} in 1990–1996. These core-based loads correspond closely with estimates derived from direct TSS monitoring, differing from one another by less than 3% for the intervals 1980–1990 and 1996–2008 (Fig. 2.6). The largest difference, for the period 1990–1996, is <15%.

Total phosphorus (TP) concentrations were relatively similar among cores and remained fairly constant between the two most recent time periods, neither increasing nor

decreasing significantly. Thus, whole-basin TP accumulation rates followed a spatial pattern similar to that for DMA, highest in cores from transect I in the upper end of the lake (19.1 g m^{-2} yr^{-1}) and decreasing progressively downstream, although cores from transect V (6.1 g m^{-2} yr^{-1}) were slightly higher than those in transect IV (4.2 g m^{-2} yr^{-1}). Of the ten cores, II.1, II.3, and V.1 increased in TP, with the largest increase at core site II.3, which rose from 10 to 14 g m^{-2} yr^{-1} (Fig. 2.4B). Core sites I.2 and III.4 displayed the largest decreases in TP accumulation, declining from 26 to 19 g m^{-2} yr^{-1} and 10 to 3 g m^{-2} yr^{-1}, respectively. When these core-specific TP fluxes are extrapolated to the entire lake, whole-lake TP loads declined 8%, from 920 t yr^{-1} (1990–1996) to 845 t yr^{-1} (1996–2008) (Fig. 2.5B).

In all cores, mercury (Hg) concentrations decreased between 1990–1996 and 1996–2008. The greatest drop occurred in core V.1, which decreased from 194 to 135 ng g^{-1}. In the remaining nine cores, Hg concentrations decreased 15% (σ = 5%), on average. Hg accumulation at each core location followed trends similar to DMA and TP accumulation rates (Fig. 2.4C). Hg fluxes were highest in the upper end of Lake Pepin (2.1 mg m^{-2} yr^{-1}, average of cores I.2 and I.3) and decreased in the downstream direction to 0.58 mg m^{-2} yr^{-1} (average of cores V.1 and V.4) in the lowermost transect. One exception to this trend is average fluxes in transects III and IV were identical (0.77 mg m^{-2} yr^{-1}). Two cores, II.3 and V.1 increased slightly (< 0.16 mg m^{-2} yr^{-1}), while the remaining eight cores decreased (between 0.18 and 1.56 mg m^{-2} yr^{-1}) from 1990–1996 to 1996–2008. The largest decline occurred at core site I.2; it decreased from 3.64 mg m^{-2} yr^{-1} in 1990–1996 to 2.08 mg m^{-2} yr^{-1} in 1996–2008. Proportionally, the greatest

decreases occurred at sites III.4 and V.4, which decreased 68% and 62%, respectively. Over the entire depositional area of the lake, the average Hg flux decreased by 24%, from 1.1 mg m^{-2} yr^{-1} (1990–1996) to 0.84 mg m^{-2} yr^{-1} (1996–2008). Thus, whole-basin Hg loads have declined from 110 kg yr^{-1} (1990–1996) to 85 kg yr^{-1} (1996–2008) (Fig. 2.5C), a decrease that is substantially larger than the corresponding 12% decrease in DMA for the same time period.

2.4 Discussion

2.4.1 Sediment accumulation

Long-term, direct TSS monitoring data from Lock and Dam 3 above Lake Pepin are in good agreement with sediment loads calculated from Lake Pepin sediment cores (Fig. 2.6). A previous mass balance study estimated only 50% TSS retention (Maurer et al., 1995), however, recent estimates indicate that Lake Pepin retains approximately 80% of entering TSS (James and Barko, 2004; Lafrancois et al., 2009). If 80% of the incoming TSS load is retained in Lake Pepin, the discrepancy between TSS and lake sediments should match this difference, which it does in 1990–1996. But in the other two time periods (1980–1990 and 1996–2008) it does not; TSS loads and sediment accumulation are more similar (<3% difference) than expected (Fig. 2.6).

The above comparison, however, does not take into account in-lake production of organic matter, carbonate, and other authigenic materials. Since 1980 the organic fraction has made up about 10% of the total load to Lake Pepin (as calculated from the sediment cores), whereas organic matter accounts for almost 20% of the suspended

sediment load measured at Lock and Dam 3. When organic matter, estimated by LOI, is subtracted from both the Pepin core records and TSS measurements, the two load estimates from 1990–1996 are within 2%; for the periods 1980–1990 and 1996–2008, the two estimates are within 12% and 9%, respectively. Triplett et al. (2008) calculated that 30,000 (±17,000) t yr^{-1} of biogenic silica, primarily in the form of diatom frustules, are produced in-lake during normal-flow years and contribute to the inorganic fraction in sediment cores. As a result, in-lake silica production would account for 4 (± 2)% of the recent sediment accumulation in Lake Pepin. Calcium carbonate, as measured in the cores, has composed 12-16% of the total sediment since 1980. Unfortunately, there are no continuous measurements of $CaCO_3$ in suspended sediment at Lock and Dam 3, so load comparisons between suspended sediment delivery and lake deposition are not possible, and $CaCO_3$ is combined with the inorganic fraction when comparing sediment deposition in Lake Pepin to in-coming river loads.

Coherence between recent sediment loads measured directly in the Mississippi River and sediment loads estimated from Lake Pepin sediment cores (with or without correction for organic matter) is quite good, indicating that Lake Pepin is an effective trap and accurate recorder of suspended sediment in the river. This comparison validates the multiple core strategy, including number of cores, core placement, and delineation of depositional areas implemented by Engstrom et al. (2009) in the original study. Furthermore, this comparison to modern suspended loads lends support to the claim that historical sediment loads measured in this suite of Lake Pepin cores accurately reflect suspended sediment loads in the river.

The current (1996–2008) sediment loads are in line with the overall historical increase during the last century (Fig. 2.5A). A decrease in accumulation, however, occurred relative to the preceding time interval, from 876,000 t yr^{-1} in 1990–1996, to 772,000 t yr^{-1} in 1996–2008. The likely explanation for the relative peak in the 1990–1996 accumulation rate is an increase in mean annual flow to 22,500 million m^3 yr^{-1} during that period, which was approximately 20% higher than that of the preceding decade (18,700 million m^3 yr^{-1} in 1980–1990) or the 12 years following (18,900 million m^3 yr^{-1} in 1996-2008) (Fig. 2.6).

2.4.2 Phosphorus

The current (1996–2008) whole-basin TP loading rate (845 t yr^{-1}) is similar to that in each of the previous three time intervals (828 t yr^{-1} in 1970–1980, 834 t yr^{-1} in 1980–1990, and 920 t yr^{-1} in 1990–1996), but is significantly lower than the peak in 1960–1970 (1,051 t yr^{-1}) (Fig. 2.5B). Phosphorus loads deposited in Lake Pepin, however, are not accurate measures of loads in the Mississippi River because the retention rate is quite low. Comparison of sediment data with recent TP loads measured at Lock and Dam 3 near the head of Lake Pepin indicates that from 1980 to 2008, on average, between 20 and 30% of phosphorus inputs are retained in Lake Pepin sediments. James and Barko (2004) suggest that this low retention rate is largely a consequence of diffusive P fluxes from bottom sediments and partitioning to aqueous P phases that are readily exported because of the short hydraulic residence time in the lake. Our sediment-based retention rates compare reasonably well with previous estimates of 13-25% based solely on inflow

and outflow measurements (James and Barko, 2004; Lafrancois et al., 2009; Maurer et al., 1995).

Since 2005, the average annual TP load (250 t yr^{-1}) from all wastewater treatment plants in the Twin Cities metropolitan area, including the Metro Plant, accounts for only 11% of the annual load entering Lake Pepin (2,217 t yr^{-1}). Despite these significant post-1970 improvements to wastewater treatment, TP accumulation in Lake Pepin has remained relatively constant (Fig. 2.5B). Since the retention rate of phosphorus has not changed significantly in Lake Pepin during this time period (Engstrom et al., 2009), it is likely that increases in non-point sources, which have followed the increasing trend of suspended sediment, have balanced the decrease in point sources (Mulla and Sekely, 2009).

2.4.3 Mercury

Whole-basin total Hg fluxes in Lake Pepin for the re-core period (1996–2008) were 0.84 mg m^{-2} yr^{-1}. This flux is almost two orders of magnitude greater than the present-day atmospheric Hg deposition (0.011 mg m^{-2} yr^{-1}) calculated by Drevnick et al. (2012) from 44 inland lakes in the western Great Lakes region, primarily in Minnesota, and from nine sediment cores taken in Lake Superior (0.010 mg m^{-2} yr^{-1}). Considering that atmospheric Hg deposition peaked at 0.013 mg m^{-2} yr^{-1} around 1980 (Drevnick et al., 2012), which is still less than 2% of the current Hg flux to Pepin, atmospheric Hg is not the primary driver of Hg loading to Lake Pepin.

Based on the sediment accrual in Lake Pepin, whole-basin Hg accumulation has declined from 110 kg yr^{-1} in 1990–1996 to 85 kg yr^{-1} in 1996–2008 (Fig. 2.5C). Mercury accumulation in Lake Pepin sediments remains well above the accumulation rate of 3 kg yr^{-1} prior to Euro-American settlement, but loads have been reduced significantly since they peaked at 357 kg yr^{-1} in the 1960s (Balogh et al., 1999). In their analysis of the Hg record in Lake Pepin, Balogh et al. (1999) attributed the major decline in Hg loads to wastewater treatment advances that were implemented at the Metro Plant in St. Paul and reductions from other industrial point sources. Recent data indicate that the Metro Plant discharges only 2 g day^{-1}, or 0.73 kg yr^{-1} (Balogh and Nollet, 2008), less than 1% of the 85 kg yr^{-1} currently accumulating in Lake Pepin. Thus the majority of Hg accumulating in Lake Pepin today is from non-point sources, principally erosion of soils and their associated burden of atmospheric Hg. This means that the 23% reduction in Lake Pepin Hg loads from 1990–1996 to 1996–2008 is likely tied to the 12% reduction in DMA during those same time periods. It is unclear, however, why the recent Hg reduction is proportionally greater than the DMA reduction, though perhaps some of the major non-point source is legacy Hg that is trapped in floodplain sediments, deposited when point-source loads and sediment concentrations were much higher. Thus, the recent decline in Hg inputs to Lake Pepin may be a result of natural cleansing of floodplain sediments by the river itself.

Alternatively, changes in erosion sources may have contributed to the decrease in non-point Hg loads. Non-field erosion (from stream banks, bluffs, and ravines) is currently the major source of sediment to Lake Pepin (Schottler et al., 2010), and these

sources have minimal exposure to atmospheric deposition and are low in Hg (and other atmospheric tracers), compared to field soils that are enriched in Hg from prolonged exposure. A decrease in field erosion owing to improved agricultural practices could have reduced Hg inputs to the river. If partially offset by increased non-field erosion, total DMA rates would show a much smaller reduction, as we observed.

2.5 Conclusions

We demonstrated a novel repeat-coring approach to establish recent sediment, TP, and Hg accumulation rates, one that requires only a single marker at a depth below the effects of compaction. In the case of Lake Pepin, we used the magnetic susceptibility profile, which features a prominent excursion that begins in the early 19th century. Good agreement between our estimated whole-basin sediment accumulation in Lake Pepin and direct measures of TSS loads in the Mississippi River validates the accuracy of this approach. Because the proposed method relies on just two dates, i.e. the date of the sediment surface in the original and repeat-cores at the time of core collection, it yields only an average accumulation rate between the two coring dates. Analysis of ^{210}Pb on sediments deposited between the first and second coring efforts could, however, provide greater dating resolution if needed.

Multiple-core lake studies are valuable for mass-balance estimates of sediment, nutrients, and contaminant loads (Birks and Birks, 2006; Brenner et al., 2001; Brezonik and Engstrom, 1998; Engstrom and Rose, 2013; Engstrom et al., 2009; Hiriart-Baer et al., 2011). This approach is imperative in Lake Pepin where deposition rates vary by an order of magnitude across the basin. The utility of sediment re-core efforts is also

apparent. Following an initial paleo-assessment, the re-core method outlined above allowed us to track the effectiveness of management efforts to improve water quality. In Lake Pepin, Hg accumulation has declined, whereas only modest improvements in sediment and TP deposition have occurred over the past decade, despite significant remediation efforts. Dating repeat sediment cores using immobile stratigraphic markers allowed us to re-visit Lake Pepin and track recent environmental trends. This re-core method can be similarly applied to other systems to monitor water quality trends, provided a chronology was established during the initial paleo-study and the sediments contain suitable stratigraphic markers.

Figures

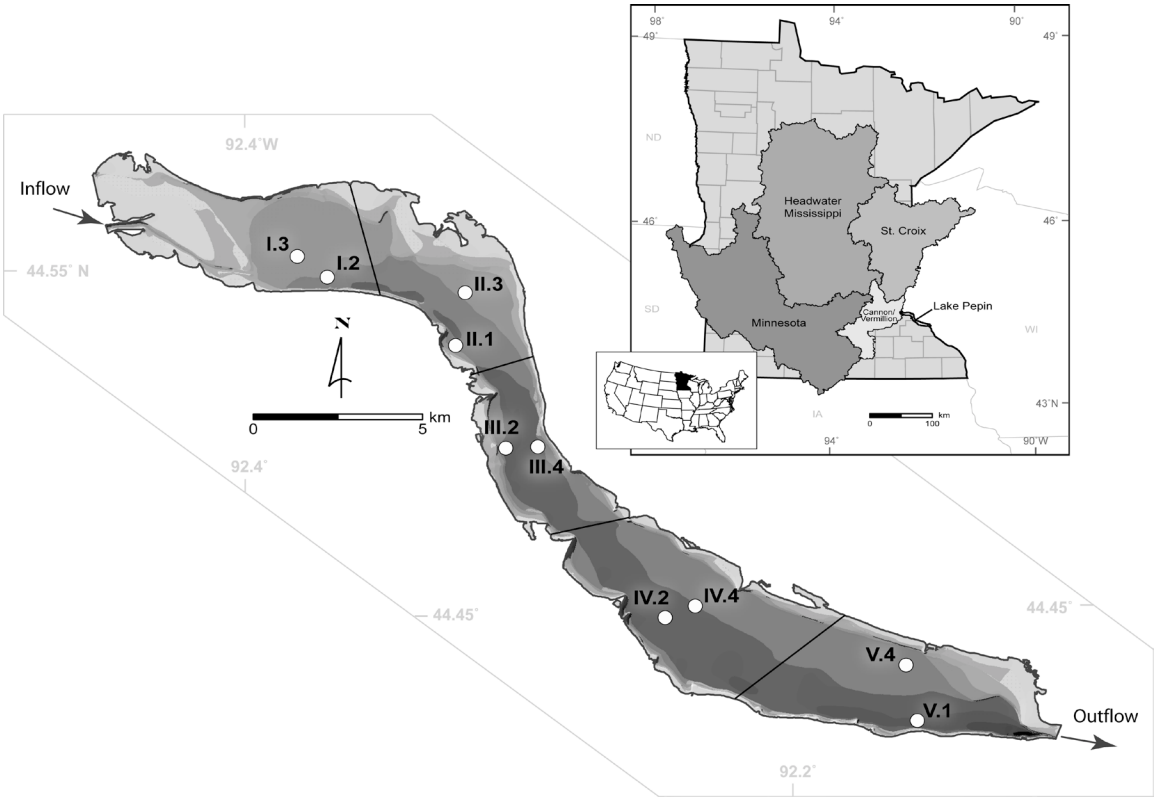

Fig. 2.1 Location of core sites in Lake Pepin, a natural riverine lake located on the border of Minnesota and Wisconsin, USA. Core transects are indicated by a Roman numeral followed by the core number for that transect. Sub-basins represented by each core transect are delineated. Lighter shades represent shallow non-depositional areas of the lake, and darker shades are deeper portions. The Lake Pepin watershed (inset) is 122,000 km^2 and comprised of three main river basins, the Minnesota, headwater Mississippi, and St. Croix rivers; the Cannon and Vermillion river basins also make up a smaller part of the Pepin watershed.

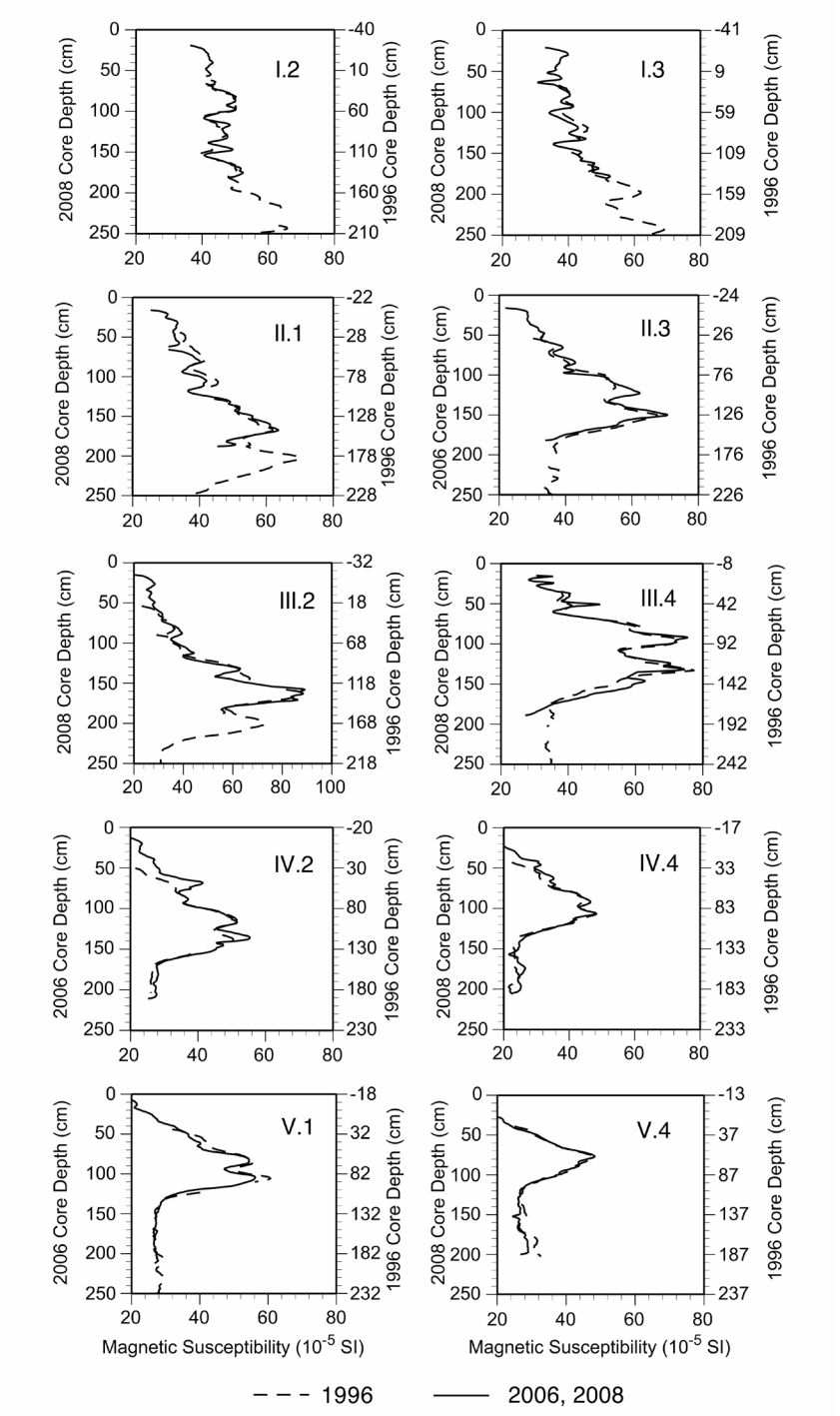

Fig. 2.2 Magnetic susceptibility (MS) profiles for each core. Transect I (top two profiles) is located at the upstream end of Lake Pepin and transect V at the downstream end (bottom two profiles). Dashed lines represent MS from the earlier (1996) set of cores and solid lines are MS profiles from the later core set (2006 and 2008). The negative number on the 1996 Core Depth axis is the depth of new sediment deposited between coring dates.

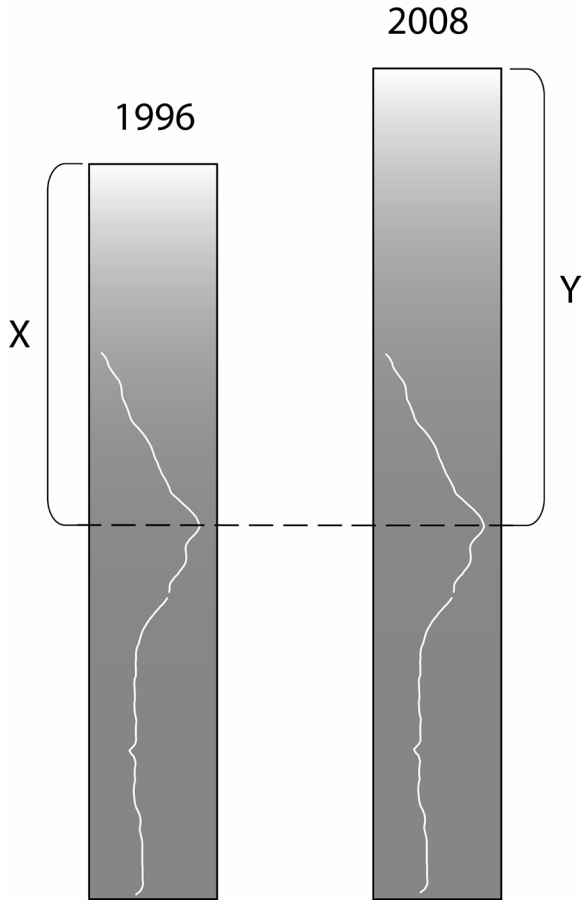

Fig. 2.3 The peaks in magnetic susceptibility profiles (white lines) are the tie points between cores taken from the same location in different years, 1996 and 2008. The cumulative dry mass above each tie point is represented by X (1996) and Y (2008). The amount of new sediment is then the difference between X and Y.

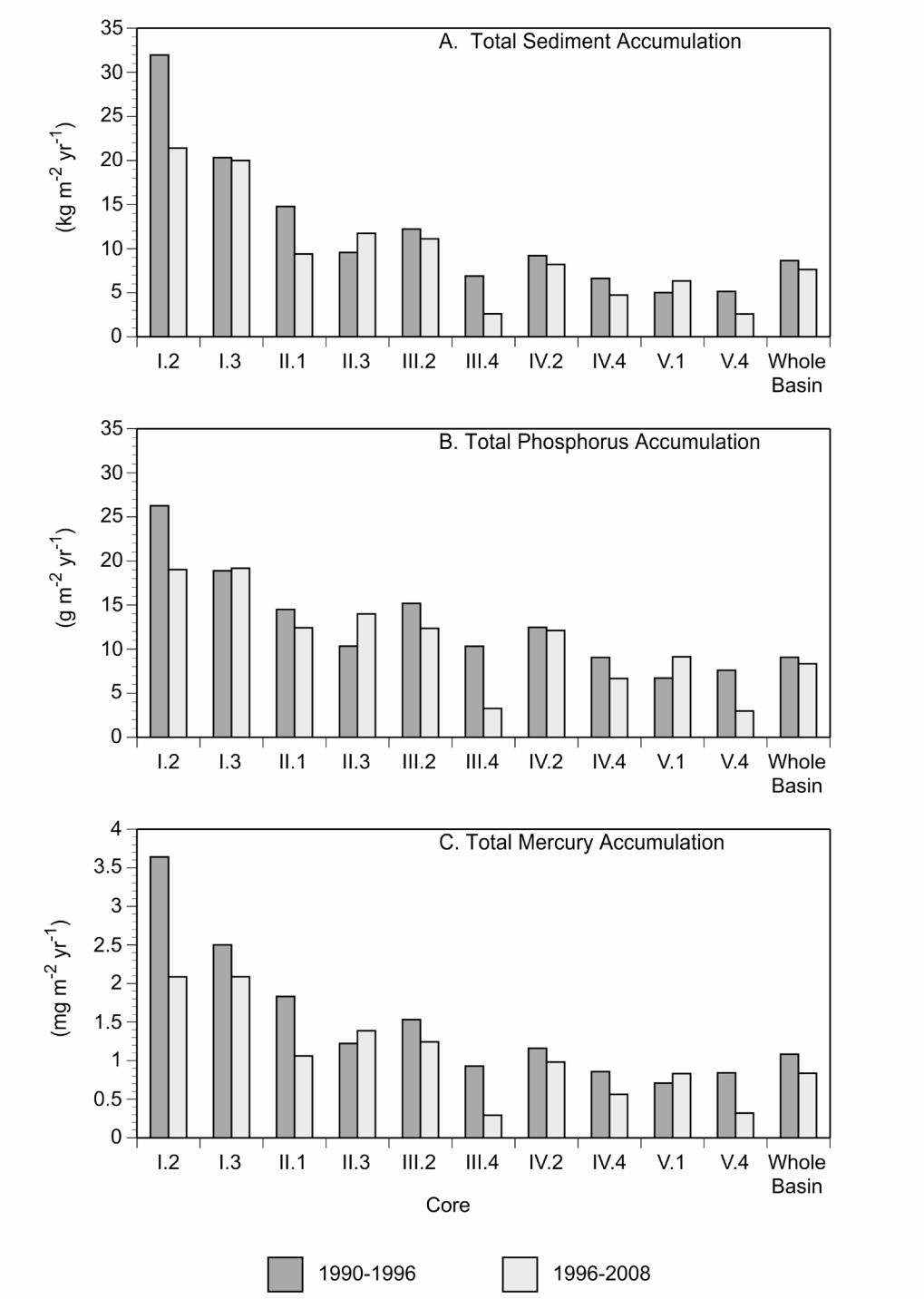

Fig. 2.4 Core-by-core comparison of estimated accumulation rates in Lake Pepin between 1990–1996 and 1996–2008 for total sediment (A), TP (B), and total Hg (C). Rates are generally highest in the upstream portion of the lake (transect I) and decrease to the downstream end (transect V). Each core is weighted to the lake area it represents to determine the accumulation rate of the whole basin.

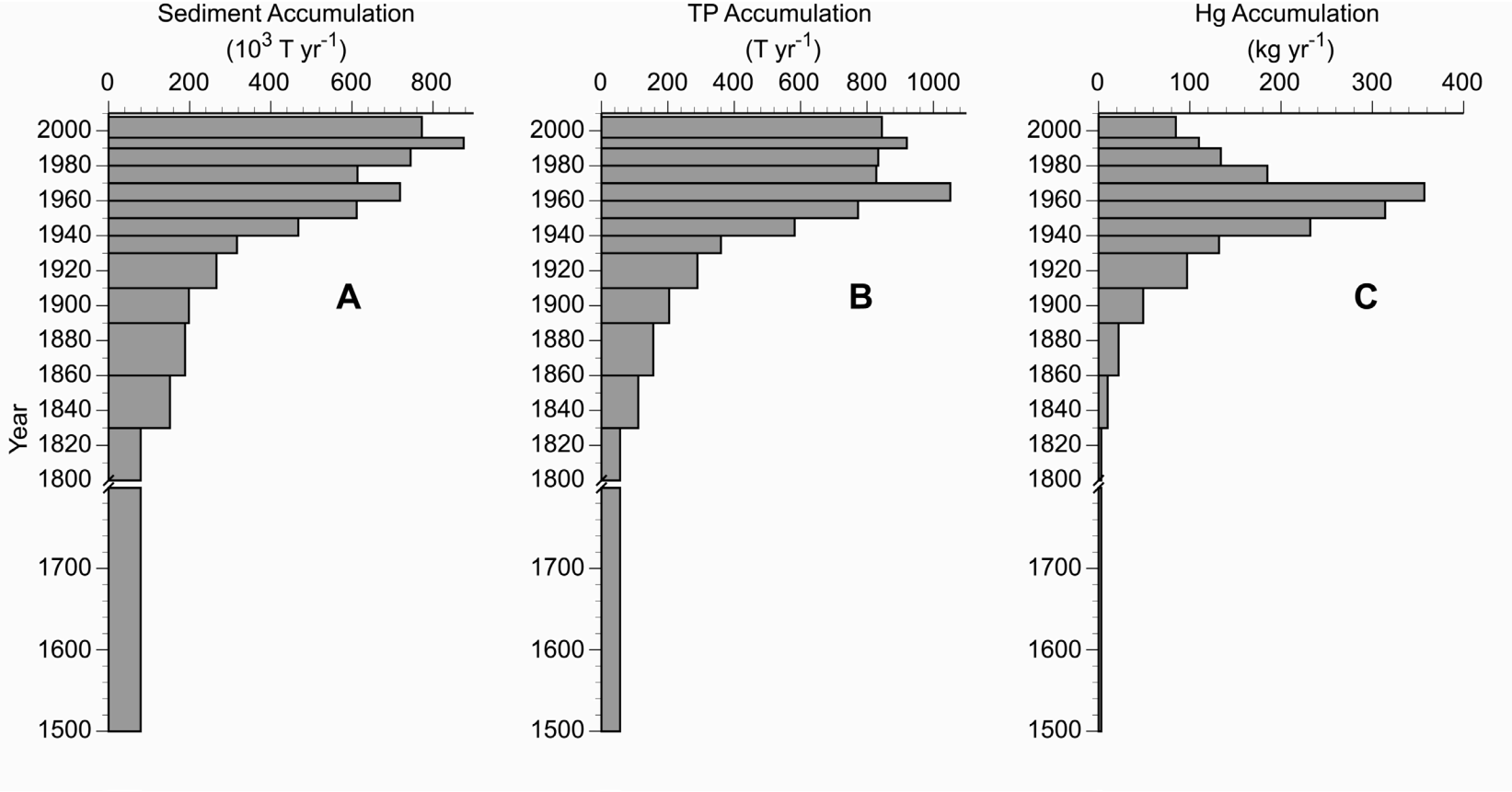

Fig. 2.5 Recent estimated whole-basin sediment (A), TP (B), and Hg (C) accumulation in Lake Pepin from this study (1996-2008) plotted with historical estimates from Engstrom et al. (2009) for (A) and (B) and Balogh et al. (1999) for (C). Sediment accumulation (A) in Lake Pepin has been steadily increasing since the 1930s and is currently almost an order of magnitude greater than prior to Euro-American settlement; TP accumulation (B) peaked in the 1960s and has remained relatively constant since its decline in the 1970s; and Hg accumulation (C), like TP, peaked in the 1960s. However, Hg has been in steady decline since then.

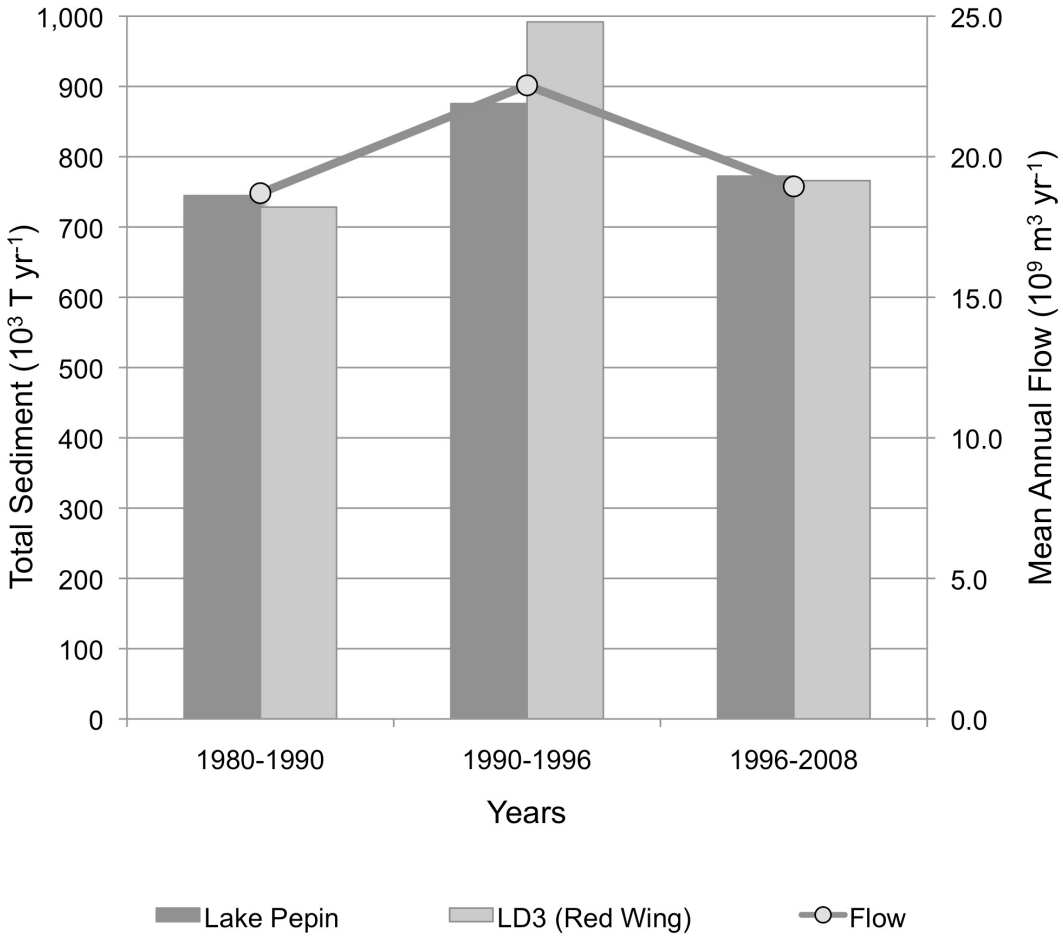

Fig. 2.6 Estimated Lake Pepin total sediment load compared to measured TSS loads estimated from monitoring data collected at Lock and Dam 3 (LD3) near Red Wing, approximately 15 km upstream of Lake Pepin, for three different time periods. The loads calculated by these two independent methods agree well for 1980–1990 and 1996–2008. The largest discrepancy occurs during the high-flow period (1990–1996), but is still in reasonable agreement (<15%).

Chapter 3: A comparison of magnetic susceptibility measurement techniques and ferrimagnetic component analysis from recent sediments in Lake Pepin (USA)

Dylan J. Blumentritt[1], Ioan Lascu[2]

[1]*Limnological Research Center, Department of Earth Sciences, University of Minnesota, Minneapolis, MN, USA*

[2]*Institute for Rock Magnetism and Limnological Research Center, Department of Earth Sciences, University of Minnesota, Minneapolis, MN, USA*

Magnetic susceptibility (MS) is commonly measured on lake sediments as a proxy for soil erosion, for correlating among cores in the same lake basin, and to align successive overlapping drives of the same core. There are several common techniques for measuring MS, each with its own advantages. Here we review three such techniques measured on a sediment core from Lake Pepin, a natural impoundment of the upper Mississippi River: 1) loop-sensor MS logging on wet sediment of the intact core; 2) point-sensor MS logging on wet sediment of a split (lengthwise) core; and 3) discrete MS measurements of dried sub-samples using a susceptibility bridge. To obtain further information about the origin of down-core MS variability, additional magnetic measurements were performed to model ferrimagnetic sedimentary components. Overall trends and individual features in the MS curves agree reasonably well between MS techniques; however, the amplitude of local minima and maxima varies according to the technique used. All three MS techniques captured two distinct events in 1900 and 1940, attributed to increases in the superparamagnetic component. A notable increase in interacting single domain particles was captured by the point sensor log and susceptibility bridge, but was not distinct in the loop sensor MS curve. This highlights possible discrepancies between MS techniques on lake-sediment cores.

3.1 Introduction

Magnetic susceptibility (MS) is a magnetic parameter commonly measured on lake-sediment cores as a cross-correlation tool or to provide an initial approximation of

the sediment magnetic composition. There are multiple ways to obtain MS, and here we compare three of those methods and also examine the ferrimagnetic components that contribute to MS in a sediment core from Lake Pepin on the upper Mississippi River, USA.

Magnetic susceptibility is a measure of the ability of a material to be magnetized in the presence of a magnetic field (Thompson and Oldfield, 1986), which in natural sediments allows inferences to be made about the iron-bearing minerals, including the formation, erosion, and transport of the sediment (Dearing, 1999). Bulk MS measurements incorporate magnetism of all material being measured, which makes MS an important source of magnetic information, but also lends to problematic interpretations owing to the synthetic quality of the signal. MS logging is frequently measured in lake cores for correlation of overlapping sections from the same core site to create a composite core section (Nowaczyk et al., 2007), for correlation of cores across a lake basin (Engstrom et al., 2009; Thompson et al., 1975), to align and date repeat-cores where a location was revisited after an initial paleo-study (Blumentritt et al., 2013), or as a marker for erosion within the lake catchment (Eriksson and Sandgren, 1999; Sandgren and Snowball, 2002; Thompson et al., 1975).

In this study a single sediment core (Pepin III.4, Fig. 3.1) was measured using three MS acquisition techniques to explore the advantages and differences among each method. The three methods include (1) whole-core scan with a loop sensor susceptibility meter, (2) split-core scan with a point sensor susceptibility meter, and (3) discrete single-sample measurements with a susceptibility bridge.

Magnetite is the most abundant natural ferrimagnetic mineral and is likely the dominant source of magnetism (and hence MS) in most environmental samples (Dearing, 1999; Sandgren and Snowball, 2002). Deconstructing the ferrimagnetic signal into multiple magnetic components, according to magnetic grain size and the nature of magnetic interactions among grains, may provide insight to the sources of magnetism in bulk sediment samples (Egli, 2004; Evans and Heller, 2003; Lascu et al., 2010; Lascu et al., 2012). Ferrimagnetic components can be separated according to grain size. The remanence-carrying components are larger multi-domain (MD) particles and smaller single domain (SD) particles. SD particles can be further segregated in interacting single domain (ISD) and uniaxial non-interacting single domain (UNISD) particles. Ultra-fine, nano-sized, superparamagnetic (SP) grains represent the non-remanence ferrimagnetic component at room temperature.

Our study site, Lake Pepin, is a riverine lake on the Mississippi River on the border between southeastern Minnesota and western Wisconsin (Fig. 3.1). The lake formed approximately 10 ka ago as the result of natural damming of the Mississippi by its tributary, the Chippewa River (Wisconsin), after the high-discharge Glacial River Warren subsided as the southern outlet of Glacial Lake Agassiz was abandoned (Fisher, 2003b; Wright et al., 1998). Lake Pepin trends from the inflow in the northwest approximately 34 km southeast to the outflow and is confined between steep bluffs on both sides, resulting in mean width of only 3 km. Lake Pepin is, on average, 5.4 m deep; it is most shallow near the inflow and increases in depth downstream toward a maximum depth (18 m) near the outflow. The surface area is 103 km^2 and the mean water residence

time is 6–47 days, depending on flow conditions (Heiskary and Vavricka, 1993). The Lake Pepin watershed is 122,000 km^2 and drains much of southern Minnesota and a portion of western Wisconsin (Fig. 3.1). Although the Pepin watershed is comprised of three larger river basins (Minnesota, Headwater Mississippi, and St. Croix), the majority of sediment (80-90%) deposited in Lake Pepin is derived from the Minnesota River watershed (Kelley et al., 2006; Kelley and Nater, 2000).

3.2 Methods

3.2.1 Sampling

Lake Pepin core III.4 (Fig. 3.1) is one of 10 cores collected throughout the lake basin in June of 2008 (Blumentritt et al., 2013). Core site III.4 was selected for further magnetic investigation because it exhibited well-defined MS peaks, high mass accumulation, and a well-established chronology. Sediments were collected in a single drive using a piston corer fitted with a 2 m long and 7 cm diameter removable polycarbonate core barrel. The top 14 cm of wet sediment was sectioned off in the field at 2-cm intervals and placed in polypropylene jars. The remaining core section was transported intact to the Limnological Research Center (LRC) at the University of Minnesota where it was scanned for MS using a Geotek scanning multi-sensor core logger outfitted with a loop sensor. The core was then split lengthwise into two halves; one half was catalogued and stored in the National Lacustrine Core Facility (LacCore), and MS was measured on the other half, this time with a point sensor Geotek multi-sensor core logger. This working half of the core was then transported to the St. Croix

Watershed Research Station where it was sectioned into 2-cm intervals. Water content and sediment composition were measured on an amalgamated aliquot of wet sediment from each interval by drying and loss-on-ignition (LOI) techniques (Dean, 1974; Heiri et al., 2001); the remaining portion was freeze-dried.

3.2.2 Core Chronology

The chronology of the Pepin III.4 core site was initially developed by Engstrom et al. (2009) on an earlier core collected in June 1995. Radiometric ^{210}Pb dating was performed using the constant rate of supply method (Appleby, 2001; Appleby and Oldfield, 1978; Appleby et al., 1979) along with several dating markers to anchor the dating model. These markers included the ^{137}Cs peak of 1964 that corresponds with the ban on above-ground nuclear bomb testing and also the appearance of ragweed pollen associated with land clearing upon the arrival of European settlers to the region. The more recent 2008 core, on which the magnetic measurements of this study were performed, was dated by aligning it with the 1996 core using the prominent MS features measured with a loop sensor (Blumentritt et al., 2013). The MS curves from the 1996 and 2008 cores were aligned using two prominent magnetic excursions, ca. 1900 and 1940, as tie points. The chronology of the 2008 core was established by subtracting the dry mass accumulation above the MS tie points of the 1996 core from the dry mass accumulation above the same MS tie points of the 2008 core. The most recent chronology (1996–2008) of the 2008 core was then estimated by assuming a constant accumulation rate over that 12-year period.

3.2.3 Magnetic Susceptibility

Continuous whole-core (loop sensor) and split-core (point sensor) MS measurements were scanned on intact core sections shortly after collection, and single-sample measurements were taken later on freeze-dried sediment. Loop sensor measurements were first performed on the whole core, which was passed through a loop of a known volume. The volume susceptibility (κ) was calculated using the ratio of loop volume to core volume. Because this method employs a pass-through type sensor, the core occupies it for the entire length of measurement, precluding re-calibration during the scan (Nowaczyk, 2002). The core was stored at room temperature for 12 hours prior to scanning, so there was not significant warming of the sediment during measurement, which could otherwise introduce significant measurement drift. The loop sensor MS measurement is a magnetic signal integrated over a portion of the core longer than just that section occupying the inside of the loop. The result is a smoothed MS signal, and data points should be considered weighted running averages (Nowaczyk, 2002).

Point sensor susceptibility meters obtain measurements while in direct contact with the core surface. To accommodate this technique, the core was carefully split lengthwise according to LRC protocol to provide a flat surface for complete contact with the point sensor. The core was covered with a single layer of plastic film to prevent sediment from sticking to the sensor, which is housed in a robotic carriage that moves along the stationary core. After each measurement the sensor is raised above the sediment, recalibrated, and then lowered onto the next specified measurement point – at

1–cm intervals for the Pepin III.4 core. The point sensor records the response of small, discrete volumes of sediment with each measurement and may achieve sub-centimeter resolution. Point sensor results are reported as normalized by a defined volume of sediment that depends on the diameter of the core.

Following whole-core MS measurements on wet sediment, single-sample measurements were obtained from dry sediment. Aliquots of approximately 2.5–3g from each freeze-dried 2-cm interval sample was packed into plastic boxes for further magnetic measurements at the Institute for Rock Magnetism, University of Minnesota. Single-sample MS measurements were obtained with a Kappabridge KLY-2 susceptometer. Unlike the core loggers that measure volume-normalized MS, the Kappabridge measures mass-specific low frequency MS (χ_{lf}) at a frequency of 920 hz and AC field amplitude of 300 A/m.

3.2.4 Ferrimagnetic Components

In addition to MS, several other magnetic parameters were measured on the Pepin III.4 freeze-dried samples to model component sources of ferrimagnetism and thus provide further insight to the causes of MS variations in the lake. Measurements were acquired following procedures detailed in Lascu et al. (2010) and summarized as follows. Anhysteretic remanent magnetization (ARM) and ARM susceptibility (χ_a) were acquired using a D-Tech 2000 demagnetizer; samples were imparted with a 0.1 mT steady field superimposed on an alternating frequency field, which decayed from a 200 mT peak at 5 μT per half cycle. Isothermal remanent magnetization (IRM) was obtained by pulsing

samples with a 2G core pulse magnetizer followed by demagnetization with the same procedure used for ARM. Hysteresis loops were measured on a Princeton Measurements vibrating sample magnetometer with a 1 T maximum applied field. Saturation magnetization (M_s), saturation remanence (M_{rs}), and high field susceptibility (χ_{hf}) were all obtained from the hysteresis loops after correction for the high-field slope.

The ferrimagnetic components of each sample were modeled according to mathematical methods that are fully described in Lascu et al. (2010). Briefly, M_s was used as a proxy for the total ferrimagnetic concentration. The saturation remanence ratio (M_{rs}/M_s) was used as a magnetic grain size proxy, allowing separation of SD particles from the larger MD particles. SD particles were further classified into ISD and UNISD using anhysteretic remanence ratio (χ_a/M_{rs}) to estimate inter-particle magnetostatic interactions. The proportion of ultrafine (<0.03 μm) SP particles was calculated from the normalized susceptibility of the ferrimagnetic fraction (χ_f/M_s).

3.3 Results

3.3.1 Magnetic susceptibility

Magnetic susceptibility profiles from the Lake Pepin III.4 core compare reasonably well among the three MS measuring techniques: loop sensor, discrete single-sample, and point sensor (Fig. 3.2). As expected, the loop sensor and single-sample techniques provide much smoother profiles than the point sensor because they integrate the magnetic signal over a larger portion of the core. There are three evident MS excursions in the profiles noted in figure 3.2 as $E_{1\text{-}3}$. E_1, which begins at approximately

1890 and lasts until about 1920, is apparent in all three profiles. The loop sensor captures a double peak during E_1, ca. 1900 and 1910, whereas the point sensor profile displays two additional distinct peaks, one near 1890 and the other about 1915. The single-sample profile only displays a plateau with no distinct peaks during E_1. E_2 (ca. 1930–1945) has very similar structures in the single-sample and loop sensor profiles, again with the possibility of a double peak. Like E_1, the point sensor profile exhibits multiple distinct peaks within E_2, the two largest being on both ends of the overall excursion (ca. 1930 and 1940). Near the top of the core E_3 occurs ca. 1970–1980 and is defined by a single peak in the single-sample profile and a double peak in the point sensor profile; the peaks of these two profiles are of amplitude similar to peaks from E_1 and E_2 from the same profiles. The loop sensor profile does indicate a small peak within E_3; however, the amplitude is far less dramatic than in the other excursions.

3.3.2 Ferrimagnetic components

The UNISD component has relatively low and consistent mass concentrations (0.02–0.06 mg Fe_3O_4 g^{-1}) throughout the entire core section (Fig. 3.3). The SP mass concentrations are quite low (<0.05 mg Fe_3O_4 g^{-1}) in the early 1800s and remain so until an increase to 0.10 mg Fe_3O_4 g^{-1} ca. 1880 and again ca. 1930, corresponding with E_1 and E_2. The ISD component increases steadily from 0.05 mg Fe_3O_4 g^{-1} in 1810 to 0.12 mg Fe_3O_4 g^{-1} around 1890. ISD concentrations then fluctuate slightly up-core, but remain fairly consistent until a large increase to 0.32 mg Fe_3O_4 g^{-1} ca. 1980, which aligns well with E_3. Following this late excursion, ISD mass concentrations fall to <0.10 mg Fe_3O_4

g^{-1}. MD mass concentrations are the largest of the four ferrimagnetic components; they follow a similar pattern as the ISD component, steadily rising in the early to mid 1800s, remaining fairly consistent in the late 1800s to mid 1900s (0.33–0.43 mg Fe_3O_4 g^{-1}) before a large spike in 1980 (0.73 mg Fe_3O_4 g^{-1}). After 1980, MD concentrations decreased dramatically, like ISD concentrations, to levels similar to the early 1800s.

Flux estimations of the ferrimagnetic components in the Pepin III.4 core (Fig. 3.4) display little difference in profile structure from the mass concentrations (Fig. 3.3), with the exception of the MD profile. MD mass concentrations remain fairly steady from 1855 to 1955; however, the MD flux increases quite dramatically over that same time interval from 0.068 mg cm^{-2} yr^{-1} to 0.19 mg cm^{-2} yr^{-1}.

3.4 Discussion

3.4.1 Magnetic susceptibility

All three MS acquisition techniques explored in this study are fairly rapid, non-destructive, and inexpensive methods for measuring MS. Acquiring MS with a loop sensor susceptibility meter is extremely fast (<1 hr/m of core) and completely non-destructive, as it is performed on an intact sediment core with little or no preparation. Scans can be made directly following core collection to provide near-instant data that might better inform sampling strategies. However, the loop sensor does not provide a high level of detail because the magnetometer integrates a longer section of the core than the other two methods. Results are typically reported as volume-normalized susceptibility (κ), but mass-normalized (χ) MS values may be estimated if simultaneous

density measurements are made concurrently with MS. Caution should be exercised though, as gas pockets or extensional gaps in the sediment from the core extraction process, which may not be noticeable from the outside of the core tube, can introduce a significant source of error in calculating χ.

The point sensor susceptibility meter provides a very high level of detail with only slightly more preparation than using the loop sensor. MS acquisition takes more time than the actual preparation work, but can be programmed to run without supervision if an automatic sampler is available. Preparation and measurement time on the order of several hours per meter of core can be expected with the point sensor technique, depending on the prescribed resolution. The point sensor magnetometer only comes in contact with a very small section of the core with each measurement, so the value obtained is very discrete compared to the loop sensor technique. This can be advantageous in cores with very low sediment accumulation rates, but in our Lake Pepin III.4 core (0.44 g cm^{-2} yr^{-1}) the level of detail was quite high and would make meaningful comparisons to other cores from within Lake Pepin more difficult. Further processing to smooth the data, such as applying a weighted moving average filter to the point sensor MS data, could be applied to highlight the broader trends, as is the case here.

Our single-sample MS data do not provide as high a level of detail as do the point sensor data, but resolution at 2-cm sample intervals is sufficient for examining integrated MS trends; this level of detail aligns well with the loop sensor resolution. Single-sample resolution will, of course, primarily depend on the level of detail used in sub-sampling the core. Sample preparation is the most time and labor intensive portion of the single-

sample MS technique, whereas the measurement portion is quite fast. The time spent obtaining single-sample MS measurements will ultimately depend on the chosen sub-sample resolution, but several days per meter of core should be expected. This technique may be a good option if samples are being prepared in the same way for other magnetic measurements or if accurate mass-normalized susceptibility is essential.

Loop sensor and single-sample MS sample resolution is sufficient for recognizing E_1 and E_2, which are ideal markers for core comparison across the lake basin (Engstrom et al., 2009) and for repeat-core dating (Blumentritt et al., 2013). Each excursion (E_{1-3}) is evident in the loop sensor and single-sample MS profiles by single or double peaks, with the exception that the loop sensor profile does not display a prominent peak associated with E_3. Each excursion is comprised of multiple peaks in the point sensor profile, which makes visual cross-correlation among cores throughout the lake basin more difficult.

All three MS profiles (Fig. 3.2) display steadily increasing values from the early 1800s to approximately 1870. This time period corresponds with Euro-American settlement in the region, when aggressive land clearing and conversion of forests and prairies to agriculture increased sediment delivery to Lake Pepin (Fig. 3.5) (Engstrom et al., 2009). This large-scale landscape alteration, which would have made sediment particles more available for erosion, is the likely cause of large MS fluctuations that began in the late 1800s and are evident in the three MS profiles, particularly the point sensor profile.

3.4.2 Ferrimagnetic components

Mass concentrations of the SP component are elevated ca. 1900–1915 and 1930–1950, corresponding well to MS peaks during E_1 and E_2 (Fig. 3.3). The other three ferrimagnetic components (UNISD, ISD, and MD) lack the same increases during E_1 and E_2, although ISD and MD concentrations rise slightly during the onset of E_2. ISD and MD have very significant peaks centered on 1980 (E_3), but SP concentrations remain quite low. This complex pattern illustrates that MS can have a variety of magnetic sources. It also confirms that a relatively small change in the concentration of SP particles can have a dramatic effect on MS (Dearing, 1999), whereas it takes a much larger relative increase in ISD and MD concentrations to have a similar effect (single-sample and point sensor), or far less dramatic effect (loop sensor) on MS (E_3 in Figs. 3.2). It thus appears that the loop sensor is biased toward SP particles, as E_1 and E_2, which corresponded to the SP excursions, registered nicely in the loop sensor profiles, but E_3 with no related SP increases, did not register as significantly.

3.4.3 Sediment Sources

Current MS and ferrimagnetic concentrations and fluxes have reached levels similar to what they were in the early 1800s. However, sediment accumulation in Lake Pepin, is currently almost an order magnitude higher than it was prior to Euro-American settlement in the early 1800s (Fig. 3.5) (Blumentritt et al., 2013; Engstrom et al., 2009). Fluxes of each ferrimagnetic parameter increased from the early 1800s to the mid-1900s and reached a general trend maximum ca. 1940 (UNISD, ISD, and SP) and 1960 (MD),

perhaps owing to the increase in erosion during this time, illustrated by the increase in sediment delivery to Lake Pepin (Fig. 3.5). Fluxes then began to decline toward current low values, with the exception of the 1980 peak in ISD and MD. This decrease in flux back to pre-settlement values suggests that either the erosional sources of sediment has changed to those deficient in ferrimagnetic mineral grains, or that the sediment source has remained the same, but has been depleted of ferrimagnetic particles. If high MS and ferrimagnetic fluxes are primarily the result of soil erosion, then the MS and ferrimagnetic flux shifts over the past half century would indicate a shift from an erosional regime dominated by field erosion in the early 1900s to the present regime dominated by non-field erosion, such as from banks, bluffs, and ravines. This mid-1900s shift in sediment sources agrees well with recent work that used radiometric fingerprinting and geomorphic mass balance techniques in Lake Pepin and the Minnesota River basin (Belmont et al., 2011; Schottler et al., 2010).

3.5 Conclusions

Measuring MS on lake sediment cores is relatively fast, inexpensive, and non-destructive, regardless of the chosen acquisition method. MS profiles among loop-sensor, single-sample, and point sensor methods all matched up reasonably well (Fig. 3.3), especially if a filter is applied to the highly detailed point sensor profile. Ultra-fine SP particles appear to have the greatest influence on our Lake Pepin MS profile. Small increases in SP concentrations correlate well with the first two MS excursions (E_1 and E_2). However, MD and ISD particles were the primary contributors to MS during E_3,

illustrating that MS is a measure that incorporates the magnetic properties of all material being measured. The decreasing flux of the ferrimagnetic components as well as MS values over the past half-century offers further evidence that there has been a major shift from field-dominated erosion to a system dominated by non-field erosion sources.

Figures

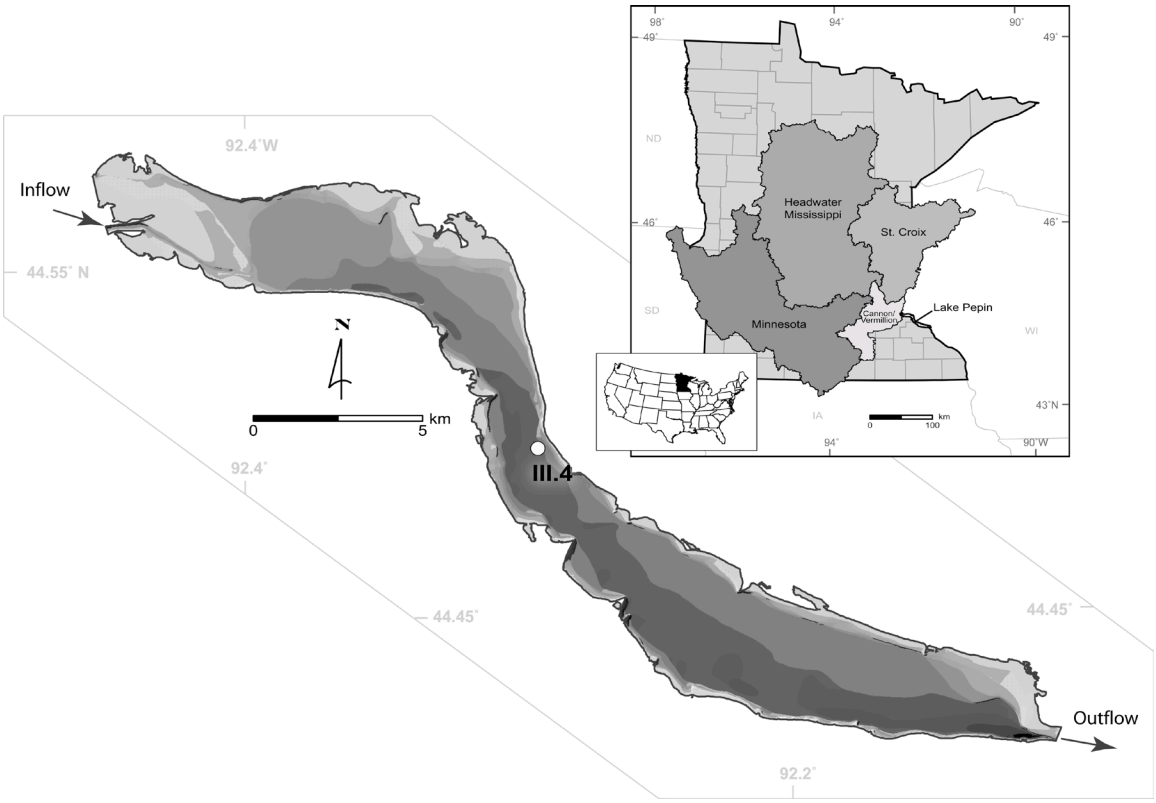

Fig. 3.1 Location of core site III.4 in Lake Pepin, a natural riverine impoundment on the Mississippi River located on the border between Minnesota and Wisconsin, USA. The Lake Pepin watershed (inset) is 122,000 km^2 and comprised of three main river basins, the Minnesota, headwater Mississippi, and St. Croix rivers; the Cannon and Vermillion river basins also make up a smaller part of the Pepin watershed.

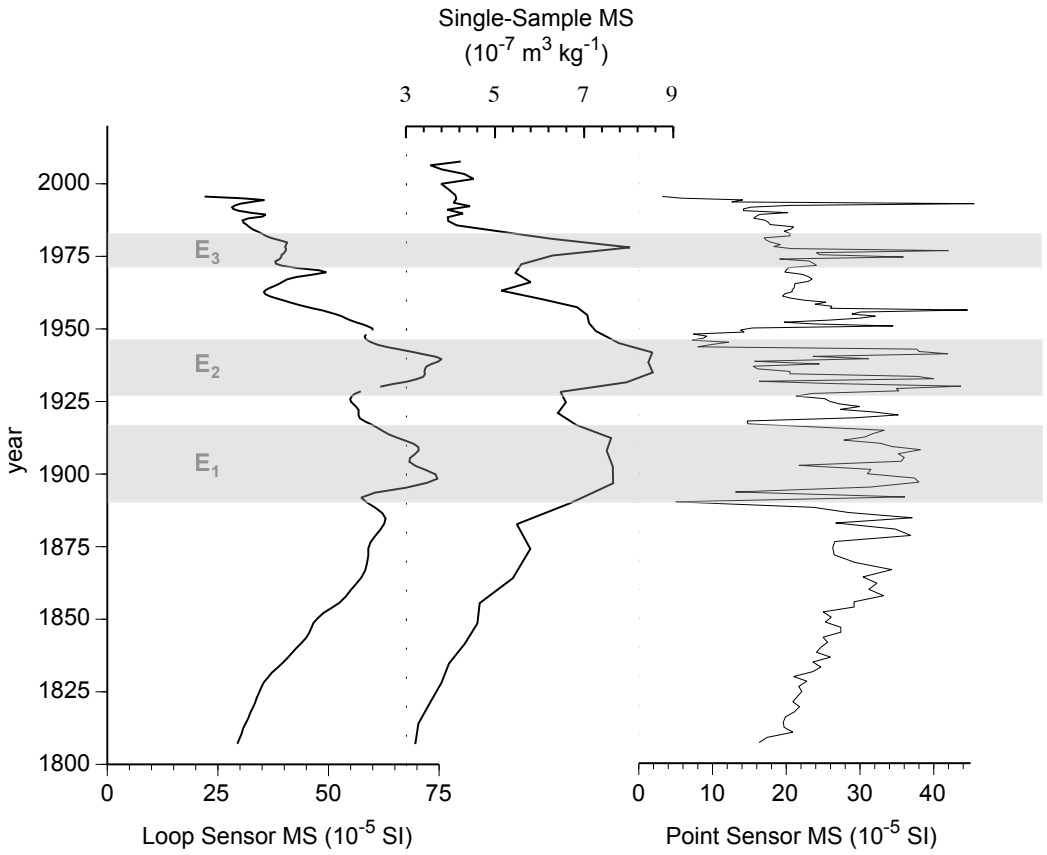

Fig. 3.2 Magnetic susceptibility profiles of the Lake Pepin III.4 core obtained using three acquisition techniques. The loop sensor profile represents a running average of MS; the single-sample profile was obtained by measuring single 2-cm sub-samples; and the point sensor profile measures only a small (sub-cm) portion of the sediment, providing the greatest detail of the three methods. High susceptibility excursions are indicated by $E_{1\text{-}3}$.

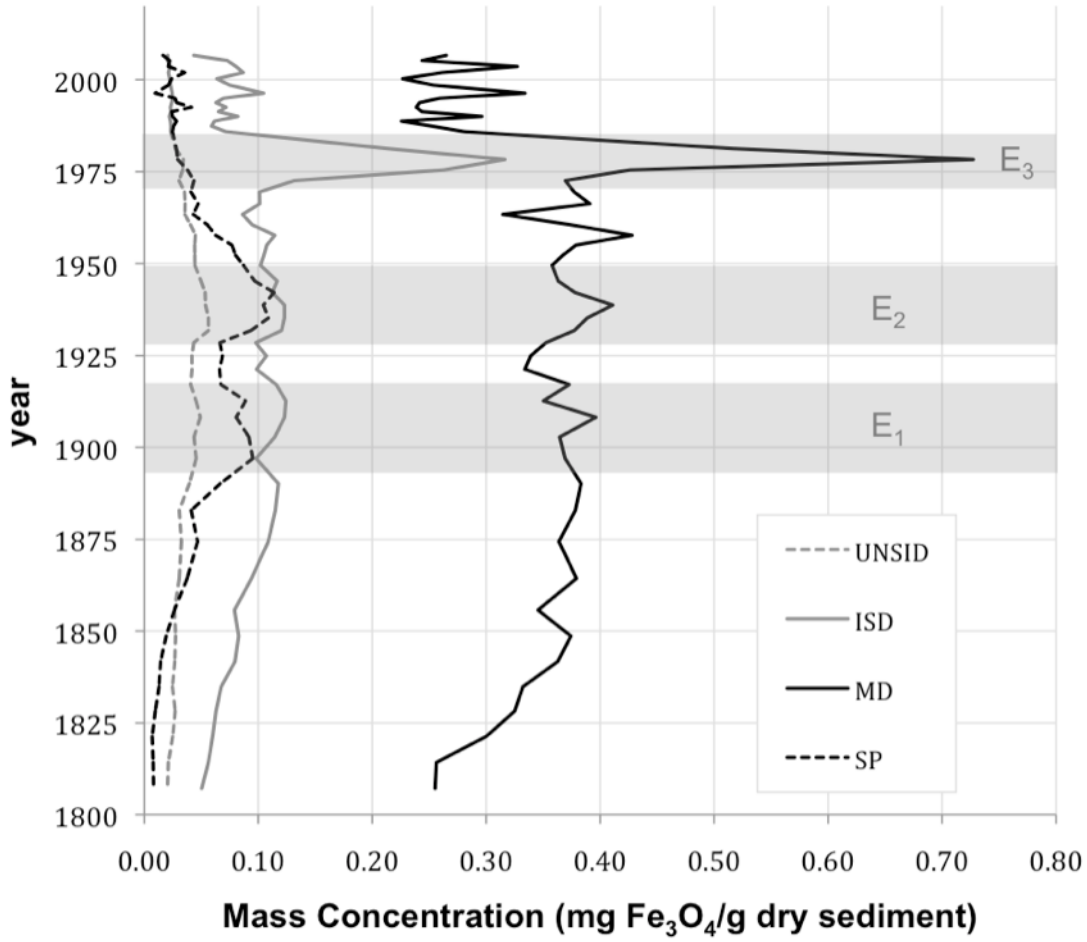

Fig. 3.3 Mass-concentration profiles of modeled ferrimagnetic components for Lake Pepin III.4 core. Larger MD particles have the highest concentrations, whereas UNISD, ISD, and SP particles are substantially lower. Increases in SP concentrations ca. 1900–1915 and 1930–1950 correspond to E_1 and E_2 in the MS profiles (Fig. 3.2); peak concentrations in ISD and MD (ca. 1980) correspond to MS E_3.

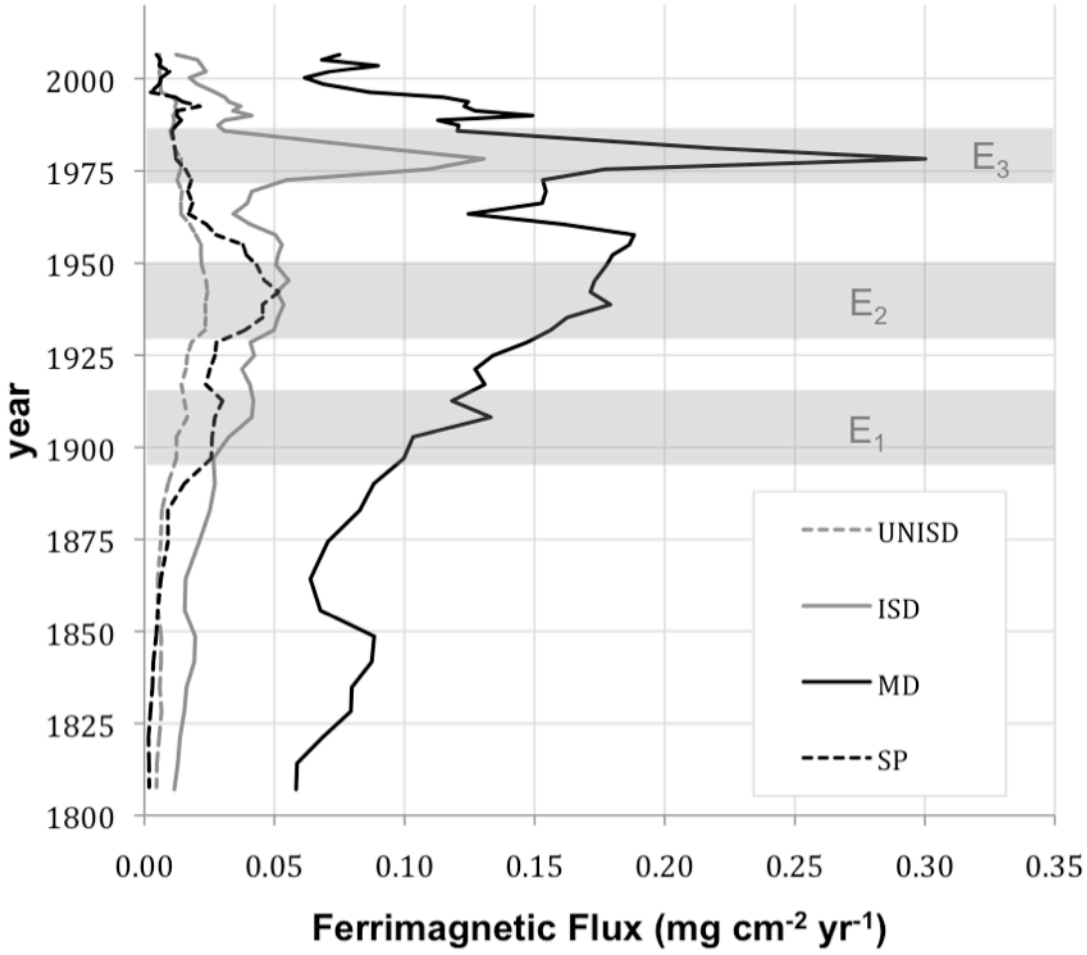

Fig. 3.4 Fluxes of ferrimagnetic components for Lake Pepin III.4 core. Fluxes were estimated from modeled ferrimagnetic component concentrations and sediment dry mass accumulation. General trends for all components indicate an increase in fluxes from the late 1800s to the mid 1900s, after which fluxes generally decrease toward the present, with the exception of ISD and MD peaks ca. 1980.

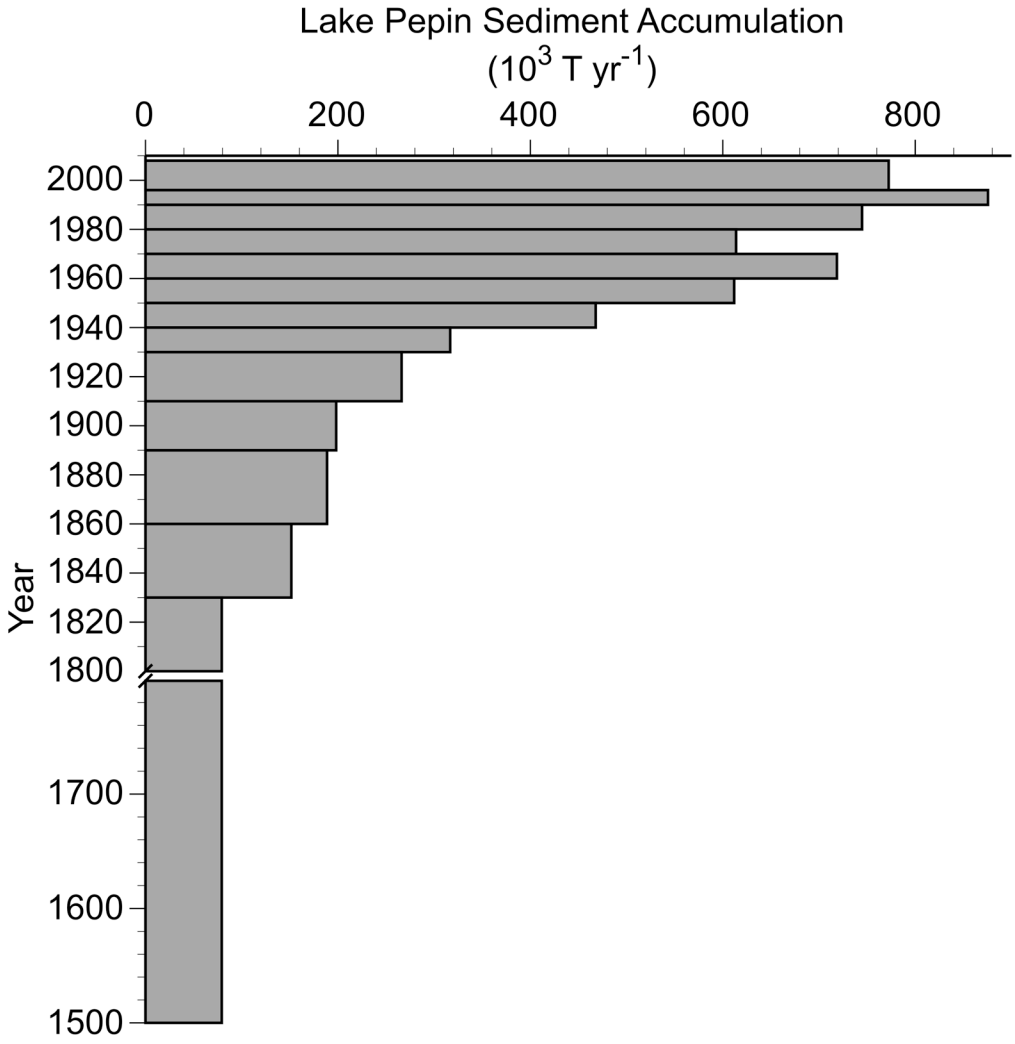

Fig. 3.5 Whole-basin sediment accumulation in Lake Pepin calculated from a suite of 10 cores (Blumentritt et al., 2013; Engstrom et al., 2009). Accumulation begins to increase in the early to mid 1800s, corresponding with Euro-American settlement in the region. Accumulation accelerated in the early 1900s to the current rate, which is almost an order of magnitude greater than pre-settlement rates.

Chapter 4: Investigation of direct deposition of atmospheric ^{210}Pb to river surfaces: Implications for sediment fingerprinting

Dylan J. Blumentritt[1], Shawn Schottler[2], Daniel R. Engstrom[2]

[1]*Department of Earth Sciences, University of Minnesota, Minneapolis, MN, USA*

[2]*St. Croix Watershed Research Station, Science Museum of Minnesota, St. Paul, MN, USA*

Many streams and rivers throughout the world are impaired with excess sediment, the result of increasing erosion and sediment delivery in these watersheds. Sediment fingerprinting using atmospheric radioisotopes (ARI) is a useful tool for determining the provenance of this excess sediment. Specifically, short-lived ARI such as ^{7}Be, ^{137}Cs, and ^{210}Pb fall to the surface of the earth through precipitation and enrich soil surfaces (*field* sources) with maximum exposure. Other sediment sources such as streambanks, bluffs, and ravines (collectively called *non-field* sources) are largely absent of any appreciable short-lived ARI. Therefore, it is possible to discern field sources from non-field sources from a suspended sediment sample collected in a river using sediment fingerprinting techniques. Although ARI sediment fingerprinting is a rather well established method, it relies on the assumption that ARI deposited directly to the surface of the water is negligible. We have devised a strategy for measuring the amount of ^{210}Pb deposited directly to the river (ie. did not enter on eroded particles) by utilizing the initial disequilibrium between ^{210}Pb and its granddaughter ^{210}Po. Samples were collected bi-weekly for one year at four locations with large watersheds (42,000–123,000 km^2) in southern Minnesota. Direct ^{210}Pb deposition (Pb_w) was estimated by modeling ^{210}Po ingrowth; we optimized the ingrowth curve to ^{210}Po activities measured three times after sample collection. The Pb_w fraction of total unsupported ^{210}Pb varied considerably in individual samples. A significant amount of Pb_w was detected at each site, ranging from 20–90% of the total unsupported ^{210}Pb load, and generally increased with watershed size. Our ^{210}Po ingrowth method works well for estimating Pb_w for individual samples; however, significant errors are associated with annual load estimates.

Keywords: Sediment fingerprinting • ^{210}Pb • Atmospheric radioisotopes • Erosion

4.1 Introduction

Excess sediment is a recognized pollutant that can negatively affect natural ecosystem functions, particularly in landscapes where anthropogenic activities have accelerated sediment delivery. Determining sediment sources is important for erosion control and turbidity issues in many streams and rivers throughout the world. Restoration efforts to remediate sediment issues are numerous and costly, so it is important to understand the sources. Sediment fingerprinting determines the sediment source-type, or provenance from a position on the landscape such as bank, bluff, ravine, or field erosion. Understanding these sources of suspended sediment in rivers is important for targeting problem areas in an impaired watershed during remediation efforts.

Atmospheric radioisotopes (ARI), such as ^{7}Be, ^{137}Cs, and ^{210}Pb, are ubiquitous in the atmosphere and are delivered to the earth's surface by precipitation. ARI are highly particle reactive (He and Walling, 1996), such that sediments derived from a surface with prolonged exposure to precipitation, such as an agricultural field, are enriched in ARI. Conversely, sediment sources that are not directly exposed to rainfall (i.e. streambanks, ravines, or bluffs) are largely depleted in ARI. Thus, ARI are effective at differentiating sediment source-types – specifically field-derived sediment from non-field sediment in rivers (Mabit et al., 2008) – providing a powerful tool for sediment management efforts.

Numerous studies have been performed on suspended sediment in rivers using ARI (e.g. Aalto et al., 2008; Aalto and Nittrouer, 2012; Belmont et al., 2011; Nagle et al., 2007; Owens et al., 2012; Schottler et al., 2010; Walling et al., 1999; Walling and Woodward, 1992; Yin and Li, 2008). Central to this work is the assumption that ARI

concentrations measured on river sediment are proportional to the concentrations of the sediment sources. Inherent in this is the assumption that there is not a significant contribution from precipitation-deposited ARI directly to the surface of the river. This assumption, an important tenet to sediment fingerprinting, has never been tested.

We have developed a method to quantify the amount of Pb_w by utilizing the disequilibrium of freshly deposited ^{210}Pb and its granddaughter product ^{210}Po. Lead-210[^{210}Po] are assumed to be at or near equilibrium on soil source material because of longer accumulation time; however, ^{210}Pb[^{210}Po] are not at equilibrium in the atmosphere, due to a short residence time, nor when they are deposited to the earth by precipitation. We have devised a strategy to estimate the contribution of Pb_w from rainfall that utilizes ^{210}Po, the short-lived granddaughter of ^{210}Pb, by measuring the appearance of ^{210}Po over time.

We hypothesize that Pb_w is not negligible, that not all unsupported ^{210}Pb in rivers entered on eroded particles, especially in large rivers. The purpose of this study is to evaluate the amount of Pb_w on sediment particles in rivers of varying watershed size to: (1) develop a method to quantify Pb_w on suspended sediment particles in a river system; and (2) determine if Pb_w is a significant portion of total ^{210}Pb and if there is a relationship to watershed size. Our findings provide a tool for detecting if Pb_w is significant, and correcting for it when necessary.

4.1.1 Study area

There are three major watersheds that cover more than half the state of Minnesota and converge and flow through Lake Pepin, on its southeastern border with Wisconsin (Fig. 4.1A). The Minnesota River (MNR; 44,000 km^2) drains the southwest portion of the Lake Pepin watershed and is dominated by row-crop agriculture land-use. This basin has a relatively low population and is generally drier than the other two owing to a west-to-east gradient of increasing precipitation across Minnesota. The headwaters Mississippi River (HMR; 51,000 km^2) and St. Croix River (SCR; 20,000 km^2) make up the north-central and northeast sections of the Lake Pepin watershed and have significant portions in forest, agriculture, and urban land cover. These watersheds are generally wetter and more populated than the MNR basin. HMR and MNR join together between the city centers of Minneapolis and St. Paul and with the SCR 50 km downstream from there. The lower 40 km of SCR is a natural impoundment (Lake St. Croix) with a residence time of 20-50 days, and so serves as an effective sediment (and ^{210}Pb) trap (Triplett et al., 2008). Another 40 km downstream from the SCR confluence, the Mississippi River flows through its own natural impoundment, Lake Pepin. Lake Pepin – also an efficient sediment trap – is currently filling in at a rate of 772,000 metric tons yr^{-1} (Blumentritt et al., 2013), and both present-day and historically 80-95% of that sediment is sourced in the MNR basin (Kelley et al., 2006; Kelley and Nater, 2000).

The four primary sampling locations (Jordan, Fort Snelling, St. Paul, and LD3) were selected above and below major river confluences (Fig. 4.1B) to best determine the effects of these major inputs associated with increasing watershed sizes and water surface area. These sites also correspond to long-term gauging stations where flow conditions

are continuously monitored, allowing annual sediment loads to be calculated. A fifth location (Minneapolis) was added near the end of the sample-collection period to obtain independent confirmation of HMR inputs and isotopic signatures.

Jordan is the most upstream sampling site and is on MNR (river mile 39.4); this location is associated with USGS gauge station 0530000 and has a watershed area of 42,000 km^2. The Fort Snelling sampling site (44,000 km^2 watershed area) is located in Fort Snelling State Park near the mouth of MNR (USGS gauge station 05330920), 36 km downstream from Jordan (river mile 3.5). The St. Paul sampling site (USGS gauge station 05331000) is located just 5.5 km downstream of the confluence of MNR and HMR (river mile 839.1); this site has a watershed area of 95,000 km^2. Note that the watershed area approximately doubles at this confluence, so the mainstem Mississippi River will be called, for our purposes here, the Upper Mississippi River (UMR) below this point. The fourth primary sampling location is at Lock and Dam 3 (LD3), which is maintained by the U.S. Army Corps of Engineers and is located 68 km downstream from the St. Paul site, and 17 km upstream of Lake Pepin (river mile 796.9). SCR enters UMR between St. Paul and LD3 and represents about 15% of the contributing watershed above LD3 (122,000 km^2). The mean discharge for Jordan, Fort Snelling, St. Paul, and LD3 for the time period of this study (April, 2009 through May, 2010) is 221, 237, 462, and 571 $m^3\ s^{-1}$, respectively. The supplemental sampling site on HMR in Minneapolis is not associated with a gauging station and is located near the Franklin Avenue Bridge approximately 21 km upstream of the St. Paul site.

4.1.2 ^{210}Pb[^{210}Po] disequilibrium theory

The methods used in this study are reliant on the disequilibrium held between ^{210}Pb ($t_{1/2}$ = 22.3 yr) and ^{210}Po ($t_{1/2}$ = 138 days) that occurs upon the creation of ^{210}Pb. Radium-226 is a product of ^{238}U decay and is sourced in soils and rock throughout the world; it decays to ^{222}Rn and escapes to the atmosphere as a gas. Lead-210 is formed in the atmosphere through a series of short-lived decay products (Fig. 4.2) and is readily scavenged by atmospheric particulates and washed out of the atmosphere through precipitation and deposited on the surface of the earth (Nozaki et al., 1978); the atmospheric residence time is quite short (~5-22 days) compared to its much longer half-life (McNeary and Baskaran, 2007; Poet et al., 1972; Tokieda et al., 1996). Once deposited, ^{210}Pb quickly adsorbs to particles on the landscape and in surface waters; this is the excess (unsupported) component of ^{210}Pb ($^{210}Pb_{ex}$). Supported ^{210}Pb ($^{210}Pb_{sup}$) is the component found inside mineral lattices or sorbed to particles when ^{222}Rn gas becomes trapped in the soil and cannot escape to the atmosphere.

Polonium-210 is the granddaughter of ^{210}Pb and quickly forms through the intermediary ^{210}Bi ($t_{1/2}$ = 5 days; Fig. 4.2). Freshly created ^{210}Pb is not in equilibrium with ^{210}Po until the activity of ^{210}Po is sufficient where decay balances formation. When this condition occurs (approximately six half-lives) ^{210}Po is at equilibrium with, and may be used as a surrogate for, ^{210}Pb in laboratory measurements. This decay mode is analytically advantageous because ^{210}Po is a strong alpha emitter and is readily analyzed by isotope-dilution methods for great precision. The activity of ^{210}Po can be calculated at any given time if the initial activity of ^{210}Pb is known:

$$Po_x = K_1 Pb_0 e^{-\lambda_p t}(1 - e^{-K_2 t}) \quad \text{(Eqn. 1)}$$

where Po_x is the activity of ^{210}Po at time t (years). Pb_0 is the initial activity of ^{210}Pb at $t = 0$, λ_p is the decay constant for the ^{210}Pb parent radioisotope (0.03114 year^{-1}), K_1 (1.017) is the decay constant ratio of ^{210}Po/^{210}Pb at secular equilibrium, and K_2 (1.7929) is the difference between parent and daughter decay constants. 85% of ^{210}Po ingrowth occurs within 12 months from the creation of ^{210}Pb, and after 24 months 99% ingrowth is achieved.

4.2 Methods

4.2.1 Sampling

Samples were collected once every two weeks during the open water season from April, 2009 through May, 2010 at the four primary sample locations (Jordan, Fort Snelling, St. Paul, and LD3). Samples were collected with a bailer at Jordan (Hwy 9 bridge crossing), St. Paul (sheet-pile wall on Randolph Ave. under the Smith Ave. High Bridge), and LD3 (lock wall near the Tainter gate). At Fort Snelling (near Post Rd.) we used water pumped from a pier that extended out into the channel at an automatic sampling site. The four samples from the Minneapolis site (April and May, 2010) were collected from a concrete wall near the Franklin Ave. bridge crossing. At each location care was taken so that the channel bottom was not disturbed and only the particles in suspension were collected. Each sample consisted of approximately 40 liters of water

from Jordan and Fort Snelling, 60 liters from St. Paul and LD3, and 80 liters from Minneapolis.

After samples were collected, the suspended sediment was allowed to settle undisturbed for approximately 14 days before the supernatant was siphoned off and the residual sediment was concentrated into a smaller container. The concentrated sample was allowed to settle for an additional 14 days; overlying water was then extracted using a vacuum pump, and the remaining sediment slurry freeze dried.

4.2.2 Analytical

Polonium-210 was measured on each freeze-dried sample three times over the course of approximately one year to determine the amount of ingrowth during that time. The first measurement was taken soon after sample collection (approximately 1 month). The second and third measurements were obtained, on average, 6 months and 12.5 months after sample collection, respectively. Samples (0.1–1.0 g) were initially spiked with ^{209}Po as an internal yield tracer and the Po isotopes distilled at 550° C, and plated directly onto silver planchets in a weak HCl solution according to methods outlined by Eakins and Morrison (1978). Activity was measured on an Ortec alpha spectrometry system for 8-70 x 10^4 s. Supported values were estimated from a subset of samples (n = 29) measured with Ortec ultra-low background well-type gamma spectrometers. Excess ^{210}Pb (^{210}Po) was then calculated by subtracting the supported activity from the total activity.

4.2.3 Ingrowth Modeling

The purpose of ingrowth modeling is to determine the activity of ^{210}Pb recently deposited directly from the atmosphere to the surface of the water (Pb_w). Knowing the value of Pb_w allows us to estimate the proportion of excess ^{210}Pb on suspended sediment that comes from direct atmospheric deposition and that delivered through erosion of catchment soils. To model Pb_w, we measured ^{210}Po activity at three times during ingrowth, following the analytical procedure above. The nature of ingrowth over that time is described in Figure 4.3 and by the following set of equations:

$$\begin{aligned} Po_1 &= K_1 Pb_w(1 - e^{-K_2 t_1}) + Pb_0 e^{-\lambda_p t_1} \\ Po_2 &= K_1 Pb_w(1 - e^{-K_2 t_2}) + Pb_0 e^{-\lambda_p t_2} \\ Po_3 &= K_1 Pb_w(1 - e^{-K_2 t_3}) + Pb_0 e^{-\lambda_p t_3} \end{aligned} \qquad \text{Eqs. 2-4}$$

where Po_1 is the activity of ^{210}Po when first measured (t_1), Po_2 is the activity at the second measurement (t_2), and Po_3 is the activity at the third time of measurement (t_3). K_1 (1.017) and K_2 (1.7929) constants are related to the ratio of ^{210}Po:^{210}Pb at secular equilibrium. K_2 is the difference of the ^{210}Po (daughter) decay constant (λ_d, 1.824 yr^{-1}) and the ^{210}Pb (parent) decay constant (λ_p, 0.03114 yr^{-1}) and K_1 is the λ_d:K_2 ratio. Pb_0 is the initial ^{210}Pb activity before ingrowth begins. The following set of equations describe the time components ($t_{1\text{-}3}$) of equations 2-4:

$$t_2 = t_1 + \Delta t_a$$
$$t_3 = t_2 + \Delta t_b \qquad \text{Eqs. 5 \& 6}$$

where t_1 is the time elapsed between atmospheric deposition of ^{210}Pb (t_0) and the first activity measurement. Then t_2 is the sum of t_1 and the time elapsed between the first and second activity measurements (Δt_a), and t_3 is the sum of t_2 and the time between the second and third activity measurements (Δt_b).

Pb_w, t_1, and Pb_0 are all unknown variables in this set of simultaneous nonlinear equations (eqns. 2-4). To solve for them, we optimized the right-hand solutions by adjusting the three unknown variables to the measured left-hand values ($Po_{1,2,3}$).

Because this equilibrium curve is an inverse exponential growth function, the Pb_0 variable is particularly sensitive near t=0. Therefore we ran the optimization method (OM) for three different scenarios, each representing different constraints on t_1 (Fig. 4.4). For scenario OM1, t_1 was set to the time between sample collection and the first activity measurement; this method assumes there is no Pb_w residence time in the river channel before sample collection and is regarded as the minimum Pb_w scenario. The estimate for t_1 in OM2 was a process-based minimum estimate. We estimated the time it would take a particle in continuous suspension to reach each sampling location established on base-flow conditions and the distance to the headwaters or major impoundment (where all upstream ^{210}Pb or ^{210}Po would settle out). This transport time estimate is 45 days at Jordan, 58 days at Fort Snelling, 22 days at Minneapolis, 59 days at St. Paul, and 65 days

at LD3. No constraints were imposed on t_1 for OM3; in this method all unknown variables were allowed to optimize freely as long as values were ≥0.

4.2.4 Flux Modeling

Once Pb_w was determined for each sample using the three OM scenarios, the annual load (April, 2009 through May, 2010) was estimated at each of the four primary sample locations (Jordan, Fort Snelling, St. Paul, and LD3). We used the U.S. Army Corps of Engineers Flux32 model (Walker, 1999), as it is widely used by Metropolitan Council Environmental Services (MCES) for determining sediment and nutrient loads at our four primary sites, and MCES has developed a comprehensive SOP for its application. Flux32 requires only two input files, one that has daily flow over the period of interest for that site, and one that has constituent concentrations (Pb_w) and associated dates. Daily flow and total suspended solids (TSS) data were obtained from MCES; TSS information was necessary for converting activities from mass concentrations to volume concentrations. Flux32 allows for stratification of data based on flow, date, or season, and calculates loads by six different load estimate methods with associated errors (coefficient of variance, CV). Briefly, our strategy for using this model was to run all combinations of stratification and load estimate methods and choose the estimate with the lowest associated error. All load estimates selected were within the guidelines (CV<0.3) recommended in the MCES SOP.

4.3 Results

4.3.1 Ingrowth Modeling

The three optimization techniques for estimating Pb_w yielded different levels of ^{210}Po ingrowth depending on the OM used and the trend in ^{210}Po activities measured during the ingrowth period. Figure 4.5 shows three representative plots illustrating these varying patterns of ingrowth. In some cases there was no ingrowth and activities were steady or decreased over the incubation period (Fig. 4.5A). In this scenario ^{210}Pb and ^{210}Po are initially at secular equilibrium, and therefore Pb_w is zero. In other cases, the modeled Pb_0 parameter (y-intercept) goes to zero and all Pb_{eq} is attributed to Pb_w (Fig. 4.5C). Most cases, however, were an intermediate of these two end-members and yielded measurable activities for both Pb_w and Pb_0 (Fig 4.5B).

A total of 24 samples were collected at each primary sampling location, and 5 samples at the Minneapolis site. Relatively few samples (0-3) were excluded at each site for a given OM because of poor optimization results of the three unknown variables (Pb_w, t_1, and Pb_0). Table 1 contains a summary of Pb_w ingrowth results for individual samples at each site for all three OMs. Many samples have a minimum Pb_w activity of 0 Bq g^{-1}. However, maximum activities are generally much larger than the minimum, and the standard deviation indicates a large variance in all cases. Mean Pb_w activities increase incrementally from Jordan to Fort Snelling to St. Paul and then decrease slightly at LD3. The Minneapolis site, representing a limited number of samples from the headwaters Mississippi River (HMR), has mean Pb_w activities more than 2.5x greater than the other sites for OM1 and OM2, and 4x greater for OM3.

Mean Pb_{eq}, the sum of Pb_w and Pb_0, is very similar between model runs at each site. The mean Pb_{eq} activities at Jordan for OM1, OM2, and OM3 are 0.038, 0.038, and 0.040 Bq g^{-1}, respectively. Pb_{eq} activities increase at Fort Snelling to 0.067 (OM1), 0.070 (OM2), and 0.067 (OM3) Bq g^{-1}. At St. Paul, below the confluence of HMR, the activities again increase significantly and are very consistent (0.146 for OM1, OM2, and OM3). At LD3 Pb_{eq} activities decrease slightly from St. Paul and are 0.130 (OM1), 0.130 (OM2), and 0.133 (OM3) Bq g^{-1}.

4.3.2 Flux Modeling

Annual load estimates were made at each of the four primary sites for both Pb_w and Pb_{eq} using the Flux32 model (Table 2). Annual estimates of Pb_{eq} are quite consistent among OMs at each site (within 5%), and loads increase incrementally downstream from Jordan to LD3 in all cases.

Annual estimates for Pb_w loads are relatively low at Jordan (0.686–1.81 x10^{10} Bq yr^{-1}) and Fort Snelling (0.604–0.931 x10^{10} Bq yr^{-1}) and dramatically higher at St. Paul (2.61–4.24 x10^{10} Bq yr^{-1}) and LD3 (2.63–5.72 x10^{10} Bq yr^{-1}) (Fig. 4.6A, Table 2). The largest difference between Pb_w load estimates for OM1 and OM3 occurs at Jordan (163% increase), which is higher than at LD3 (117% increase). Pb_w load estimate increases between OM1 and OM3 at Fort Snelling and St. Paul are more modest (54% and 62%, respectively). Errors are relatively consistent throughout, with the exception of higher errors for Pb_w estimates at the LD3 site for all three OMs (Table 1). The Pb_w/Pb_{eq} ratio – the fraction of Pb_{eq} attributed to Pb_w – is 0.44 (OM3) at Jordan and decreases slightly to

0.32 at Fort Snelling (Fig. 4.6B). This ratio is quite consistent for the remaining three sites (Minneapolis, 0.90; St. Paul, 0.85; and LD3, 0.89). Note that the Minneapolis site is based on the average activity of only four samples (Table 1) and hence loads could not be reliably modeled as was done for the four primary sample locations.

4.4 Discussion

The objective of this study is to determine if the amount of ^{210}Pb deposited directly to the water surface is significant relative to the amount entering on eroded particles. Our approach models the ingrowth of ^{210}Po directly following sample collection. If significant ingrowth occurs, then a measurable amount of ^{210}Pb is from atmospheric deposition to the water surface.

4.4.1 Ingrowth Modeling

Our ingrowth model successfully solves the set of three simultaneous equations (Eqs. 2–4) for the unknown variables Pb_w, t_1, and Pb_0, and then uses those values to plot the non-linear ingrowth curve fitted to three measured data points. The model is particularly sensitive near the vertical-axis intercept where the activity component has the largest rate of change and is mostly affected by the t_1 variable. In order to explore this relationship and to obtain a minimum estimate of Pb_w, we ran the model for each sample with different constraints on t_1.

Optimization method 1 (OM1) constrains t_1 to zero. Essentially OM1 is estimating Pb_w as if the activity at the time of sample collection was entirely Pb_0. The

ingrowth that follows sample collection is then attributed to Pb_w. OM1 is thus a minimum estimate of Pb_w and assumes there is no storage or transit time for the directly deposited ^{210}Pb in the river channel or floodplain. OM2 estimates higher Pb_w values by constraining t_1 based on river flow velocity and travel distance. Here we set t_1 to the time, estimated under baseflow conditions, it would take a package of water to reach the sampling site from either the headwaters or the last major impoundment. While OM2 takes into account water residence time, it is not a maximum estimate of Pb_w because it does not consider sediment storage of the suspended particle load. Neither is it a minimum estimate in the strictest sense, because Pb_w may be deposited to the surface of the water at any time during transit to the sampling station. OM3 allows t_1 to vary to achieve the best possible fit of the model to the actual measured points. Although OM3 represents the maximum Pb_w values we can model using this approach, the actual Pb_w component could be higher if there is significant temporary storage of ^{210}Pb in the river channel or floodplain. Storage is the major source of uncertainty in the study. If particles are deposited in the floodplain for a period of time greater than the ingrowth life of ^{210}Po (i.e. six half-lives) and then re-suspended and delivered to the sampling site, that component of "aged" Pb_w will register in the model as Pb_0, because ^{210}Po will be at equilibrium with ^{210}Pb.

4.4.2 ^{210}Pb Load Estimates

In general ^{210}Pb loads increase in the downstream direction of the four primary sampling sites. The exception is Fort Snelling where Pb_w loads decrease from Jordan, but

Pb_{eq} increases (Table 2, Fig. 4.6A). Overall there is a decrease in Pb_w/Pb_{eq} in this stretch of the Minnesota River (MNR) (Fig. 4.6B), which may be evidence of gaining particles with little or no Pb_w, perhaps a result of floodplain exchange. Moreover, there are no major tributaries to transport fresh Pb_w to this river reach, which may contribute further to the observed drop-off in Pb_w between Jordan and Fort Snelling.

Loading of both Pb_w and Pb_{eq} increase dramatically between Fort Snelling and St. Paul, despite the fact that these sampling sites are only 10 km apart. However, the headwaters Mississippi (HMR) enters between Fort Snelling and St. Paul, more than doubling the watershed area between these two sites and increasing the surface area of water. Pb_w/Pb_{eq} increases from 0.32 at Fort Snelling to 0.85 at St. Paul (OM3). Therefore, it would stand to reason that the Pb_w component must be more significant, relative to Pb_{eq}, in HMR than in MNR. However, Pb_w/Pb_{eq} ratios are very similar at Minneapolis and St. Paul, which would indicate that the Pb_w component is equally represented, relative to Pb_{eq}, at the two sites, indicating a dominance of the HMR signal at St. Paul. Keep in mind there is a very limited number of samples (n=4) collected at Minneapolis and these samples represent only a narrow range of flow and seasonal conditions.

4.4.3 Implications to Sediment Fingerprinting

Direct atmospheric deposition of ^{210}Pb to the river surface (Pb_w) is a significant component of the total excess ^{210}Pb (Pb_{eq}) in the large watersheds studied here. At a minimum, OM1 indicates 20-30% of Pb_{eq} can be attributed to Pb_w at Jordan and Fort

Snelling; this percentage increases to 40-55% at Minneapolis, St. Paul, and LD3. However, it is likely that percentages of Pb_w, as estimated by OM3, are higher (30-45%) at Jordan and Fort Snelling, and much higher (85-90%) at the remaining three sites. MNR has greater sediment concentration than HMR or upper Mississippi River (UMR), so its lower Pb_w fraction is likely a result of dilution by the high sediment load (from field erosion) relative to river surface area. MNR was also part of the Glacial River Warren valley, which created an over-widened river valley that MNR now occupies. This geometry result in greater floodplain exchange in MNR so that suspended-sediment samples collected in this basin have a greater portion of 'aged' ^{210}Pb that provides little or no ^{210}Po ingrowth. If this were the case, we might expect to see some decrease in the Pb_w/Pb_{eq} ratio between St. Paul and LD3 because UMR is an extension of the River Warren channel; ratios for OM1 and OM2 do decrease slightly, but the ratio for OM3 does not. It could be that UMR has steady Pb_w/Pb_{eq} ratios because of the added watershed area, and thus, added Pb_w is balanced by high floodplain exchange. Despite these differences between MNR and UMR, the Pb_w component of ^{210}Pb is quite high for all sites in this study, and the direct deposition of Pb and Po isotopes to the water surface should be considered in any atmospheric radioisotopic fingerprinting work on watersheds of this magnitude.

4.5 Conclusions

The methods we developed here were successful for measuring the amount of ^{210}Pb deposited directly to the water surface (Pb_w). As expected, many samples taken

from these large rivers displayed ^{210}Po ingrowth, indicating significant Pb_w inputs. Error estimations, however, were a bit more problematic. Estimations of Pb_w minima, based on the first optimization method (OM1), were reliable. OM3 represents the maximum Pb_w estimations presented in this study, but because OM3 is the best fit of each ingrowth curve, true maximum values may be higher. Individual Pb_w samples varied widely (0–100% of Pb_{eq}), illustrating the transient nature of direct atmospheric deposition, likely related to localized rainfall events somewhere in the watershed prior to sample collection. Pb_w can easily be corrected for using this method if performed on individual samples used for fingerprinting studies.

Modeling annual loads based on our bi-weekly sampling program was successful, but resulted in significant errors. These errors would have likely been greatly reduced with more frequent sampling, which is prohibitive due to high cost and time associated with each sample. The percentage of Pb_{eq} attributed to Pb_w for annual load estimates ranged from 20% at Fort Snelling (OM1) to 89% at LD3 (OM3). There appears to be a correlation between Pb_w contribution and watershed size, although the relationship is likely much more complicated and could involve water surface area and floodplain exchange dynamics in these large rivers.

Tables

Table 1. Summary of Pb_w Ingrowth Results

		Min Bq g^{-1}	**Max** Bq g^{-1}	**Mean** Bq g^{-1}	**Stdev** Bq g^{-1}	**Samples** n
	Jordan	0.000	0.058	0.012	0.013	23
	Fort Snelling	0.000	0.172	0.031	0.038	23
OM1	St. Paul	0.004	0.365	0.071	0.082	24
	LD3	0.000	0.208	0.045	0.058	24
	Minneapolis	0.053	0.562	0.281	0.260	4
	Jordan	0.000	0.071	0.015	0.016	23
	Fort Snelling	0.000	0.225	0.042	0.051	22
OM2	St. Paul	0.006	0.482	0.094	0.108	24
	LD3	0.000	0.282	0.061	0.079	24
	Minneapolis	0.006	0.622	0.250	0.284	5
	Jordan	0.000	0.070	0.019	0.017	21
	Fort Snelling	0.000	0.233	0.048	0.053	23
OM3	St. Paul	0.013	0.513	0.115	0.110	24
	LD3	0.000	0.320	0.089	0.090	23
	Minneapolis	0.142	0.818	0.466	0.347	4

Table 2. Summary of Annual Load Estimates (10^{10} Bq yr^{-1}) and Associated Errors

	OM1				OM2				OM3			
	Pb_w	CV	Pb_{eq}	CV	Pb_w	CV	Pb_{eq}	CV	Pb_w	CV	Pb_{eq}	CV
Jordan	0.686	0.155	2.15	0.126	0.890	0.153	2.14	0.129	1.81	0.166	2.06	0.080
Ft. Snelling	0.604	0.185	2.95	0.186	0.790	0.192	2.95	0.187	0.931	0.197	2.95	0.188
St. Paul	2.61	0.144	5.01	0.098	3.45	0.144	5.01	0.098	4.24	0.188	5.00	0.098
LD3	2.63	0.292	6.33	0.189	3.57	0.292	6.34	0.189	5.72	0.259	6.41	0.185

Figures

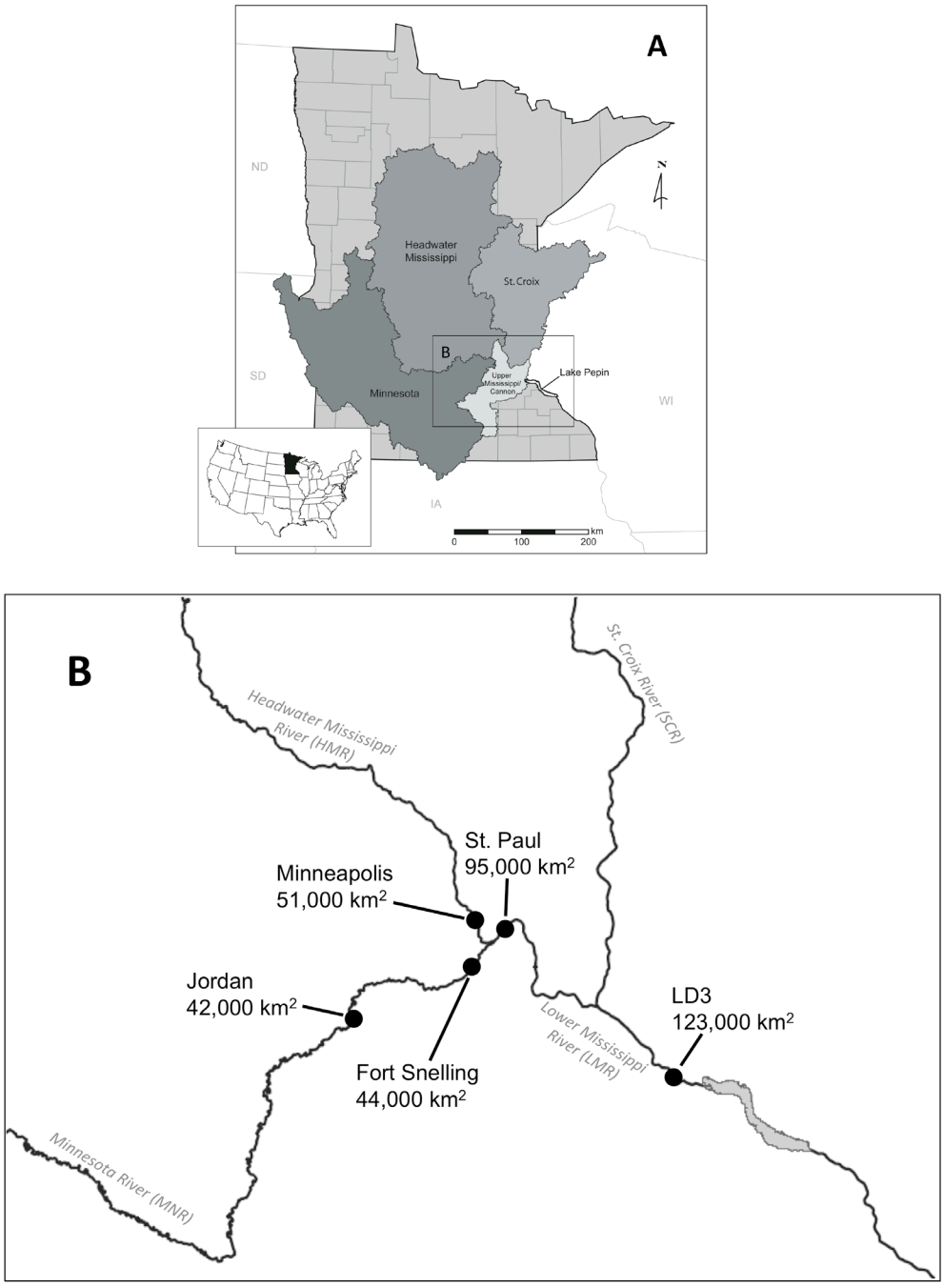

Fig. 4.1 Map of the Lake Pepin watershed (A), predominantly draining three major watersheds in Minnesota, USA: the Minnesota River, Headwater Mississippi River, and St. Croix River. Inset (B) shows the locations of the five sampling sites in this study, along with the watershed area above each site.

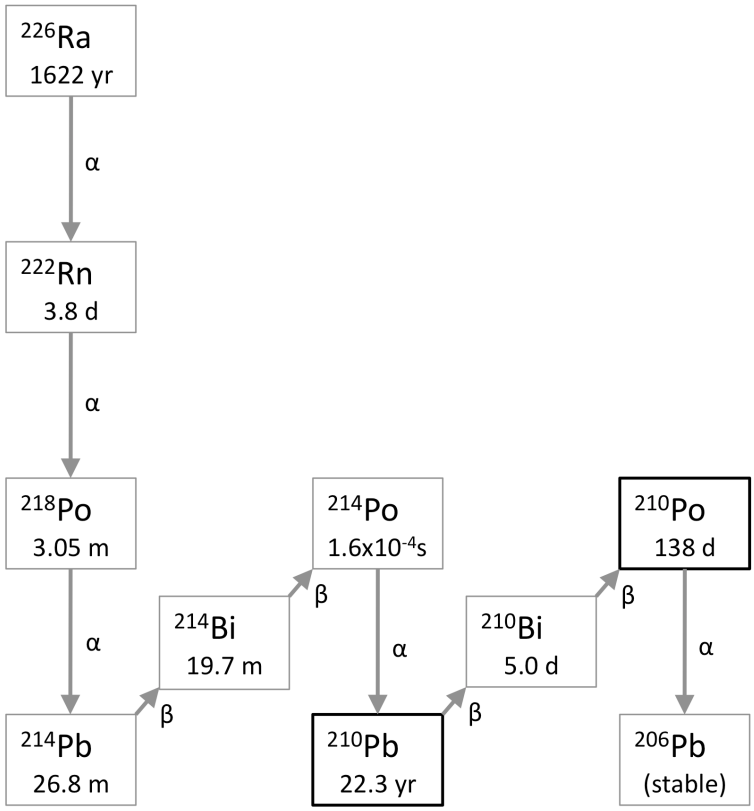

Fig. 4.2 Decay chain of radium-226 to stable lead.

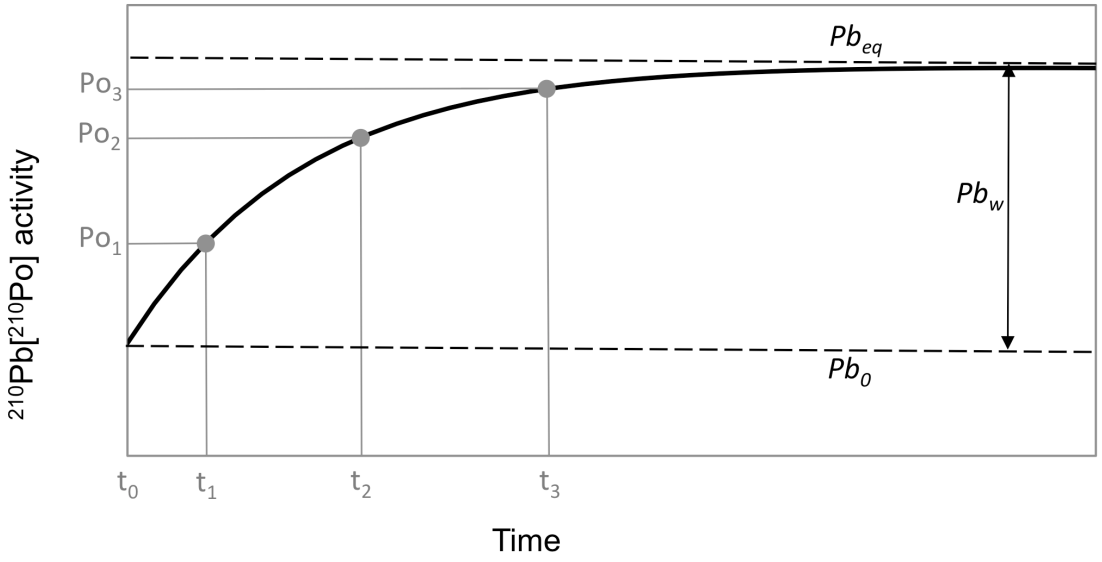

Fig. 4.3 Theoretical ingrowth curve of atmospherically deposited ^{210}Pb. Points represent three measurements of ^{210}Po taken at different times during ingrowth. The y-intercept represents the initial activity of ^{210}Pb prior to additional atmospheric loading (Pb_0). The asymptote of the curve is the new equilibrium activity (Pb_{eq}), and the amount of freshly deposited ^{210}Pb (Pb_w) is the amount of ingrowth from Pb_0 to Pb_{eq}.

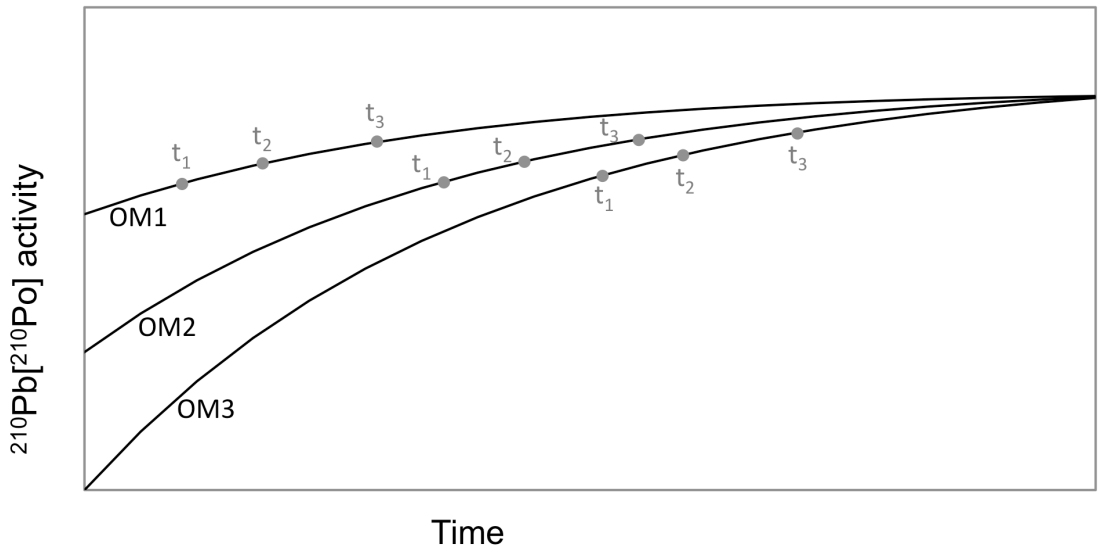

Fig. 4.4 Hypothetical ingrowth curves shown for the three different optimization methods (OM) used for ingrowth modeling. Activities are measures at three discrete times during ingrowth (t_1, t_2, and t_3); corresponding points on each curve have the same activity and time separation between points, however, t_1 is constrained differently in each OM model run because it is unknown. Changing t_1, as illustrated here, results in significant differences in Pb_0 (the y-intercept) between OMs, which then has an effect on Pb_w (Fig. 4.3). Therefore OM1, where t_1 is set to a minimum value, is a minimum estimate of Pb_w; OM2 has a t_1 value set higher, so Pb_w is higher. OM3 allows t_1 to vary, unconstrained, for optimal fit of measured data; this resulted in Pb_w values that were generally greater than OM1 or OM2 Pbw values, as illustrated here.

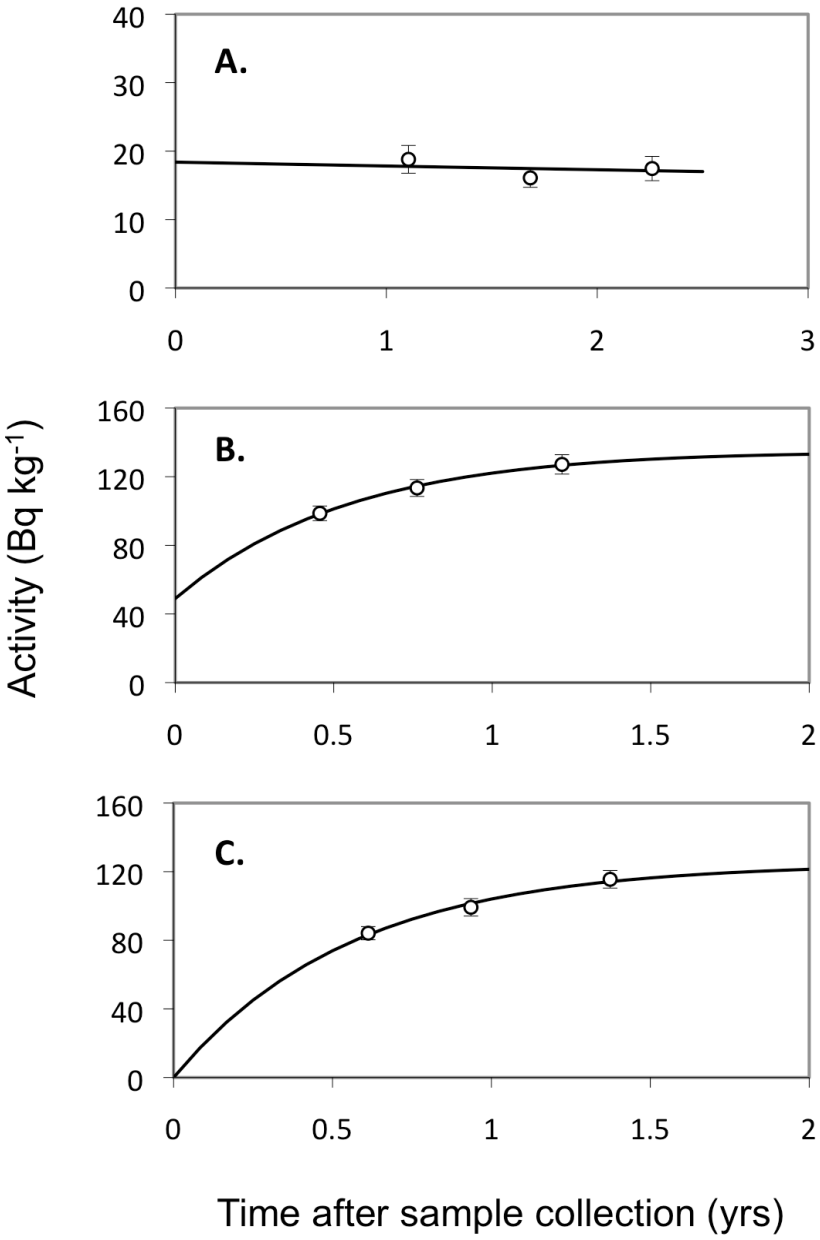

Fig. 4.5 Representative plots of three optimized curves illustrating the degree of ^{210}Po ingrowth modeling results; error bars represent analytical uncertainty. Several optimization models result in no ingrowth of ^{210}Po (A) where the Pb_w component is zero. Other samples result in maximum ingrowth (C) where the vertical-axis intercept is zero and all Pb_{eq} is attributed to Pb_w. The majority of modeled results have some component of Pb_{eq} and Pb_w and yield curves (B) that display some degree of ingrowth and initial ^{210}Pb activity (Pb_0).

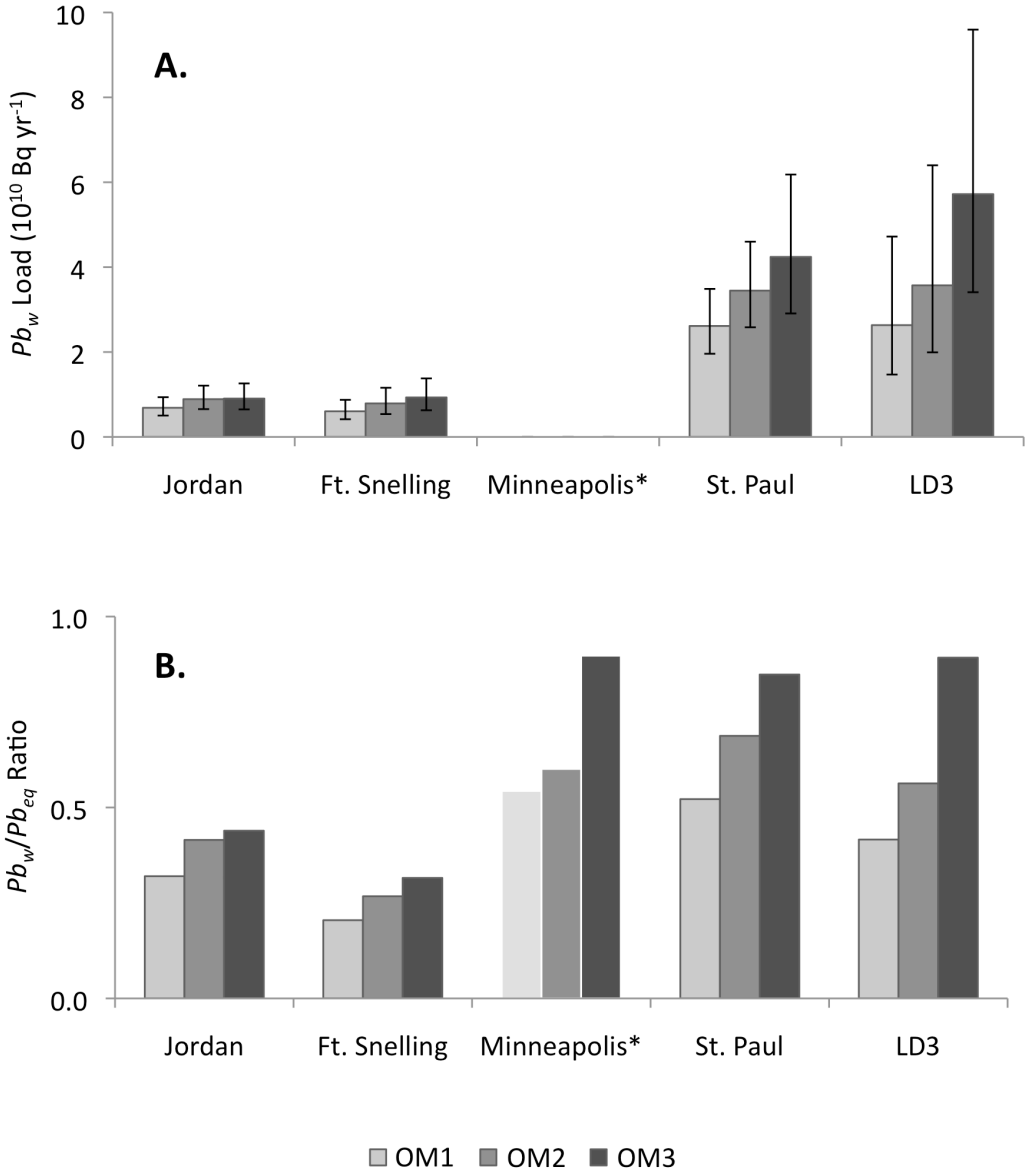

Fig. 4.6 (A) Annual Pb_w load estimates from Flux32-model runs at the four primary sample locations for the three optimization methods. Loads are relatively small in the MNR basin (Jordan and Ft. Snelling) and increase dramatically at St. Paul (below the confluence of MNR and HMR), and again at LD3. Errors were calculated using the coefficient of variance (CV) output from model results. (B) Pb_w/Pb_{eq} ratio – the portion of Pb_{eq} attributed to Pb_w – at each sample location. *Ratios at the four primary sites are based on annual load estimates, but because of a limited number of samples at the Minneapolis site, annual loads could not be calculated; hence ratios for this site are based on mean activities of only four (OM1 and OM3) or five (OM2) samples. Ratios for OM3 at Jordan and Ft. Snelling indicate a significant fraction (0.3–0.5) of Pb_{eq} is from direct atmospheric deposition of ^{210}Pb (Pb_w), and the Pb_w component dominates at Minneapolis, St. Paul, and LD3 (0.90, 0.85, and 0.89, respectively).

Complete Reference List

Aalto, R., Lauer, J.W., Dietrich, W.E., 2008. Spatial and temporal dynamics of sediment accumulation and exchange along Strickland River floodplains (Papua New Guinea) over decadal-to-centennial timescales. J. Geophys. Res, 113, F01S04.

Aalto, R., Nittrouer, C.A., 2012. 210Pb geochronology of flood events in large tropical river systems. Philosophical Transactions of the Royal Society A: Mathematical, Physical and Engineering Sciences, 370(1966), 2040-2074.

Appleby, P.G., 2001. Chronostratigraphic Techniques in Recent Sediments. In: W.M. Last, J.P. Smol (Eds.), Tracking Environmental Change Using Lake Sediments. Developments in Paleoenvironmental Research. Springer Netherlands, pp. 171-203.

Appleby, P.G., Oldfield, F., 1978. The calculation of lead-210 dates assuming a constant rate of supply of unsupported 210Pb to the sediment. CATENA, 5(1), 1-8.

Appleby, P.G., Oldfield, F., Thompson, R., Huttunen, P., Tolonen, K., 1979. 210Pb dating of annually laminated lake sediments from Finland. Nature, 280(5717), 53-55.

Balogh, S., Engstrom, D., Almendinger, J., McDermott, C., Hu, J., Nollet, Y., Meyer, M., Johnson, D., 2009. A sediment record of trace metal loadings in the Upper Mississippi River. J. Paleolimnol., 41(4), 623-639.

Balogh, S.J., Engstrom, D.R., Almendinger, J.E., Meyer, M.L., Johnson, D.K., 1999. History of Mercury Loading in the Upper Mississippi River Reconstructed from the Sediments of Lake Pepin. Environmental Science and Technology, 33, 3297-3302.

Balogh, S.J., Nollet, Y.H., 2008. Mercury mass balance at a wastewater treatment plant employing sludge incineration with offgas mercury control. Sci. Total Environ., 389(1), 125-131.

Battarbee, R.W., 1978. Biostratigraphical evidence for variations in the recent pattern of sediment accumulation in Lough Neagh, N. Ireland. Verh. Internat. Verein. Limnol., 20, 624-629.

Belmont, P., 2011. Floodplain width adjustments in response to rapid base level fall and knickpoint migration. Geomorphology, 128(1-2), 92-102.

Belmont, P., Gran, K.B., Schottler, S.P., Wilcock, P.R., Day, S.S., Jennings, C., Lauer, J.W., Viparelli, E., Willenbring, J.K., Engstrom, D.R., Parker, G., 2011. Large Shift in Source of Fine Sediment in the Upper Mississippi River. Environ. Sci. Technol., 45(20), 8804-8810.

Bennion, H., Battarbee, R., 2007. The European Union Water Framework Directive: opportunities for palaeolimnology. J. Paleolimnol., 38(2), 285-295.

Birks, H., Birks, H., 2006. Multi-proxy studies in palaeolimnology. Vegetation History and Archaeobotany, 15(4), 235-251.

Blumentritt, D., Engstrom, D., Balogh, S., 2013. A novel repeat-coring approach to reconstruct recent sediment, phosphorus, and mercury loading from the upper Mississippi River to Lake Pepin, USA. J. Paleolimnol., 1-12.

Blumentritt, D.J., Wright Jr., H.E., Stefanova, V., 2009. Formation and early history of Lakes Pepin and St. Croix of the Mississippi River. J. Paleolimnol., 41(4), 545-562.

Brachfeld, S.A., Banerjee, S.K., 2000. A new high-resolution geomagnetic relative paleointensity record for the North American Holocene; a comparison of

sedimentary and absolute intensity data. Journal of Geophysical Research, 105(B1), 821-834.

Brenner, M., Schelske, C.L., Keenan, L.W., 2001. Historical rates of sediment and nutrient accumulation in marshes of the Upper St. Johns River Basin, Florida, USA. J. Paleolimnol., 26(3), 241-257.

Brezonik, P.L., Engstrom, D.R., 1998. Modern and historic accumulation rates of phosphorus in Lake Okeechobee, Florida. J. Paleolimnol., 20(1), 31-46.

Dean, W.E., 1974. Determination of carbonate and organic matter in calcareous sediments and sedimentary rocks by loss on ignition: Comparison with other methods. Journal of Sedimentary Petrology, 44(1), 242-248.

Dearing, J., 1999. Magnetic susceptibility. In: J. Walden, F. Oldfield, J. Smith (Eds.), Environmental magnetism: A pracitcal guide. Quaternary Research Association, London, pp. 35-62.

Dobbs, C.A., Mooers, H., 1990. A Phase I archaeological and geomorphological study of navigation pool 4, Upper Mississippi River. 44, Institute for Minnesota Archaeology, Minneapolis.

Drevnick, P.E., Engstrom, D.R., Driscoll, C.T., Swain, E.B., Balogh, S.J., Kamman, N.C., Long, D.T., Muir, D.G.C., Parsons, M.J., Rolfhus, K.R., Rossmann, R., 2012. Spatial and temporal patterns of mercury accumulation in lacustrine sediments across the Laurentian Great Lakes region. Environ. Pollut., 161(0), 252-260.

Eakins, J.D., Morrison, R.T., 1978. NEW PROCEDURE FOR DETERMINATION OF PB-210 IN LAKE AND MARINE-SEDIMENTS. International Journal of Applied Radiation and Isotopes, 29(9-10), 531-536.

Egli, R., 2004. Characterization of individual rock magnetic components by analysis of remanence curves, 1. Unmixing natural sediments. Studia Geophysica Et Geodaetica, 48(2), 391-446.

Engstrom, D., Rose, N., 2013. A whole-basin, mass-balance approach to paleolimnology. J. Paleolimnol., 1-15.

Engstrom, D.R., Almendinger, J.E., Wolin, J.A., 2009. Historical changes in sediment and phosphorus loading to the upper Mississippi River: mass-balance reconstructions from the sediments of Lake Pepin. J. Paleolimnol., 41(4), 563-588.

Engstrom, D.R., Wright Jr., H.E., 1984. Chemical stratigraphy of lake sediments as a record of environmental change. In: E.Y. Haworth, W. Tutin, J.W.G. Lund (Eds.), Lake Sediments and Environmental History: Studies in Palaeolimnology and Palaeoecology in Honour of Winifred Tutin. University of Minnesota Press, pp. 11-67.

Eriksson, M.G., Sandgren, P., 1999. Mineral magnetic analyses of sediment cores recording recent soil erosion history in central Tanzania. Palaeogeogr., Palaeoclimatol., Palaeoecol., 152(3,Äì4), 365-383.

Evans, M.E., Heller, F., 2003. Environmental Magnetism: Principles and Applications of Environmagnetics. Academic Press, Elsevier Science, Amsterdam.

Eyster-Smith, N.M., 1977. Holocene pollen stratigraphy of Lake St. Croix, Minnesota-Wisconsin, and some aspects of the depostional history. M.S. Thesis (M.S.), M.S. Thesis, University of Minnesota., Minneapolis.

Fisher, T.G., 2003a. Chronology of glacial Lake Agassiz meltwater routed to the Gulf of Mexico. Quaternary Research, 59(2), 271-276.

Fisher, T.G., 2003b. Chronology of glacial Lake Agassiz meltwater routed to the Gulf of Mexico. Quatern. Res., 59, 271-276.

Gälman, V., Petterson, G., Renberg, I., 2006. A comparison of sediment varves (1950-2003 AD) in two adjacent lakes in northern Sweden. J. Paleolimnol., 35(4), 837-853.

Gälman, V., Rydberg, J., de-Luna, S.S., Bindler, R., Renberg, I., 2008. Carbon and Nitrogen Loss Rates during Aging of Lake Sediment: Changes over 27 Years Studied in Varved Lake Sediment. Limnol. Oceanogr., 53(3), 1076-1082.

Gran, K.B., Belmont, P., Day, S.S., Jennings, C., Johnson, A., Perg, L., Wilcock, P.R., 2009. Geomorphic evolution of the Le Sueur River, Minnesota, USA, and implications for current sediment loading. Geological Society of America Special Papers, 451, 119-130.

Gumus-Dawes, B., 2012. Population Returns to the Core: The Twin Cities Metropolitan Area in 2011. 74-11-027, Metropolitan Council Publication No. 74-11-027, St. Paul.

He, Q., Walling, D.E., 1996. Interpreting particle size effects in the adsorption of ^{137}Cs and unsuported ^{210}Pb by mineral soils and sediments. J. Environ. Radioact., 30(2), 117-137.

Heiri, O., Lotter, A.F., Lemcke, G., 2001. Loss on ignition as a method for estimating organic and carbonate content in sediments: reproducibility and comparability of results. J. Paleolimnol., 25, 101-110.

Heiskary, S., Vavricka, M., 1993. Lake Pepin water quality. Section 3, Mississippi river phosphorus study. Minnesota Pollution Control Agency, St. Paul, MN, 105 pp.

Hiriart-Baer, V.r.P., Milne, J.E., Marvin, C.H., 2011. Temporal trends in phosphorus and lacustrine productivity in Lake Simcoe inferred from lake sediment. J. Great Lakes Res., 37(4), 764-771.

Hodell, D.A., Schelske, C.L., 1998. Production, Sedimentation, and Isotopic Composition of Organic Matter in Lake Ontario. Limnol. Oceanogr., 43(2), 200-214.

James, T.R., Chimney, M.J., Sharfstein, B., Engstrom, D.R., Schottler, S.P., East, T., Jin, K.-R., 2008. Hurricane effects on a shallow lake ecosystem, Lake Okeechobee, Florida (USA). Fundamental and Applied Limnology / Archiv für Hydrobiologie, 172(4), 273-287.

James, W.F., Barko, J.W., 2004. Diffusive fluxes and equilibrium processes in relation to phosphorus dynamics in the Upper Mississippi River. River Res. Appl., 20(4), 473-484.

Johnson, D.K., Aasen, P.W., 1989. The Metropolitan Wastewater Treatment Plant and the Mississippi River: 50 Years of Improving Water Quality Journal of the Minnesota Academy of Science, 55(1), 134-138.

Kelley, D.W., Brachfeld, S.A., Nater, E.A., Wright Jr., H.E., 2006. Sources of sediment in Lake Pepin on the Upper Mississippi River in response to Holocene climatic changes. J. Paleolimnol., 35, 193-206.

Kelley, D.W., Nater, E.A., 2000. Source apportionment of lake bed sediments to watersheds in an Upper Mississippi basin using a chemical mass balance method. Catena, 41, 277-292.

Klaminder, J., Appleby, P., Crook, P., Renberg, I., 2012. Post-deposition diffusion of 137Cs in lake sediment: Implications for radiocaesium dating. Sedimentology, 59(7), 2259-2267.

Knox, J.C., 2001. Agricultural influence on landscape sensitivity in the Upper Mississippi River Valley. Catena, 42, 193-224.

Lafrancois, B.M., Magdalene, S., Johnson, D.K., 2009. Recent water quality trends and a comparison to sediment-core records for two riverine lakes of the Upper Mississippi River basin: Lake St. Croix and Lake Pepin. J. Paleolimnol., 41(4), 603-622.

Lascu, I., Banerjee, S.K., Berquó, T.S., 2010. Quantifying the concentration of ferrimagnetic particles in sediments using rock magnetic methods. Geochemistry, Geophysics, Geosystems, 11(8), Q08Z19.

Lascu, I., McLauchlan, K.K., Myrbo, A., Leavitt, P.R., Banerjee, S.K., 2012. Sediment-magnetic evidence for last millennium drought conditions at the prairie–forest ecotone of northern United States. Palaeogeogr., Palaeoclimatol., Palaeoecol., 337,Äì338(0), 99-107.

Lepper, K., Fisher, T.G., Hajdas, I., Lowell, T.V., 2007. Ages for the Big Stone Moraine and the oldest beaches of glacial Lake Agassiz: Implications for deglaciation chronology. Geology, 35(7), 667-670.

Liu, K.-b., Fearn, M.L., 1993. Lake-sediment record of late Holocene hurricane activities from coastal Alabama. Geology, 21(9), 793-796.

Lund, S.P., Banerjee, S.K., 1985. Late Quaternary paleomagnetic field secular variation from two Minnesota lakes. Journal of Geophysical Research, 90(B1), 803-825.

Mabit, L., Benmansour, M., Walling, D.E., 2008. Comparative advantages and limitations of the fallout radionuclides Cs-137, Pb-210(ex) and Be-7 for assessing soil erosion and sedimentation. J. Environ. Radioact., 99(12), 1799-1807.

Maurer, W.R., Claflin, T.O., Rada, R.G., Rogala, J.T., 1995. Volume loss and mass-balance for selected physicochemical constituents in Lake Pepin, upper

Mississippi River, USA Regulated Rivers-Research & Management, 11(2), 175-184.

McNeary, D., Baskaran, M., 2007. Residence times and temporal variations of 210Po in aerosols and precipitation from southeastern Michigan, United States. J. Geophys. Res., 112(D4), D04208.

Mrachek, J.H., Sullivan, J.E., Mooers, H.D., 1994. The development of a model of archaeological sensitivity for landforms in the Red Wing locality, Pierce County, Wisconsin. Geology Department, University of Minnesota Duluth, unpublished report.

Mulla, D.J., Sekely, A.C., 2009. Historical trends affecting accumulation of sediment and phosphorus in Lake Pepin, upper Mississippi River, USA. J. Paleolimnol., 41(4), 589-602.

Musser, K., Kudelka, S., Moore, R., 2009. Minnesota River Trends Report.

Nagle, G.N., Fahey, T.J., Ritchie, J.C., Woodbury, P.B., 2007. Variations in sediment sources and yields in the Finger Lakes and Catskills regions of New York. Hydological Processes, 21, 828-838.

Nowaczyk, N., 2002. Logging of Magnetic Susceptibility. In: W. Last, J. Smol (Eds.), Tracking Environmental Change Using Lake Sediments. Developments in Paleoenvironmental Research. Springer Netherlands, pp. 155-170.

Nowaczyk, N., Melles, M., Minyuk, P., 2007. A revised age model for core PG1351 from Lake El,Äôgygytgyn, Chukotka, based on magnetic susceptibility variations tuned to northern hemisphere insolation variations. J. Paleolimnol., 37(1), 65-76.

Nozaki, Y., DeMaster, D.J., Lewis, D.M., Turekian, K.K., 1978. Atmospheric 210Pb Fluxes Determined From Soil Profiles. J. Geophys. Res., 83(C8), 4047-4051.

Owens, P.N., Blake, W.H., Giles, T.R., Williams, N.D., 2012. Determining the effects of wildfire on sediment sources using Cs-137 and unsupported Pb-210: the role of landscape disturbances and driving forces. J. Soils Sed., 12(6), 982-994.

Poet, S.E., Moore, H.E., Martell, E.A., 1972. Lead 210, Bismuth 210, and Polonium 210 in the Atmosphere: Accurate Ratio Measurement and Application to Aerosol Residence Time Determination. J. Geophys. Res., 77(33), 6515-6527.

Rippey, B., Anderson, N.J., Renberg, I., Korsman, T., 2008. The accuracy of methods used to estimate the whole-lake accumulation rate of organic carbon, major cations, phosphorus and heavy metals in sediment. J. Paleolimnol., 39(1), 83-99.

Rose, N.L., Yang, H., 2007. Temporal and spatial patterns of spheroidal carbonaceous particles (SCPs) in sediments, soils and deposition at Lochnagar. In: N.L. Rose (Ed.), Lochnagar: The Natural History of a Mountain Lake. Springer, Dordrecht, pp. 403-423.

Rydberg, J., Galman, V., Renberg, I., Bindler, R., Lambertsson, L., Martinez-Cortizas, A., 2008. Assessing the stability of mercury and methylmercury in a varved lake sediment deposit. Environ. Sci. Technol., 42(12), 4391-4396.

Sandgren, P., Snowball, I., 2002. Application of Mineral Magnetic Techniques to Paleolimnology. In: W. Last, J. Smol (Eds.), Tracking Environmental Change Using Lake Sediments. Developments in Paleoenvironmental Research. Springer Netherlands, pp. 217-237.

Schottler, S., Engstrom, D.R., Blumentritt, D.J., 2010. Fingerprinting sources of sediment in large agricultural river systems. Final Report to Minnesota Pollution Control Agency, St. Paul.

Schottler, S.P., Ulrich, J., Belmont, P., Moore, R., Lauer, J.W., Engstrom, D.R., Almendinger, J.E., 2013. Twentieth century agricultural drainage creates more erosive rivers. Hydrological Processes, 1-11.

Shay, C.T., 1967. Vegetation history of the southern Lake Agassiz Basin during the past 12,000 years. In: W.J. Mayer-Oakes (Ed.), Life, Land, and Water, Proceedings of the 1960 Conference on Environmental Studies of the Glacial Lake Agassiz Basin. University of Manitoba Press.

Teller, J.T., 1987. Proglacial lakes and the southern margin of the Laurentide ice sheet. In: W.F. Ruddiman, H.E. Wright, Jr. (Eds.), North America and Adjacent Ocean during the Last Deglaciation. The Geology of North America. Geol. Soc. Am., Boulder, pp. 38-69.

Thompson, R., Battarbee, R.W., O'Sullivan, P.E., Oldfield, F., 1975. Magnetic susceptibility of lake sediments. Limnol. Oceanogr., 20(5), 687-698.

Thompson, R., Clark, R.M., Boulton, G., 2012. Core Correlation. In: H.J.B. Birks, A.F. Lotter, S. Juggins, J.P. Smol (Eds.), Tracking Environmental Change Using Lake Sediments. Developments in Paleoenvironmental Research. Springer Netherlands, pp. 415-430.

Thompson, R., Oldfield, F., 1986. Environmental Magnetism. Allen and Unwin, London.

Tokieda, T., Yamanaka, K., Harada, K.O.H., Tsunogai, S., 1996. Seasonal variations of residence time and upper atmospheric contribution of aerosols studied with Pb-210, Bi-210, Po-210 and Be-7. Tellus B, 48(5), 690-702.

Triplett, L., Engstrom, D., Edlund, M., 2009. A whole-basin stratigraphic record of sediment and phosphorus loading to the St. Croix River, USA. J. Paleolimnol., 41(4), 659-677.

Triplett, L.D., Engstrom, D.R., Conley, D.J., Schellhaass, S.M., 2008. Silica fluxes and trapping in two contrasting natural impoundments of the upper Mississippi River. Biogeochemistry, 87(3), 217-230.

Walker, W.W., 1999. Simplified procedures for eutrophication assessment and prediction: user manual. (Instruction report W-96-2), U.S. Army Engineer Research and Development Center, Vicksburg, MS.

Walling, D.E., Owens, P.N., Leeks, G.J.L., 1999. Fingerprinting suspended sediment sources in the catchment of the River Ouse, Yorkshire, UK. Hydological Processes, 13, 955-975.

Walling, D.E., Woodward, J.C., 1992. Use of radiometric fingerprints to drive information on suspended sediment sources, Erosion and Sediment Transport Monitoring Programmes in River Basins (proceedings of the Oslo Symposium, August 1992). Publication no. 210. IAHS.

Winchell, N.H., Upham, W., 1884. 1872-1882 The Geology of Minnesota: Vol.1 of the final report, The Geological and Natural History Survey of Minnesota, Minneapolis.

Wright, H.E., Jr., 1993. History of the landscape in the Itasca region. Special Paper - Geological Society of America, 276, 7-17.

Wright, H.E., Jr., Lease, K., Johnson, S., 1998. Glacial River Warren, Lake Pepin, and the environmental history of southeastern Minnesota. 49, Minnesota Geological Survey Report on Investigations.

Yin, C.Q., Li, L.Q., 2008. An investigation on suspended solids sources in urban stormwater runoff using (7)Be and (210)Pb as tracers. Water Science and Technology, 57(12), 1945-1950.

Zumberge, J.H., 1952. The lakes of Minnesota; their origin and classification. Minnesota Geological Survey Bulletin, 25, 99.